The SWMS_3D Code for Simulating Water Flow and Solute Transport in Three-Dimensional Variably-Saturated Media

Version 1.0

by

J. Šimůnek, K. Huang, and M. Th. van Genuchten

U. S. SALINITY LABORATORY
AGRICULTURAL RESEARCH SERVICE
U. S. DEPARTMENT OF AGRICULTURE
RIVERSIDE, CALIFORNIA

ABSTRACT

J. Šimůnek, K. Huang, and M. Th. van Genuchten. 1995. The SWMS_3D Code for Simulating Water Flow and Solute Transport in Three-Dimensional Variably-Saturated Media, Version 1.O. Research Report No, 139, U.S. Salinity Laboratory, USDA, ARS, Riverside, California.

      This report documents version 1.0 of SWMS_3D, a computer program for simulating water and solute movement in three-dimensional variably saturated media. The program numerically solves the Richards' equation for saturated-unsaturated water flow and the convection-dispersion equation for solute transport. The flow equation incorporates a sink term to account for water uptake by plant roots. The transport equation includes provisions for linear equilibrium adsorption, zero-order production, and first-order degradation. The program may be used to analyze water and solute movement in unsaturated, partially saturated, or fully saturated porous media. SWMS_3D can handle flow regions delineated by irregular boundaries. The flow region itself may be composed of nonuniform soils having an arbitrary degree of local anisotropy. The water flow part of the model can deal with prescribed head and flux boundaries, as well as boundaries controlled by atmospheric conditions.

      The governing flow and transport equations are solved numerically using Galerkin-type linear finite element schemes. Depending upon the size of the problem, the matrix equations resulting from discretization of the governing equations are solved using either Gaussian elimination for banded matrices, or a conjugate gradient method for symmetric matrices and the ORTHOMIN method for asymmetric matrices. The program is written in ANSI standard FORTRAN 77. Computer memory is a function of the problem definition, mainly the total number of nodes and elements. This report serves as both a user manual and reference document. Detailed instructions are given for data input preparation. Example input and selected output files are also provided.

CONTENTS

LIST OF FIGURES

LIST OF TABLES

LIST OF VARIABLES

a dimensionless water stress response function [-]

a_{ij} cosine of angle between the ith principal direction of the anisotropy tensor $\boldsymbol{K}^A$ and the j-axis of the global coordinate system

A_{qh} parameter in equation (6.1) [LT^{-1}]

$[A]$ coefficient matrix in the global matrix equation for water flow [L^{2}T^{-1}]

b normalized root water uptake distribution [L^{-3}]

b' arbitrary root water uptake distribution [L"]

b_i, c_i, d_i geometrical shape factors [L^2]

B_{qh} parameter in equation (6.1) [L^{-1}]

$\{B\}$ vector in the global matrix equation for water flow [L^{3}T^{-1}]

c solution concentration [ML"]

c' finite element approximation of c [ML^{-3}]

c_i initial solution concentration [ML^{-3}]

c_n value of the concentration at node n [ML"]

c_s concentration of the sink term [ML"]

$\mathbf{co}$ prescribed concentration boundary condition [ML^{-3}]

C_d factor used to adjust the hydraulic conductivity of elements in the vicinity of drains [-]

Cr_i^e local Courant number [-]

d effective drain diameter [L]

D side length of the square in the finite element mesh surrounding a drain (elements have adjusted hydraulic conductivities) [L]

D_d ionic or molecular diffusion coefficient in free water [L^{2}T^{-1}]

D_{ij} components of the dispersion coefficient tensor [L^{2}T^{-1}]

D_L longitudinal dispersivity [L]

D_T transverse dispersivity [L]

$\{D\}$ vector in the global matrix equation for water flow [L^{3}T^{-1}]

e_n subelements which contain node n [-]

E	maximum (potential) rate of infiltration or evaporation under the prevailing atmospheric conditions [LT']
$\{f\}$	vector in the global matrix equation for solute transport [MT']
$[F]$	coefficient matrix in the global matrix equation for water flow $[L^3]$
$\{g\}$	vector in the global matrix equation for solute transport $[MT^{-1}]$
$[G]$	coefficient matrix in the global matrix equation for solute transport $[L^3T^{-1}]$
h	pressure head [L]
$h^{\bullet}$	scaled pressure head [L]
h'	finite element approximation of h [L]
h_A	minimum pressure head allowed at the soil surface [L]
h_n	nodal values of the pressure head [L]
h_s	air-entry value in the soil water retention function [L]
h_S	maximum pressure head allowed at the soil surface [L]
h_0	initial condition for the pressure head [L]
k	distribution coefficient $[L^3M^{-1}]$
K	unsaturated hydraulic conductivity $[LT^{-1}]$
$K^{\bullet}$	scaled unsaturated hydraulic conductivity $[LT^{-1}]$
$\boldsymbol{K}^A$	dimensionless anisotropy tensor for the unsaturated hydraulic conductivity K [-]
K_{drain}	adjusted hydraulic conductivity in the elements surrounding a drain [LT"]
K_{ij}^{A}	components of the dimensionless anisotropy tensor $\boldsymbol{K}^A$ [-]
K_k	measured value of the unsaturated hydraulic conductivity corresponding to $\theta_k [LT^{-1}]$
K_r	relative hydraulic conductivity [-]
K_s	saturated hydraulic conductivity $[LT^{-1}]$
L	length of the side of an element [L]
L_i	local coordinate [-]
L_n	area of a boundary segment connected to node n [L']
L_x	width of the root zone [L]
L_y	width of the root zone [L]
L_z	depth of the root zone [L]
m	parameter in the soil water retention function [-]

M^0	cumulative amount of solute removed from the flow region by zero-order reactions [M]
M^1	cumulative amount of solute removed from the flow region by first-order reactions [M]
M_r	cumulative amount of solute removed from the flow region by root water uptake [M]
M_t	amount of solute in the flow region at time t [M]
M_t^e	amount of solute in element e at time t [M]
M_0	amount of solute in the flow region at the beginning of the simulation [M]
M_0^e	amount of solute in element e at the beginning of the simulation [Mj
n	exponent in the soil water retention function [-]
n_i	components of the outward unit vector normal to boundary Γ_N [-]
N	total number of nodes [-]
N_e	number of subelements e_n which contain node n [-]
O	actual rate of inflow/outflow to/from a subregion [L^{3}T^{-1}]
Pe_i^e	local Peclet number [-]
q_i	components of the Darcian fluid flux density [LT"]
Q_n^A	convective solute flux at node n [MT?]
Q_n^D	dispersive solute flux at node n [MT']
Q_n^T	total solute flux at node n [MT^{-1}]
$\{Q\}$	vector in the global matrix equation for water flow [L^{3}T^{-1}]
$[Q]$	coefficient matrix in the global matrix equation for solute transport [L^3]
R	retardation factor [-]
s	adsorbed solute concentration [-]
S	sink term [T^{-1}]
S_e	degree of saturation [-]
S_{ek}	degree of saturation corresponding to θ_k [-I
S_p	spatial distribution of the potential transpiration rate [T"]
S_t	soil surface associated with transpiration [L^2]
$[S]$	coefficient matrix in the global matrix equation for solute transport [L^{3}T^{-1}]
t	time [T]
T_a	actual transpiration rate per unit surface length [LT"]

T_p	potential transpiration rate $[LT^{-1}]$
v	average pore-water velocity $[LT^{-1}]$
V	volume of water in each subregion $[L^3]$
V_e	volume of a tetrahedral element $[L^3]$
V_{new}	volume of water in each subregion at the new time level $[L^3]$
V_{old}	volume of water in each subregion at the previous time level $[L^3]$
V_t	volume of water in the flow domain at time t $[L^3]$
V_t^e	volume of water in element e at time t $[L^3]$
V_0	volume of water in the flow domain at time zero $[L^3]$
V_0^e	volume of water in element e at time zero $[L^3]$
x_i	spatial coordinates (i=1,2,3) $[L]$
Z_0	characteristic impedance of a transmission line analog to drain
Z_0'	characteristic impedance of free space ($\approx$376.7 ohms)
α	coefficient in the soil water retention function $[L^{"}]$
α^w	weighing factor $[-]$
α_K	scaling factor for the hydraulic conductivity $[-]$
α_h	scaling factor for the pressure head $[-]$
α_θ	scaling factor for the water content $[-]$
γ_s	zero-order rate constant for solutes adsorbed onto the solid phase $[T^{-1}]$
γ_w	zero-order rate constant for solutes in the liquid phase $[ML^{-3}T^{-1}]$
Γ_e	boundary segments connected to node n
Γ_D	part of the flow domain boundary where Dirichlet type conditions are specified
Γ_G	part of the flow domain boundary where gradient type conditions are specified
Γ_N	part of the flow domain boundary where Neumann type conditions are specified
Γ_C	part of the flow domain boundary where Cauchy type conditions are specified
δ_{ij}	Kronecker delta $[-]$
Δt	time increment $[T]$
Δt_{max}	maximum permitted time increment $[T]$
Δt_{min}	minimum permitted time increment $[T]$

ϵ	temporal weighing factor [-]
ϵ_a^c	absolute error in the solute mass balance [M]
ϵ_a^w	absolute error in the water mass balance [L^3]
ϵ_r^c	relative error in the solute mass balance [%]
ϵ_r^w	relative error in the water mass balance [%]
ϵ_0	permittivity of free space (used in electric analog representation of drains)
θ	volumetric water content [L^{3}L^{-3}]
θ^*	scaled volumetric water content [L^{3}L^{-3}]
θ_a	parameter in the soil water retention function [L^{3}L^{-3}]
θ_k	volumetric water content corresponding to K_k [L^{3}L^{-3}]
θ_m	parameter in the soil water retention function [L^{3}L^{-3}]
θ_r	residual soil water content [L^{3}L^{-3}]
θ_s	saturated soil water content [L^{3}L^{-3}]
λ	first-order rate constant [T^{-1}]
μ_s	first-order rate constant for solute adsorbed onto the solid phase [T^{-1}]
μ_w	first-order rate constant for solutes in the liquid phase [T^{-1}]
μ_0	permeabihty of free space
ρ	bulk density [ML"]
ρ_d	dimensionless ratio between the side of the square in the finite element mesh surrounding the drain, D, and the effective diameter of a drain, d
σ	prescribed flux boundary condition at boundary Γ_N [LT^{-1}]
τ	tortuosity factor [-]
ϕ_n	linear basis functions [-]
ϕ_n^u	upstream weighted basis functions [-]
ψ	prescribed pressure head boundary condition at boundary Γ_D [L]
ω_s	performance index used as a criterion to minimize or eliminate numerical oscillations [-]
Ω	flow region
Ω_e	domain occupied by element e
Ω_R	region occupied by the root zone

1. INTRODUCTION

The importance of the unsaturated zone as an integral part of the hydrological cycle has long been recognized.   The zone plays an inextricable role in many aspects of hydrology, including infiltration, soil moisture storage, evaporation, plant water uptake, groundwater recharge, runoff and erosion.   Initial studies of the unsaturated (vadose) zone focused primarily on water supply studies, inspired in part by attempts to optimally manage the root zone of agricultural soils for maximum crop production. Interest in the unsaturated zone has dramatically increased in recent years because of growing concern that the quality of the subsurface environment is being adversely affected by agricultural, industrial and municipal activities. Federal, state and local action and planning agencies, as well as the public at large, are now scrutinizing the intentional or accidental release of surface-applied and soil-incorporated chemicals into the environment. Fertilizers and pesticides applied to agricultural lands inevitably move below the soil root zone and may contaminate underlying groundwater reservoirs.   Chemicals migrating from municipal and industrial disposal sites also represent environmental hazards. The same is true for radionuclides emanating from energy waste disposal facilities.

The past several decades have seen considerable progress in the conceptual understanding and mathematical description of water flow and solute transport processes in the unsaturated zone. A variety of analytical and numerical models are now available to predict water and/or solute transfer processes between the soil surface and the groundwater table.   The most popular models remain the Richards' equation for variably saturated flow, and the Fickian-based convection-dispersion equation for solute transport. Deterministic solutions of these classical equations have been used, and likely will continue to be used in the near future, for predicting water and solute movement in the vadose zone, and for analyzing specific laboratory or field experiments involving unsaturated water flow and/or solute transport. These models are also helpful tools for extrapolating information from a limited number of field experiments to different soil, crop and climatic conditions, as well as to different tillage and water management schemes.

The purpose of this report is to document version 1.0 of the SWMS_3D computer program simulating water and solute movement in three-dimensional variably saturated media. The program numerically solves the Richards' equation for saturated-unsaturated water flow and

the convection-dispersion equation for solute transport. The flow equation incorporates a sink term to account for water uptake by plant roots. The solute transport equation includes provisions for linear equilibrium adsorption, zero-order production, and first-order degradation. The program may be used to analyze water and solute movement in unsaturated, partially saturated, or fully saturated porous media. SWMS_3D can handle flow domains delineated by irregular boundaries. The flow region itself may be composed of nonuniform soils having an arbitrary degree of local anisotropy. The water flow part of the model considers prescribed head and flux boundaries, as well as boundaries controlled by atmospheric conditions or free drainage. A simplified representation of nodal drains using results of electric analog experiments is also included. First- or third-type boundary conditions can be prescribed in the solute transport part of the model.

The governing flow and transport equations are solved numerically using Galerkin-type linear finite element schemes. Depending upon the size of the problem, the matrix equations resulting from discretization of the governing equations are solved using either Gaussian elimination for banded matrices, or the conjugate gradient method for symmetric matrices and the ORTHOMIN method for *asymmetric* matrices *[Mendoza et. al.,* 1991]. The program *is an* extension of the variably saturated transport code SWMS_2D (version 1.2) of *Šimůnek et al. [1994].* The SWMS_3D code is written in ANSI standard FORTRAN 77, and hence can be compiled, linked and run on any standard micro-, mini-, or mainframe *system,* as well as on personal computers. The source code was developed and tested on a P5 using the Microsoft FORTRAN PowerStation.

This report serves as both a user manual and reference document. Detailed instructions are given for data input preparation. Example input and selected output files are aiso provided. 3 ½ inch floppy diskette containing the source code and the selected input and output files of four examples discussed in this report are available upon request from the authors.

2. VARIABLY SATURATED WATER FLOW

2.1. Governing Flow Equation

Consider three-dimensional isothermal Darcian flow of water in a variably saturated rigid porous medium and assume that the air phase plays an insignificant role in the liquid flow process. The governing flow equation for these conditions is given by the following modified form of the Richards' equation:

$$\frac{\partial \theta}{\partial t} = \frac{\partial}{\partial x_i}\left[K\left(K_{ij}^{A}\frac{\partial h}{\partial x_j} + K_{iz}^{A}\right)\right] - S \tag{2.1}$$

where θ is the volumetric water content [$L^3 L^{-3}$], h is the pressure head [L], S is a sink term [T^{-1}], x_i (i=1,2,3) are the spatial coordinates [L], t is time [T], K_{ij}^{A} are components of a dimensionless tensor K^A representing the possible anisotropic nature of the medium, and K is the unsaturated hydraulic conductivity function [LT^{-1}] given by

$$K(h,x,y,z) = K_s(x,y,z)\, K_r(h,x,y,z) \tag{2.2}$$

where K_r is the relative hydraulic conductivity [-] and K_s the principal saturated hydraulic conductivity [LT^{-1}]. According to this definition, the value of K_{ij}^{A} in (2.1) must be positive and less than or equal to unity. The diagonal entries of K_{ij}^{A} equal one and the off-diagonal entries zero for an isotropic medium. Einstein's summation convention is used in (2.1) and throughout this report. Hence, when an index appears twice in an algebraic term, this particular term must be summed over all possible values of the index.

2.2. Root Water Uptake

The sink term, S, in (2.1) represents the volume of water removed per unit time from a unit volume of soil due to plant water uptake. *Feddes et al.* [1978] defined S as

$$S(h) = a(h)S_p \qquad\qquad (2.3)$$

where the water strkss response function a(h) is a prescribed dimensionless function (Fig. 2.1) of the soil water pressure head $(0 \le a \le 1)$, and S_p is the potential water uptake rate $[T^{-1}]$. Figure 2.1. gives a schematic plot of the stress response function as used by *Feddes et al.* [1978]. Notice that water uptake is assumed to be zero close to saturation (i.e., wetter than some arbitrary "anaerobiosis point", h_1). For $h < h_4$ (the wilting point pressure head), water uptake is also assumed to be zero. Water uptake is considered optimal between pressure heads h_2 and h_3, whereas for pressure head between h_3 and h_4 (or h, and h,), water uptake changes linearly with h. *The* potential water uptake S_p is equal to the water uptake rate during periods of no water stress, i.e., *a(h)=l.*

When the potential water uptake rate is equally distributed over a three-dimensional rectangular root domain, S_p becomes
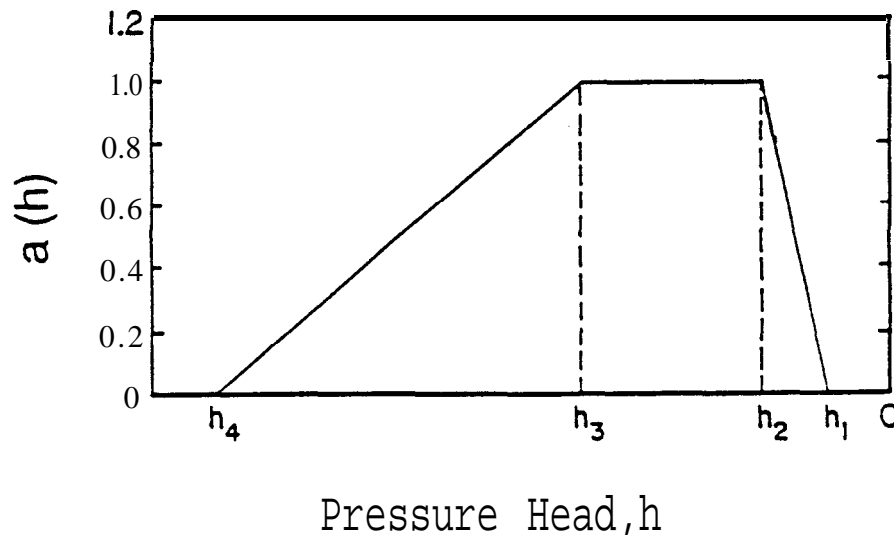
Fig. 2.1. Schematic of the plant water stress response function, a(h),
as used by *Feddes et al. [1978].*
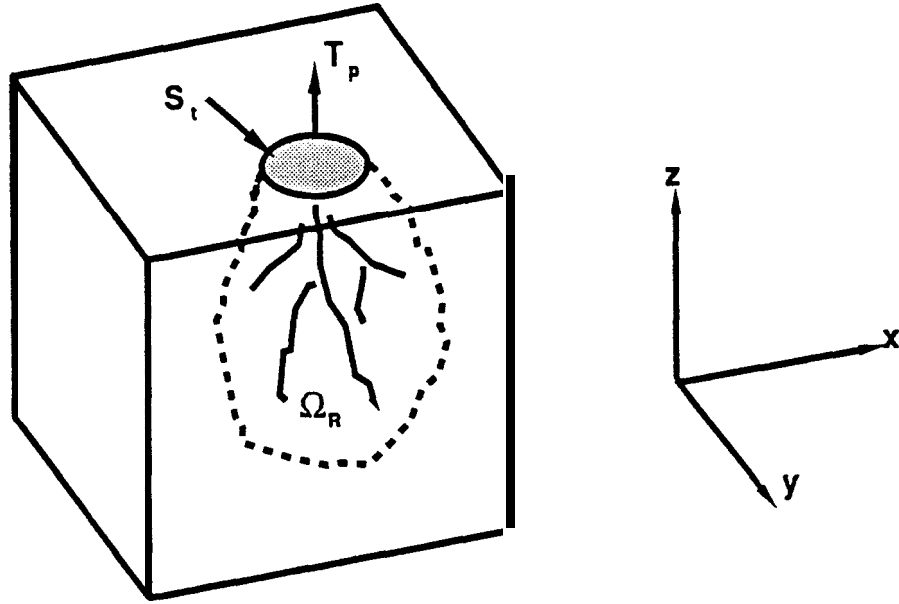
Fig. 2.2. Schematic of the potential water uptake distribution function, $b(x,y,z)$, in the soil root zone.

$$S_p = \frac{1}{L_x L_y L_z} S_t T_p \qquad (2.4)$$

where T_p is the potential transpiration rate [LT^{-1}], L_z is the depth [L] of the root zone, L_x and L_y *are the* lateral widths [L] of the root zone, and S, is the area of the soil surface [L'] associated with the transpiration process. Notice that S_p reduces to T_p/L_z when $S_t=L_x L_y$.

Equation (2.4) may be generalized by introducing a non-uniform distribution of the potential water uptake rate over a root zone of arbitrary shape:

$$S_p = b(x, y, z) \, S_t \, T_p \qquad (2.5)$$

where $b(x,y,z)$ is the normalized water uptake distribution [L^{-3}]. This function describes the spatial variation of the potential extraction term, S_p, over the root zone (Fig. 2.2), and is obtained from $b'(x,y,z)$ as follows

$$b(x,y,z) = \frac{b'(x,y,z)}{\int_{\Omega_R} b'(x,y,z)\, d\Omega} \tag{2.6}$$

where Ω_R is the region occupied by the root zone, and $b'(x,y,z)$ is an arbitrarily prescribed distribution function. Normalizing the uptake distribution ensures that $b(x,y,z)$ integrates to unity over the flow domain, i.e.,

$$\int_{\Omega_R} b(x,y,z)\, d\Omega = 1 \tag{2.7}$$

From (2.5) and (2.7) it follows that S_p is related to T_p by the expression

$$\frac{1}{S_t} \int_{\Omega_R} S_p\, d\Omega = T_p \tag{2.8}$$

The actual water uptake distribution is obtained by substituting (2.5) into (2.3):

$$S(h,x,y,z) = a(h,x,y,z)\, b(x,y,z)\, S_t\, T_p \tag{2.9}$$

whereas the actual transpiration rate, T_a, is obtained by integrating (2.9) as follows

$$T_a = \frac{1}{S_t} \int_{\Omega_R} S\, d\Omega = T_p \int_{\Omega_R} a(h,x,y,z)\, b(x,y,z)\, d\Omega \tag{2.10}$$

2.3. *The Unsaturated Soil Hydraulic Properties*

The unsaturated soil hydraulic properties in the SWMS_3D code are described by a set of closed-form equations resembling those of *van Genuchten [1980]* who used the statistical pore-size distribution model of *Mualem [* 1976] to obtain a predictive equation for the unsaturated hydraulic conductivity function. The original van Genuchten equations were modified to add extra flexibility in the description of the hydraulic properties near saturation [*Šír et al.,* 1985; Vogel *and Císlerová,* 1988]. The soil water retention, *B(h),* and hydraulic conductivity, *K(h),* functions in SWMS_3D are given by

$$\theta(h) = \begin{cases} \theta_a + \dfrac{\theta_m - \theta_a}{(1 + |\alpha h|^n)^m} & h < h_s \\[3ex] es & h \geq h_s \end{cases} \qquad (2.11)$$

and

$$K(h) = \begin{cases} K_s K_r(h) & h \leq h_k \\[2ex] K_k + \dfrac{(h - h_k)(K_s - K_k)}{h_s - h_k} & h_k < h < h_s \\[3ex] K_s & h \geq h_s \end{cases} \qquad (2.12)$$

respectively, where

$$K_r = \frac{K_k}{K_s} \left[\frac{S_e}{S_{ek}} \right]^{1/2} \left[\frac{F(\theta_r) - F(\theta)}{F(\theta_r) - F(\theta_k)} \right]^2 \qquad (2.13)$$

$$F(\theta) = \left[1 - \left| \frac{e - \theta_a}{\theta_m - \theta_a} \right|^{1/m} \right]^m \qquad (2.14)$$

$$m = 1 - 1/n \quad , \qquad n > 1 \qquad (2.15)$$

$$S_e = \frac{e - \theta_r}{\theta_s - \theta_r} \qquad (2.16)$$

$$S_{ek} = \frac{\theta_k - \theta_r}{\theta_s - \theta_r} \qquad (2.17)$$

in which θ_r and θ_s denote the residual and saturated water contents, respectively, and K_s is the saturated hydraulic conductivity. To increase the flexibility of the analytical expressions, and to allow for a non-zero air-entry value, $h,$, the parameters θ_r and θ_s in the retention function were
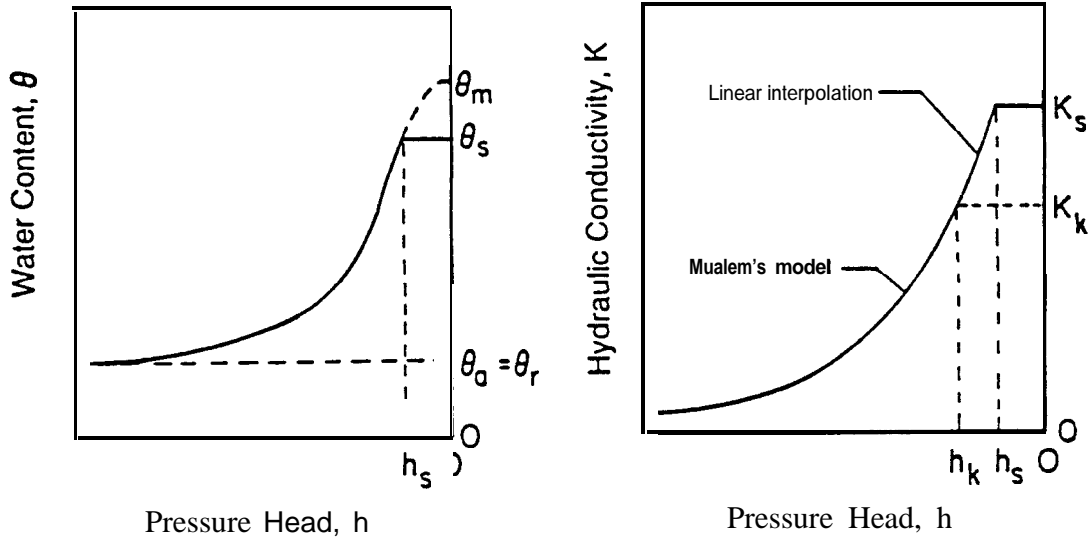
Fig. 2.3. Schematics of the soil water retention (a) and hydraulic conductivity (b) functions as given by equations (2.11) and (2.12), respectively.

replaced by the fictitious (extrapolated) parameters $\theta_a \leq \theta_r$ and $\theta_m \geq \theta_s$ as shown in Fig. 2.3. The approach maintains the physical meaning of θ_r and θ_s as measurable quantities. Equation (2.13) assumes that the predicted hydraulic conductivity function is matched to a measured value of the hydraulic conductivity, $K_k = K(\theta_k)$, at some water content, θ_k, less that or equal to the saturated water content, i.e., $\theta_k \leq \theta_s$ and $K_k \leq K_s$ [Vogel **and Císlerová**, 1988; **Luckner et al., 1989**].

Inspection of (2.11) through (2.17) shows that the hydraulic characteristics contain 9 unknown parameters: θ_r, θ_s, θ_a, θ_m, α, n, K_s, K_k, and θ_k. When $\theta_a = \theta_r$, $\theta_m = \theta_k = \theta_s$ and $K_k = K_s$, the soil hydraulic functions reduce to the original expressions of **van Genuchten** [1980]:

$$\theta(h) = \begin{cases} \theta_r + \dfrac{\theta_s - \theta_r}{[1 + |\alpha h|^n]^m} & h < 0 \\[3mm] \theta_s & h \geq 0 \end{cases} \qquad (2.18)$$

8

$$K(h) = \begin{cases} K_s K_r(h) & h < 0 \\ K_s & h \geq 0 \end{cases} \qquad (2.19)$$

where

$$K_r = S_e^{1/2} [1 - (1 - S_e^{1/m})^m]^2 \qquad (2.20)$$

2.4. *Scaling of the Soil Hydraulic Functions*

SWMS_3D implements a scaling procedure designed to simplify the description of the spatial variability of the unsaturated soil hydraulic properties in the flow domain. The code assumes that the hydraulic variability in a given area can be approximated by means of a set of linear scaling transformations which relate the individual soil hydraulic characteristics $\theta(h)$ and $K(h)$ to reference characteristics $\theta^*(h^*)$ and $K^*(h^*)$. The technique is based on the similar media concept introduced by *Miller and Miller* [1956] for porous media which differ only in the scale of their internal geometry.   The concept was extended by *Simmons et al.* [1979] to materials which differ in morphological properties, but which exhibit 'scale-similar' soil hydraulic functions. Three independent scaling factors are embodied in SWMS_3D. These three scaling parameters may be used to define a linear model of the actual spatial variability in the soil hydraulic properties as follows [Vogel *et al.,* 1991]:

$$K(h) = \alpha_K K^*(h^*)$$

$$\theta(h) = \theta_r + \alpha_\theta [\theta^*(h^* - \theta_r^*] \qquad (2.21)$$

$$h = \alpha_h h^*$$

in which, for the most general case, α_θ, α_h and α_K are mutually independent scaling factors for the water content, the pressure head and the hydraulic conductivity, respectively. Less general scaling methods arise by invoking certain relationships between α_θ, α_h and/or α_K. For example, the original Miller-Miller scaling procedure is obtained by assuming $\alpha_\theta = 1$ (with $\theta_r^* = \theta_r$), and

$\alpha_K = \alpha_h^{-2}$. A detailed discussion of the scaling relationships given by (2.21), and their application to the hydraulic description of heterogeneous soil profiles, is given by Vogel et *al. [* 1991].

2.5. *Initial and Boundary Conditions*

The solution of Eq. (2.1) requires knowledge of the initial distribution of the pressure head within the flow domain, Ω:

$$h(x,y,z,t) = h_0(x,y,z) \qquad \textit{for } t = 0 \qquad (2.22)$$

where h_0 is a prescribed function of *x,* y and *z.*

SWMS_3D implements three types of conditions to describe system-independent interactions along the boundaries of the flow region. These conditions are specified pressure head (Dirichlet type) boundary conditions of the form

$$h(x,y,z,t) = \psi(x,y,z,t) \qquad \textit{for } (x,y,z) \varepsilon \; \Gamma_D \qquad (2.23)$$

specified flux (Neumann type) boundary conditions given by

$$-[K(K_{ij}^A \frac{\partial h}{\partial x_j} + K_{iz}^A)] n_i = \sigma_1(x,y,z,t) \qquad \textit{for } (x,y,z) \; \varepsilon \; \Gamma_N \qquad (2.24)$$

and specified gradient boundary conditions

$$(K_{ij}^A \frac{\partial h}{\partial x_j} + K_{iz}^A) n_i = \sigma_2(x,y,z,t) \qquad \textit{for } (x,y,z) \; \varepsilon \; \Gamma_G \qquad (2.25)$$

where Γ_D, Γ_N, and Γ_G indicate Dirichlet, Neumann, and gradient type boundary segments, respectively; ψ [L], $\sigma_1 [LT^{-1}]$, and σ_2 [-] are prescribed functions of x, y, z and t; and n_i *are the* components of the outward unit vector normal to boundary Γ_N or Γ_G. As pointed out by *McCord [199 1], the use* of the term "Neumann type boundary condition" for the flux boundary is not very appropriate since this term should hold for a gradient type condition (see also Section 3.2 for solute transport). However, since the use of the Neumann condition is standard in the hydrologic literature *[Neuman,* 1972; *Neuman et al., 1974], we* shall also use this term to indicate flux

10

boundaries throughout this report. SWMS_3D implements the gradient boundary condition only in terms of a unit vertical hydraulic gradient ($\sigma_2 = 1$) simulating free drainage from a relatively deep soil profile. This situation is *often* observed in field studies of water flow and drainage in the vadose zone [Sisson, 1987; McCord, 1991]. *McCord [1991]* states that the most pertinent application of (2.25) is its use as a bottom outflow boundary condition for situations where the water table is situated far below the domain of interest.

In addition to the system-independent boundary conditions given by (2.23), (2.24), and (2.25), SWMS_3D considers three different types of system-dependent boundary conditions which cannot be defined a priori. One of these involves soil-air interfaces which are exposed to atmospheric conditions. The potential fluid flux across these interfaces is controlled exclusively by external conditions. However, the actual flux depends also on the prevailing (transient) soil moisture conditions. Soil surface boundary conditions may change from prescribed flux to prescribed head type conditions (and vice-versa). In the absence of surface ponding, the numerical solution of (2.1) is obtained by limiting the absolute value of the flux such that the following two conditions are satisfied [Neuman et *al.,* 1974]:

$$|K(K_{ij}^{A} \frac{\partial h}{\partial x_j} + K_{iz}^{A})n_i| \leq E \qquad (2.26)$$

and

$$h_A \leq h \leq h_S \qquad (2.27)$$

where E is the maximum potential rate of infiltration or evaporation under the current atmospheric conditions, h is the pressure head at the soil surface, and h_A and h_S are, respectively, minimum and maximum pressure heads allowed under the prevailing soil conditions. The value for h_A is determined from the equilibrium conditions between soil water and atmospheric water vapor, whereas h_S is usually set equal to zero. SWMS_3D assumes that any excess water on the soil surface is immediately removed. When one of the end points of (2.27) is reached, a prescribed head boundary condition will be used to calculate the actual surface flux. Methods of calculating E and h_A on the basis of atmospheric data have been discussed by *Feddes et al. [1974].*

A second type of system-dependent boundary condition considered in SWMS_3D is a seepage face through which water leaves the saturated part of the flow domain. In this case, the length of the seepage face is not known a priori. SWMS_3D assumes that the pressure head is always uniformly equal to zero along a seepage face. Additionally, the code assumes that water leaving the saturated zone across a seepage face is immediately removed by overland flow or some other removal process.

Finally, a third class of system-dependent boundary conditions in SWMS_3D concerns tile drains. Similarly as for seepage phase, SWMS_3D assumes that as long as a drain is located in the saturated zone, the pressure head along the drain will be equal to zero; the drain then acts as a pressure head sink. However, the drain will behave as a nodal sink/source with zero recharge when located in the unsaturated zone. More information can be found in Section 4.3.7.

3. SOLUTE TRANSPORT

3.1. *Governing Transport Equation*

The partial differential equation governing three-dimensional chemical transport during transient water flow in a variably saturated rigid porous medium is *taken as*

$$\frac{\partial \theta c}{\partial t} + \frac{\partial \rho s}{\partial t} = \frac{\partial}{\partial x_i}(\theta D_{ij}\frac{\partial c}{\partial x_j}) - \frac{\partial q_i c}{\partial x_i} + \mu_w \theta c + \mu_s \rho s + \gamma_w \theta + \gamma_s \rho - S c_s \qquad (3.1)$$

where c is the solution concentration [ML^-3], s is the adsorbed concentration [-], q_i is the *i-th* component of the volumetric flux [LT^{-1}], μ_w and μ_s are first-order rate constants for solutes in the liquid and solid phases [T^{-1}], respectively; γ_w and γ_s are zero-order rate constants for the liquid [ML^{-3}T^{-1}] and solid [T^{-1}] phases, respectively; ρ is the soil bulk density [ML^-3], S is the sink term in the water flow equation (2.1), c_s is the concentration of the sink term [ML^{-3}], and D_{ij} is the dispersion coefficient tensor [L^{2}T^{-1}]. The four zero- and first-order rate constants in (3.1) may be used to represent a variety of reactions or transformations including biodegradation, volatilization, precipitation and radioactive decay.

SWMS_3D assumes equilibrium interactions between the solution (c) and adsorbed (s) concentrations of the solute in the soil system. The adsorption isotherm relating s and c is further assumed to be described by a linear equation of the form

$$s = kc \qquad (3.2)$$

where k is an empirical constant [L^{3}M^{-1}].

The continuity equation for water flow in a three-dimensional variably-saturated medium is given by

$$\frac{\partial \theta}{\partial t} = -\frac{\partial q_i}{\partial x_i} - S \qquad (3.3)$$

where q_i is the Darcian fluid flux density. Substituting (3.2) and (3.3) into (3.1) gives

$$-\theta R \frac{\partial c}{\partial t} - q_i \frac{\partial c}{\partial x_i} + \frac{\partial}{\partial x_i}(\theta D_{ij} \frac{\partial c}{\partial x_j}) + Fc + G = 0 \qquad (3.4)$$

where

$$F = \mu_w \theta + \mu_s \rho k + S$$

$$G = \gamma_w \theta + \gamma_s \rho - Sc_s \qquad (3.5)$$

and where the retardation factor R [-] is defined as

$$R = 1 + \frac{\rho k}{\theta} \qquad (3.6)$$

In order to solve equation (3.4), it is necessary to know the water content θ and the volumetric flux q_i. Both variables are obtained from solutions of the flow equation (2.1).

3.2. *Initial and Boundary Conditions*

The solution of (3.4) requires knowledge of the initial concentration within the flow region, Ω, i.e.,

$$c(x,y,z,0) = c_i(x,y,z) \qquad (3.7)$$

where c_i is a prescribed function of x, y and z.

Two types of boundary conditions (Dirichlet and Cauchy type conditions) can be specified along the boundary of Ω. First-type (or Dirichlet type) boundary conditions prescribe the concentration along a boundary segment Γ_D:

$$c(x,y,z,t) = c_0(x,y,z,t) \qquad for\ (x,y,z)\ \varepsilon\ \Gamma_D \qquad (3.8)$$

whereas third-type (Cauchy type) boundary conditions may be used to prescribe the solute flux along a boundary segment Γ_C as follows:

$$-\theta\,D_{ij}\frac{\partial c}{\partial x_j}\,n_i + q_i n_i c = q_i n_i c_0 \quad \textit{for} \quad (x,y,z)\,\varepsilon\,\Gamma_C \tag{3.9}$$

in which $q_i n_i$ represents the outward fluid flux, n_i is the outward unit normal vector, and c_0 is the concentration of the incoming fluid. In some cases, for example when Γ_C is an impermeable boundary $(q_i n_i{=}0)$ or water flow is directed out of the region $(q_i n_i c_0{=}q_i n_i c)$, (3.9) reduces to a second-type (Neumann type) boundary condition of the form:

$$\theta\,D_{ij}\frac{\partial c}{\partial x_j}\,n_i = 0 \qquad \textit{for } (x,y,z)\,\varepsilon\,\Gamma_N \tag{3.10}$$

3.3. *Dispersion Coefficient*

The components of the dispersion tensor, *D,,* in (3.1) are given by [Bear, 1972]

$$\theta\,D_{ij} = D_T|q|\,\delta_{ij} + (D_L - D_T)\frac{q_j q_i}{|q|} + \theta\,D_d \tau\,\delta_{ij} \tag{3.11}$$

where D_d is the ionic or molecular diffusion coefficient in free water $[L^2 T^{-1}]$, τ is a tortuosity factor [-], $|q|$ is the absolute value of the Darcian fluid flux density $[LT^{-1}]$, δ_{ij} is the Kronecker delta function $(\delta_{ij}{=}1$ if $i{=}j$, and $\delta_{ij}{=}0$ if $i{\neq}j)$, and D_L and D_T **are the** longitudinal and transverse dispersivities, respectively [L]. The individual components of the dispersion tensor for three-dimensional transport are as follows:

$$\theta\,D_{xx} = D_L\frac{q_x^2}{|q|} + D_T\frac{q_y^2}{|q|} + D_T\frac{q_z^2}{|q|} + \theta\,D_d\tau$$

$$\theta\,D_{yy} = D_L\frac{q_y^2}{|q|} + D^T\frac{q_x^2}{|q|} + D^T\frac{q_z^2}{|q|} + \theta\,D_d\tau$$

$$\theta\,D_{zz} = D_L \frac{q_z^2}{|q|} + D_T \frac{q_x^2}{|q|} + D_T \frac{q_y^2}{|q|} + \theta\,D_d \tau$$

$$\theta\,D_{xy} = (D_L - D_T)\frac{q_x q_y}{|q|}$$

$$\theta\,D_{xz} = (D_L - D_T)\frac{q_x q_z}{|q|} \tag{3.12}$$

$$\theta\,D_{yz} = (D_L - D_T)\frac{q_y q_z}{|q|}$$

The tortuosity factor is evaluated in SWMS_3D as a function of the water content using the relationship of *Millington and Quirk* [1961]:

$$\tau = \frac{\theta^{7/3}}{\theta_s^2} \tag{3.13}$$

16

4. NUMERICAL SOLUTION OF THE WATER FLOW EQUATION

The Galerkin finite element method with linear basis functions is used to obtain a solution of the flow equation (2.1) subject to the imposed initial and boundary conditions. Since the Galerkin method is relatively standard and has been covered in detail elsewhere [Neuman, 1975; Zienkiewicz, 1977; *Pinder and Gray,* 1977], only the most pertinent steps in the solution process are given here.

4.1. Space Discretization

The flow region is divided into a network of tetrahedral elements. The corners of these elements are taken to be the nodal points. The dependent variable, the pressure head function $h(x,y,z,t)$, is approximated by a function $h'(x,y,z,t)$ as follows

$$h'(x,y,z,t) = \sum_{n=1}^{N} \phi_n(x,y,z) \, h_n(t) \qquad (4.1)$$

where ϕ_n are piecewise linear basis functions satisfying the condition $\phi_n(x_m,y_m,z_m)=\delta_{nm}$, h_n are unknown coefficients representing the solution of (2.1) at the nodal points, and N is the total number of nodal points.

The Galerkin method postulates that the differential operator associated with the Richards' equation (2.1) is orthogonal to each of the N basis functions, i.e.,

$$\int_{\Omega} \{ \frac{\partial \theta}{\partial t} - \frac{\partial}{\partial x_i} [K(K_{ij}^A \frac{\partial h}{\partial x_j} + K_{iz}^A)] + S \} \phi_n \, d\Omega = 0 \qquad (4.2)$$

Applying Green's first identity to (4.2), and replacing h by h', leads to

$$\sum_e \int_{\Omega_e} \left(\frac{\partial \theta}{\partial t} \phi_n + KK_{ij}^A \frac{\partial h'}{\partial x_j} \frac{\partial \phi_n}{\partial x_i} \right) d\Omega =$$

$$\sum_e \int_{\Gamma_e} K\left(K_{ij}^A \frac{\partial h'}{\partial x_j} + K_{iz}^A\right) n_i \phi_n d\Gamma + \sum_e \int_{\Omega_e} \left(-KK_{iz}^A \frac{\partial \phi_n}{\partial x_i} - S\phi_n\right) d\Omega \qquad \textbf{\textit{(4.3)}}$$

where Ω_e represents the domain occupied by element e, and Γ_e is a boundary segment coinciding with element e. Natural flux-type (Neumann) and gradient type boundary conditions can be immediately incorporated into the numerical scheme by specifying the surface integral in equation (4.3).

After imposing additional simplifying assumptions to be discussed later, and performing integration over the elements, the procedure leads to a system of time-dependent ordinary differential equations with nonlinear coefficients. In matrix form, these equations are given by

$$[F] \frac{d\{\theta\}}{dt} + [A]\{h\} = \{Q\} - \{B\} - \{D\} \qquad (4.4)$$

where

$$A_{nm} = \sum_e K_l K_{ij}^A \int_{\Omega_e} \phi_l \frac{\partial \phi_n}{\partial x_i} \frac{\partial \phi_m}{\partial x_j} d\Omega$$

$$= \sum_e \frac{\bar{K}}{36V_e} [K_{xx}^A b_m b_n + K_{yy}^A c_m c_n + K_{zz}^A d_n d_m + K_{xy}^A (b_m c_n + c_m b_n) + \qquad (4.5)$$

$$+ K_{xz}^A (b_n d_m + d_n b_m) + K_{yz}^A (c_m d_n + d_m c_n)]$$

$$B_n = \sum_e K_l K_{iz}^A \int_{\Omega_e} \phi_l \frac{\partial \phi_n}{\partial x_i} d\Omega = \sum_e \frac{\bar{K}}{6} (K_{xz}^A b_n + K_{yz}^A c_n + K_{zz}^A d_n) \qquad (4.6)$$

18

$$F_{nm} = \delta_{nm} \sum_e \int_{\Omega_e} \phi_n d\Omega = \delta_{nm} \sum_e \frac{V_e}{4} \qquad (4.7)$$

$$Q_n = -\sum_e \sigma_{1_l} \int_{\Gamma_e} \phi_l \phi_n d\Gamma = -\sum_e \sigma_n L_n \qquad (4.8)$$

$$D_n = \sum_e S_l \int_{\Omega_e} \phi_l \phi_n d\Omega = \sum_e \frac{V_e}{20} (4\bar{S} + S_n) \qquad (4.9)$$

where the overlined variables represent average values over an element e, the subscripts i and j are space direction indices (i,j = 1,2,3), l = 1,2,..., N; m = 1,2,..., N; n = 1,2,..., N, and, for tetrahedral element vertexed by nodes 1, 2, 3, and 4

$$b_1 = (y_4 - y_2)(z_3 - z_2) - (y_3 - y_2)(z_4 - z_2)$$

$$b_2 = (y_4 - y_3)(z_1 - z_3) - (y_1 - y_3)(z_4 - z_3)$$

$$b_3 = (y_2 - y_4)(z_1 - z_4) - (y_1 - y_4)(z_2 - z_4)$$

$$b_4 = (y_2 - y_1)(z_3 - z_1) - (y_3 - y_1)(z_2 - z_1)$$

$$c_1 = (x_3 - x_2)(z_4 - z_2) - (x_4 - x_2)(z_3 - z_2)$$

$$c_2 = (x_1 - x_3)(z_4 - z_3) - (x_4 - x_3)(z_1 - z_3)$$

$$c_3 = (x_1 - x_4)(z_2 - z_4) - (x_2 - x_4)(z_1 - z_4) \qquad (4.10)$$

$$c_4 = (x_3 - x_1)(z_2 - z_1) - (x_2 - x_1)(z_3 - z_1)$$

$$d_1 = (x_4 - x_2)(y_3 - y_2) - (x_3 - x_2)(y_4 - y_2)$$

$$d_2 = (x_4 - x_3)(y_1 - y_3) - (x_1 - x_3)(y_4 - y_3)$$

$$d_3 = (x_2 - x_4)(y_1 - y_4) - (x_1 - x_4)(y_2 - y_4)$$

$$d_4 = (x_2 - x_1)(y_3 - y_1) - (x_3 - x_1)(y_2 - y_1)$$

$$V_e = (x_4 - x_1)b_4 + (y_4 - y_1)c_4 + (z_4 - z_1)d_4$$

19

$$\overline{K} = \frac{K_1 + K_2 + K_3 + K_4}{4} \qquad \overline{S} = \frac{S_1 + S_2 + S_3 + S_4}{4} \tag{4.11}$$

Equation (4.8) is valid for a flux-type boundary condition. For a gradient-type boundary condition the variable σ_1 in (4.8) must be replaced by the product of the hydraulic conductivity K and the prescribed gradient $\sigma_2 (=1)$. V_e is the volume of element e, $\overline{K}$ and $\overline{S}$ are the average hydraulic conductivity and root water extraction values over element e, and L_n is the area of the boundary segment connected to node n. The symbol σ_n in equation (4.8) stands for the flux $[\text{LT}^{-1}]$ across the boundary in the vicinity of boundary node n (positive when directed outward of the system). The boundary flux is assumed to be uniform over each boundary segment. The entries of the vector Q_n are zero at all internal nodes which do not act as sources or sinks for water.

The numerical procedure leading to (4.4) incorporates two important assumptions in addition to those related to the Galerkin finite element approach. One assumption concerns the time derivatives of the nodal values of the water content in (4.4). These time derivatives were weighted according to

$$\frac{d\theta_n}{dt} = \frac{\sum_e \int_{\Omega_e} \frac{\partial \theta}{\partial t} \phi_n d\Omega}{\sum_e \int_{\Omega_e} \phi_n d\Omega} \tag{4.12}$$

This assumption implements mass-lumping which has been shown to improve the rate of convergence of the iterative solution process [e.g., *Neuman,* 1973].

A second assumption in the numerical scheme is related to the anisotropy tensor K^A which is taken to be constant over each element. By contrast, the water content θ, the hydraulic conductivity K, the soil water capacity C, and the root water extraction rate S, at a given time are assumed to vary linearly over each element, e. For example, the water content is expanded over each element as follows:

$$\theta(x,y,z) = \sum_{n=1}^{4} \theta(x_n, y_n, z_n) \phi_n(x,y,z) \qquad \text{for } (x,y,z) \, \varepsilon \, V_e \qquad (4.13)$$

where n stands for the comers of element e. The advantage of linear interpolation is that no numerical integration is needed to evaluate the coefficients in (4.4).

4.2. *Time Discretization*

Integration of (4.4) in time is achieved by discretizing the time domain into a sequence of finite intervals and replacing the time derivatives by finite differences. An implicit (backward) finite difference scheme is used for both saturated and unsaturated conditions:

$$[F] \frac{\{\theta\}_{j+1} - \{\theta\}_j}{\Delta t_j} + [A]_{j+1} \{h\}_{j+1} = \{Q\}_j - \{B\}_{j+1} - \{D\}_j \qquad (4.14)$$

where $j+1$ *denotes the* current time level at which the solution is being considered, j refers to the previous time level, and $\Delta t_j = t_{j+1} - t_j$. Equation (4.14) represents the final set of algebraic equations to be solved. Since θ and the coefficients A, B, *D,* and Q (for a gradient-type boundary conditions) are functions of the dependent variable *h, the* set of equations is generally highly nonlinear. Note that vectors *D* and Q, in contrast to the fully implicit scheme, are evaluated at the old time level. This feature may, in some cases, improve the convergence rate.

4.3. Numerical Solution Strategies

4.3.1. *Iteration Process*

Because of the nonlinear nature of (4.14), an iterative process must be used to obtain solutions of the global matrix equation at each new time step. For each iteration a system of linearized algebraic equations is first derived from (4.14) which, after incorporation of the boundary conditions, is solved using either Gaussian elimination or the conjugate gradient method (see Section 6.5). The Gaussian elimination process takes advantage of the banded and

symmetric features of the coefficient matrices in (4.14). After inversion, the coefficients in (4.14) are re-evaluated using the first solution, and the new equations are again solved. The iterative process continues until a satisfactory degree of convergence is obtained, i.e., until at all nodes in the saturated (or unsaturated) region the absolute change in pressure head (or water content) between two successive iterations becomes less than the imposed absolute pressure head (or water content) tolerance [*Šimůnek and Suarez,* 1993]. The first estimate (at zero iteration) of the unknown pressure heads at each time step is obtained by extrapolation from the pressure head values at the previous two time levels.

4.3.2. *Discretization of Water Storage Term*

The iteration process is extremely sensitive to the method used for evaluating the water content term ($\Delta\theta/\Delta t$) in equation (4.14). The present version of SWMS_3D code uses the modified Picard iteration method proposed by *Celia et al.* [1990]. Their method has been shown to provide excellent results in terms of minimizing the mass balance error. The mass-conservative method proceeds by expanding the water content term into two parts:

$$[F]\frac{\{\theta\}_{j+1} - \{\theta\}_j}{\Delta t_j} = [F]\frac{\{\theta\}_{j+1}^{k+1} - \{\theta\}_{j+1}^k}{\Delta t_j} + [F]\frac{\{\theta\}_{j+1}^k - \{\theta\}_j}{\Delta t_j} \qquad (4.15)$$

where $k+1$ and k denote the current and previous iteration levels, respectively; and $j+1$ and j the current and previous time levels, respectively. Notice that the second term on the right hand side of (4.15) is known prior to the current iteration. The first term on the right hand side can be expressed in terms of the pressure head, so that (4.15) becomes

$$[F]\frac{\{\theta\}_{j+1} - \{\theta\}_j}{\Delta t_j} = [F][C]_{j+1}\frac{\{h\}_{j+1}^{k+1} - \{h\}_{j+1}^k}{\Delta t_j} + [F]\frac{\{\theta\}_{j+1}^k - \{\theta\}_j}{\Delta t_j} \qquad (4.16)$$

where $C_{nm}=\delta_{nm}C_n$, in which C_n represents the nodal value of the soil water capacity. The first term on the right hand side of (4.16) should vanish at the end of the iteration process if the numerical solution converges. This particular feature guarantees relatively small mass balance

errors in the solution.

4.3.3. *Time Step Control*

Three different time discretizations are introduced in SWMS_3D: (1) time discretizations associated with the numerical solution, (2) time discretizations associated with the implementation of boundary conditions, and (3) time discretizations which provide printed output of the simulation results (e.g., nodal values of dependent variables, water and solute mass balance components, and other information about the flow regime).

Discretizations 2 and 3 are mutually independent; they generally involve variable time steps as described in the input data file. Discretization 1 starts with a prescribed initial time increment, **At.** This time increment is automatically adjusted at each time level according to the following rules [Mls, 1982; Vogel, 1987]:

  a. Discretization 1 must coincide with time values resulting from discretizations 2 and 3.

  b. Time increments cannot become less than a preselected minimum time step, Δt_{min}, nor exceed a maximum time step, **At_** (i.e., At,, ≤ At ≤ At_).

  c. If, during a particular time step, the number of iterations necessary to reach convergence is ≤3, the time increment for the next time step is increased by multiplying At by a predetermined constant >1 (usually between 1.1 and 1.5). If the number of iterations is ≥7, At for the next time level is multiplied by a constant <1 (usually between 0.3 and 0.9).

  d. If, during a particular time step, the number of iterations at any time level becomes greater than a prescribed maximum (usually between 10 and 50), the iterative process for that time level is terminated. The time step is subsequently reset to $\Delta t/3$, and the iterative process restarted.

The selection of optimal time steps, At, is also influenced by the solution scheme for solute transport (see Section 5.3.6.).

4.3.4. *Treatment of Pressure Head Boundary Conditions*

Finite element equations corresponding to Dirichlet nodes where the pressure head is prescribed can, at least in principle, be eliminated from the global matrix equation. An alternative and numerically simpler approach is to replace the Dirichlet finite element equations by dummy expressions of the form *[Neuman,* 1974]

$$\delta_{nm} h_m = \psi_n \tag{4.17}$$

where δ_{nm} is the Kronecker delta and ψ_n is the prescribed value of the pressure head at node n. The values of h_n in all other equations are set equal to ψ_n and the appropriate entries containing ψ_n in the left hand side matrix are incorporated into the known vector on the right-hand side of the global matrix equation. When done properly, this rearrangement will preserve symmetry in the matrix equation. This procedure is applied only when Gaussian elimination is used to solve the matrix equation. When the conjugate gradient solver is used, then the finite element equation representing the Dirichlet node is modified in a way that the right hand side of this equation is set equal to the prescribed pressure head multiplied by a large number (10^{30}) and entry on the left hand side representing the Dirichlet node is set equal to this large number. After solving for all pressure heads, the value of the flux Q_n can be calculated explicitly and accurately from the original finite element equation associated with node n *(e.g., Lynch, 1984).*

4.3.5. Flux and Gradient Boundary Conditions

The values of the fluxes Q_n at nodal points along prescribed flux and gradient boundaries are computed according to equation (4.8). Internal nodes which act as Neumann type sources or sinks have values of Q_n equal to the imposed fluid injection or extraction rate.

4.3.6. Atmospheric Boundary Conditions and Seepage Faces

Atmospheric boundaries are simulated by applying either prescribed head or prescribed

flux boundary conditions depending upon whether equation (2.26) or (2.27) is satisfied [Neuman, 1974]. If (2.27) is not satisfied, node n becomes a prescribed head boundary, If, at any point in time during the computations, the calculated flux exceeds the specified potential flux in (2.26), the node will be assigned a flux equal to the potential value and treated again as a prescribed flux boundary.

All nodes expected to be part of a seepage face during code execution must be identified a priori. During each iteration, the saturated part of a potential seepage face is treated as a prescribed pressure head boundary with $h=0$, while the unsaturated part is treated as a prescribed flux boundary with $Q=0$. The lengths of the two surface segments are continually adjusted [Neuman, 1974] during the iterative process until the calculated values of Q (equation (4.8)) along the saturated part, and the calculated values of h along the unsaturated part, are all negative, thus indicating that water is leaving the flow region through the saturated part of the surface boundary only.

4.3.7. *Treatment of Tile Drains*

The representation of tile drains as boundary conditions is based on studies by *Vimoke et al. [1963]* and *Fipps et al. [1986]*. The approach uses results of electric analog experiments conducted by *Vimoke and Taylor [1962]* who reasoned that drains can be represented by nodal points in a regular finite element mesh, provided adjustments are made in the hydraulic conductivity, K, of neighboring elements. The adjustments should correspond to changes in the electric resistance of conducting paper as follows

$$K_{drain} = K\,C_d \tag{4.18}$$

where K_{drain} is the adjusted conductivity [LT^{-1}], and C_d is the correction factor [-]. C_d is determined from the ratio of the effective radius, d [L], of the drain to the side length, D [L], of the square formed by finite elements surrounding the drain node and located in a plane perpendicular to a drain [*Vimoke at al., 1962]:*

$$C_d = \frac{Z_0'}{Z_0} \approx \frac{\sqrt{\mu_0/\epsilon_0}}{138 \, \log_{10}\rho_d + 6.48 - 2.34\,A - 0.48\,B - 0.12\,C} \qquad (4.19)$$

where Z_0' is the characteristic impedance of free space (≈ 376.7 ohms), μ_0 is the permeability of free space, ϵ_0 is the permittivity of free space, and Z_0 is the characteristic impedance of a transmission line analog of the drain. The coefficients in (4.19) are given by

$$\rho_d = \frac{D}{d} \qquad\qquad A = \frac{1 + 0.405\,\rho_d^{-4}}{1 - 0.405\,\rho_d^{-4}}$$

$$\qquad\qquad (4.20)$$

$$B = \frac{1 + 0.163\,\rho_d^{-8}}{1 - 0.163\,\rho_d^{-8}} \qquad\qquad c = \frac{1 + 0.067\,\rho_d^{-12}}{1 - 0.067\,\rho_d^{-12}}$$

where the effective drain diameter, d, is to be calculated from the number and size of small openings in the drain tube *[Mohammad and Skaggs,* 1984], and D is the size of the square in the finite element mesh surrounding the drain having adjusted hydraulic conductivities. The approach above assumes that the node representing a drain must be surrounded by finite elements (either triangular or quadrilateral) which form a square whose hydraulic conductivities are adjusted according to (4.18). This method of implementing the drain by means of a boundary condition gives an efficient, yet relatively accurate, prediction of the hydraulic head in the immediate area surrounding the dram, as well as of the dram flow rates [Fipps et *al.,* 1986]. More recent studies have shown that the correction factor C_d could be further reduced by a factor of 2 [Rogers *and Fouss,* 1989] or 4 *[Tseng,* 1994, personal communication].

4.3.8. *Water Balance Evaluation*

The SWMS_3D code performs water balance computations at prescribed times for several preselected subregions of the flow domain. The water balance information for each subregion consists of the actual volume of water, V, in that subregion, and the rate, 0, of inflow or outflow to or from the subregion. V and O are given by

$$V = \sum_e V_e \frac{\theta_i + \theta_j + \theta_k + \theta_l}{4} \qquad (4.21)$$

and

$$O = \frac{V_{new} - V_{old}}{\Delta t} \qquad (4.22)$$

respectively, where θ_i, θ_j, 19, and 8, are water contents evaluated at the comer nodes of element e, and where V_{new} and V_{old} *are* volumes of water in the subregion computed at the current and previous time levels, respectively. The summation in (4.21) is taken over all elements within the subregion.

The absolute error in the mass balance is calculated as

$$\epsilon_a^w = V_t - V_0 + S_t \int_0^t T_a dt - \int_0^t \sum_{n_\Gamma} Q_n dt \qquad (4.23)$$

where *V,* and V_0 *are the* volumes of water in the flow domain at time *t* and zero, respectively, as calculated with (4.21). The third term on the right-hand side represents the cumulative root water uptake amount, while the fourth term gives the cumulative flux through nodes, n_Γ, located along the boundary of the flow domain or at internal source and sink nodes.

The accuracy of the numerical solution is evaluated in terms of the relative error, ϵ_r^w [%], in the water mass balance as follows:

$$\epsilon_r^w = \frac{|\epsilon_a^w|}{\max\left[\sum_e |V_t^e - V_0^e|, \; S_t \int_0^t T_a dt + \int_0^t \sum_{n_\Gamma} |Q_n| dt\right]} 100 \qquad (4.24)$$

where V_t^e and V_0^e *are the* volumes of water in element *e* at times *t* and zero, respectively. Note that SWMS_3D does not relate the absolute error to the volume of water in the flow domain, but instead to the maximum value of two quantities. The first quantity represents the sum of the absolute changes in water content over all elements, whereas the second quantity is the sum of the absolute values of all fluxes in and out of the flow domain. The above error criterion is

much stricter than the usual criterion involving the total volume of water in the flow domain. This is because the cumulative boundary fluxes are often much smaller than the volume in the domain, especially at the beginning of the simulation.

4.3.9. Computation of Nodal Fluxes

Components of the Darcian flux are computed at each time level during the simulation only when the water flow and solute transport equations are solved simultaneously. When the flow equation is being solved alone, the flux components are calculated only at selected print times. The x-, y-, and z-components of the nodal fluxes are computed for each node n according to:

$$q_x = -\frac{K_n}{N_e} \sum_{e_n} [\frac{\gamma_i^x h_i + \gamma_j^x h_j + \gamma_k^x h_k + \gamma_l^x h_l}{6V_e} + K_{xz}^A]$$

$$q_y = -\frac{K_n}{N_e} \sum_{e_n} [\frac{\gamma_i^y h_i + \gamma_j^y h_j + \gamma_k^y h_k + \gamma_l^y h_l}{6V_e} + K_{yz}^A]$$

$$q_z = -\frac{K_n}{N_e} \sum_{e_n} [\frac{\gamma_i^z h_i + \gamma_j^z h_j + \gamma_k^z h_k + \gamma_l^z h_l}{6V_e} + K_{zz}^A] \qquad (4.25)$$

$$\gamma_n^x = K_{xx}^A b_n + K_{xy}^A c_n + K_{xz}^A d_n$$

$$\gamma_n^y = K_{xy}^A b_n + K_{yy}^A c_n + K_{yz}^A d_n$$

$$\gamma_n^z = K_{xz}^A b_n + K_{yz}^A c_n + K_{zz}^A d_n$$

where N_e is the number of sub-elements e_n adjacent to node n. Einstein's summation convention is not used in (4.25).

4.3.10. Water Uptake by Plant Roots

SWMS_3D considers the root zone to consist of all nodes, n, for which the potential root

water uptake distribution, *b* (see Section 2.2), is greater than zero. The root water extraction rate is assumed to vary linearly over each element; this leads to approximation (4.9) for the root water extraction term D_n in the global matrix equation. The values of actual root extraction rate S_n in (4.9) are evaluated with (2.9). In order to speed up the calculations, the extraction rates S_n are calculated at the old time level and are not updated during the iterative solution process at a given time step. SWMS_3D calculates the total rate of transpiration per unit soil surface length using the equation

$$T_a = \frac{1}{S_I} \sum_e V_e \bar{S}$$

(4.26)

in which the summation takes place over all elements within the root zone.

4.3.11. *Evaluation of the Soil Hydraulic Properties*

At the beginning of a numerical simulation, SWMS_3D generates for each soil type in the flow domain a table of water contents, hydraulic conductivities, and specific water capacities from the specified set of hydraulic parameters. The values of θ_i, K_i and C_i in the table are evaluated at prescribed pressure heads h_i within a specified interval *(h_a, h_b)*. The entries in the table are generated such that

$$\frac{h_{i+1}}{h_i} = constant$$

(4.27)

which means that the spacing between two consecutive pressure head values increases in a logarithmic fashion. Values for the hydraulic properties, *8(h), K(h)* and *C(h), are* computed during the iterative solution process using linear interpolation between the entries in the table. If an argument *h* falls outside the prescribed interval *(h_a, h_b)*, the hydraulic characteristics are evaluated directly from the hydraulic functions, i.e., without interpolation. The above interpolation technique was found to be much faster computationally than direct evaluation of the hydraulic functions over the entire range of pressure heads, except when very simple hydraulic

29

models were used.

4.3.12. *Implementation of Hydraulic Conductivity Anisotropy*

Since the hydraulic conductivity anisotropy tensor, K^A, is assumed to be symmetric, it is possible to define at any point in the flow domain a local coordinate system for which the tensor K^A is diagonal (i.e., having zeroes everywhere except on the diagonal). The diagonal entries K_1^A, K_2^A and K_3^A of K^A are referred to as the principal components of K^A.

The SWMS_3D code permits one to vary the orientation of the local principal directions from element to element. For this purpose, the local coordinate axes are subjected to a rotation such that they coincide with the principal directions of the tensor K^A. The principal components K_1^A, K_2^A and K_3^A, together with the cosines of angles between the principal directions of the tensor K^A and the axis of the global coordinate system, are specified for each element. Locally determined principal components K_1^A, K_2^A and K_3^A **are** transformed to the global (x, y, z) coordinate system at the beginning of the simulation using the following rules:

$$K_{xx}^A = K_1^A a_{11} a_{11} + K_2^A a_{12} a_{12} + K_3^A a_{13} a_{13}$$

$$K_{yy}^A = K_1^A a_{12} a_{12} + K_2^A a_{22} a_{22} + K_3^A a_{23} a_{23}$$

$$K_{zz}^A = K_1^A a_{13} a_{13} + K_2^A a_{23} a_{23} + K_3^A a_{33} a_{33}$$

$$K_{xy}^A = K_1^A a_{11} a_{12} + K_2^A a_{12} a_{22} + K_3^A a_{13} a_{23}$$

$$K_{xz}^A = K_1^A a_{11} a_{13} + K_2^A a_{12} a_{23} + K_3^A a_{13} a_{33}$$

$$K_{yz}^A = K_1^A a_{12} a_{13} + K_2^A a_{22} a_{23} + K_3^A a_{23} a_{33}$$

(4.28)

where a_i represents cosine of angle between the ith principal direction of the tensor K^A and the j-axis of the global coordinate system.

30

4.3.13. Steady-State Analysis

All transient flow problems are solved by time marching until a prescribed time is reached. The steady-state problem can be solved in the same way, i.e., by time marching until two successive solutions differ less than some prescribed pressure head tolerance. *SWMS_3D* implements a faster way of obtaining the steady-state solution without having to go through a large number of time steps. The steady-state solution for a set of imposed boundary conditions is obtained directly during one set of iterations at the first time step by equating the time derivative term in the Richards' equation (2.1) to zero.

5. NUMERICAL SOLUTION OF THE SOLUTE TRANSPORT EQUATION

The Galerkin finite element method is also used to solve solute transport equation (3.4) subject to appropriate initial and boundary conditions. The solution procedure below largely parallels the approach used for the flow equation.

5.1. *Space Discretization*

The dependent variable, the concentration function $c(x,y,z,t)$, is approximated by a finite series $c'(x,y,z,t)$ of the form

$$c'(x,y,z,t) = \sum_{n=1}^{N} \phi_n(x,y,z) \, c_n(t) \tag{5.1}$$

where ϕ_n are the selected linear basis functions, c_n are the unknown time dependent coefficients which represent solutions of (3.4) at the finite element nodal points and, as before, N is the total number of nodal points. Application of the standard Galerkin method leads to the following set of N equations

$$\int_\Omega [-\theta R \frac{\partial c}{\partial t} - q_i \frac{\partial c}{\partial x_i} + \frac{\partial}{\partial x_i}(\theta D_{ij} \frac{\partial c}{\partial x_j}) + Fc + G]\phi_n \, d\Omega = 0 \tag{5.2}$$

Application of Green's theorem to the second derivatives in (5.2) and substitution of c by c' results in the following system of time-dependent differential equations

$$\sum_e \int_\Omega [(-\theta R \frac{\partial c'}{\partial t} - q_i \frac{\partial c'}{\partial x_i} + Fc' + G)\phi_n - \theta D_{ij} \frac{\partial c'}{\partial x_j} \frac{\partial \phi_n}{\partial x_i}] \, d\Omega$$

$$+ \sum_e \int_{\Gamma_N^e} \theta D_{ij} \frac{\partial c'}{\partial x_j} n_i \phi_n \, d\Gamma = 0 \tag{5.3}$$

or in matrix form:

$$[Q] \frac{d\{c\}}{dt} + [S]\{c\} + \{f\} = -\{Q^D\} \tag{5.4}$$

where

$$Q_{nm} = \sum_e (-\theta R)_l \int_{\Omega_e} \phi_l \phi_n \phi_m d\Omega = -\sum_e \frac{V_e}{20} (4\overline{\theta R} + \theta_n R_n)\delta_{nm} \tag{5.5}$$

$$S_{nm} = \sum_e [(-q_i)_l \int_{\Omega_e} \phi_l \phi_n \frac{\partial \phi_m}{\partial x_i} d\Omega - (\theta D_{ij})_l \int_{\Omega_e} \phi_l \frac{\partial \phi_n}{\partial x_i} \frac{\partial \phi_m}{\partial x_j} d\Omega + F_l \int_{\Omega_e} \phi_l \phi_n \phi_m d\Omega]$$

$$= \sum_e \{ -\frac{b_m}{120}(4\overline{q_x} + q_{xn}) - \frac{c_m}{120}(4\overline{q_y} + q_{yn}) - \frac{d_m}{120}(4\overline{q_z} + q_{zn}) +$$

$$+ \frac{V_e}{120}(4\overline{F} + F_n + F_m)(1 + \delta_{nm}) - \tag{5.6}$$

$$- \frac{1}{36V_e}[b_m b_n \overline{\theta D_{xx}} + c_m c_n \overline{\theta D_{yy}} + d_m d_n \overline{\theta D_{zz}} + (b_m c_n + c_m b_n)\overline{\theta D_{xy}} +$$

$$(b_m d_n + d_m b_n)\overline{\theta D_{xz}} + (c_m d_n + d_m c_n)\overline{\theta D_{yz}}]\}$$

$$f_n = \sum_e G_l \int_{\Omega_e} \phi_l \phi_n d\Omega = \sum_e \frac{V_e}{20}(4\overline{G} + G_n) \tag{5.8}$$

in which the overlined variables represent average values over a given element e. The notation in the above equations is similar as in (4.10). The boundary integral in (5.3) represents the dispersive flux, Q_n^D, across the boundary and will be discussed later in Section 5.3.4.

The derivation of equations (5.5) through (5.7) used several important assumptions in addition to those involved in the Galerkin finite element approach [Huyakorn *and Pinder, 1983; van Genuchten,* 1978]. First, the different coefficients under the integral signs ($\theta R, q_i, \theta D_{ij}, F$, **G**) were expanded linearly over each element, similarly as for the dependent variable, i.e., in terms of their nodal values and associated basis functions. Second, mass lumping was invoked

by redefining the nodal values of the time derivative in (5.4) as weighted averages over the entire flow region:

$$\frac{dc_n}{dt} = \frac{\sum_e \int_{\Omega_e} \theta\, R\, \frac{\partial c}{\partial t}\, \phi_n\, d\Omega}{\sum_e \int_{\Omega_e} \theta\, R\, \phi_n\, d\Omega} \tag{5.8}$$

5.2. *Time Discretization*

The Galerkin method is used only for approximating the spatial derivatives while the time derivatives are discretized by means of finite differences. A first-order approximation of the time derivatives leads to the following set of algebraic equations:

$$[Q]_{j+\epsilon}\frac{\{c\}_{j+1} - \{c\}_j}{\Delta t} + \epsilon[S]_{j+1}\{c\}_{j+1} + (1-\epsilon)[S]_j\{c\}_j + \epsilon\{f\}_{j+1} + (1-\epsilon)\{f\}_j = 0 \tag{5.9}$$

where j and $j+1$ denote the previous and current time levels, respectively; Δt is the time increment, and ϵ is a time weighing factor. The incorporation of the dispersion flux, Q_n^D, into matrix $[Q]$ and vector $\{f\}$ is discussed in Section 5.3.4. The coefficient matrix $[Q]_{j+\epsilon}$ is evaluated using weighted averages of the nodal values of θ and R at current and previous time levels. Equation (5.9) can be rewritten in the form:

$$[G]\{c\}_{j+1} = \{g\} \tag{5.10}$$

where

$$[G] = \frac{1}{\Delta t}[Q]_{j+\epsilon} + \epsilon[S]_{j+1}$$

$$\tag{5.11}$$

$$\{g\} = \frac{1}{\Delta t}[Q]_{j+\epsilon}\{c\}_j - (1-\epsilon)[S]_j\{c\}_j - \epsilon\{f\}_{j+1} - (1-\epsilon)\{f\}_j$$

Higher-order approximations for the time derivative in the transport equation were derived

by *van* Genuchten [1976, 1978]. The higher-order effects may be incorporated into the transport equation by introducing appropriate dispersion corrections as follows

$$D_{ij}^- = D_{ij} \cdot \frac{q_i q_j \Delta t}{6 \theta^2 R}$$

$$D_{ij}^+ = D_{ij} + \frac{q_i q_j \Delta t}{6 \theta^2 R}$$

(5.12)

where the superscripts + and - indicate evaluation at the old and new time levels, respectively.

5.3. Numerical Solution Strategies

5.3.1. *Solution Process*

The solution process at each time step proceeds as follows. First, an iterative procedure is used to obtain the solution of the Richards' equation (2.1) (see Section 4.3.1). After achieving convergence, the solution of the transport equation (5.10) is implemented. This is done by first determining the nodal values of the fluid flux from nodal values of the pressure head by applying Darcy's law. Nodal values of the water content and the fluid flux at the previous time level are already known from the solution at the previous time step. Values for the water content and the fluid flux are subsequently used as input to the transport equation, leading to the system of linear algebraic equations given by (5.10). The structure of the final set of equations depends upon the value of the temporal weighing factor, ϵ. The explicit ($\epsilon=0$) and fully implicit ($\epsilon=1$) schemes require that the global matrix [G] and the vector {g} be evaluated at only one time level (the previous or current time level). All other schemes require evaluation at both time levels. Also, all schemes except for the explicit formulation ($\epsilon=0$) lead to an asymmetric banded matrix [G]. The associated set of algebraic equations is solved using either a standard asymmetric matrix equation solver [e.g., *Neuman,* 1972], or the ORTHOMIN method *[Mendoza et al.,* 1991], depending upon the size of final matrix. By contrast, the explicit scheme leads to a diagonal matrix [G] which is much easier to solve (but generally requires smaller time steps). Since transport is assumed to be independent of changes in the fluid density, one may proceed directly

36

to the next time level once the transport equation is solved for the current time level.

5.3.2. *Upstream Weighted Formulation*

Upstream weighing is provided as an option in SWMS_3D to minimize some of the problems with numerical oscillations when relatively steep concentration fronts are being simulated. For this purpose the second (flux) term of equation (5.3) is not weighted by regular linear basis functions ϕ_n, but instead using the nonlinear functions ϕ_n^u

$$\phi_1^u = L_1 - 3\alpha_{12}^w L_2 L_1 + 3\alpha_{14}^w L_4 L_1 + 3\alpha_{13}^w L_1 L_3$$

$$\phi_2^u = L_2 - 3\alpha_{23}^w L_3 L_2 + 3\alpha_{12}^w L_1 L_2 + 3\alpha_{24}^w L_2 L_4$$

$$\phi_3^u = L_3 - 3\alpha_{34}^w L_4 L_3 + 3\alpha_{23}^w L_2 L_3 - 3\alpha_{13}^w L_1 L_3 \qquad (5.13)$$

$$\phi_4^u = L_4 - 3\alpha_{14}^w L_4 L_1 + 3\alpha_{34}^w L_3 L_4 - 3\alpha_{24}^w L_2 L_4$$

where α_{ij}^w is a weighing factor associated with the line connecting nodes i and j (Figure 5. 1), and L_i *are* the local coordinates. The weighing factors are evaluated using the equation of *Christie et al. [1976]:*
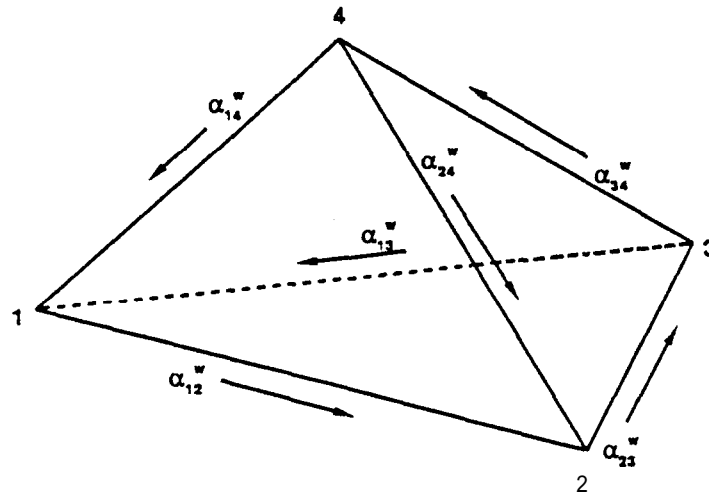
Fig. 5.1. Direction definition for the upstream weighting factors α_{ij}^w.

$$\alpha_i^w = \coth(\frac{uL}{2D}) - \frac{2D}{uL} \tag{5.14}$$

where u, D and L are the flow velocity, dispersion coefficient and length associated with side i. The weighing functions ϕ^u ensure that relatively more weight is placed on the flow velocities of nodes located at the upstream side of an element. Evaluating the integrals in (5.3) shows that the following additional terms must be added to the entries of global matrix S_{nm} in equation (5.6):

$$S_{1j}^{e'} = S_{1j}^{e} - \frac{b_j}{240} [q_{x1} (-2\alpha_{12}^w + 2\alpha_{14}^w + 2\alpha_{13}^w) + q_{x2} (-2\alpha_{12}^w + \alpha_{14}^w + \alpha_{13}^w) + $$

$$q_{x3} (-\alpha_{12}^w + \alpha_{14}^w + 2\alpha_{13}^w) + q_{x4} (-\alpha_{12}^w + 2\alpha_{14}^w + \alpha_{13}^w)] \tag{5.15}$$

$$- \frac{c_j}{240} [-q_{y1} (\ldots\ldots\ldots) + \ldots] - \frac{d_j}{240} [-q_{z1} (\ldots\ldots\ldots) + \ldots]$$

$$S_{2j}^{e'} = S_{2j}^{e} - \frac{b_j}{240} [q_{x1} (-\alpha_{23}^w + 2\alpha_{12}^w + \alpha_{24}^w) + q_{x2} (-2\alpha_{23}^w + 2\alpha_{12}^w + 2\alpha_{24}^w) + $$

$$q_{x3} (-2\alpha_{23}^w + \alpha_{12}^w + \alpha_{24}^w) + q_{x4} (-\alpha_{23}^w + \alpha_{12}^w + 2\alpha_{24}^w)] \tag{5.16}$$

$$- \frac{c_j}{240} [-q_{y1} (\ldots\ldots\ldots) + \ldots] - \frac{d_j}{240} [-q_{z1} (\ldots\ldots\ldots) + \ldots]$$

$$S_{3j}^{e'} = S_{3j}^{e} - \frac{b_j}{240} [q_{x1} (-\alpha_{34}^w + \alpha_{23}^w - 2\alpha_{13}^w) + q_{x2} (-\alpha_{34}^w + 2\alpha_{23}^w - \alpha_{13}^w) + $$

$$q_{x3} (-2\alpha_{34}^w + 2\alpha_{23}^w - 2\alpha_{13}^w) + q_{x4} (-2\alpha_{34}^w + \alpha_{23}^w - \alpha_{13}^w)] \tag{5.17}$$

$$- \frac{c_j}{240} [-q_{y1} (\ldots\ldots\ldots) + \ldots] - \frac{d_j}{240} [-q_{z1} (\ldots\ldots\ldots) + \ldots]$$

and

$$S_{4j}^{e'} = S_{4j}^{e} - \frac{b_j}{240} [q_{x1}(-2\alpha_{14}^{w} + \alpha_{34}^{w} - \alpha_{24}^{w}) + q_{x2}(-\alpha_{14}^{w} + \alpha_{34}^{w} - 2\alpha_{24}^{w}) +$$

$$q_{x3}(-\alpha_{14}^{w} + 2\alpha_{34}^{w} - \alpha_{24}^{w}) + q_{x4}(-2\alpha_{14}^{w} + 2\alpha_{34}^{w} - 2\alpha_{24}^{w})] \qquad (5.18)$$

$$-\frac{c_j}{240} [-q_{y1}(............) + ...] - \frac{d_j}{240} [-q_{z1}(............) + ...]$$

5.3.3. Implementation of First-Type Boundary Conditions

Individual equations in the global matrix equation which correspond to nodes at which the concentration is prescribed are replaced by new equations:

$$\delta_{nm} c_m = c_{n0} \qquad (5.19)$$

where c_{n0} is the prescribed value of the concentration at node n. This is done only when Gaussian elimination is used to solve the matrix equation. A similar procedure as for water flow (described in Section 4.3.4) is applied when the ORTHOMIN method is used. Because of asymmetry of the global matrix [G], no additional manipulations are needed in the resulting system of equations as was the case for the water flow solution.

The total material flux, Q_n^T, through a boundary at node n consists of the dispersive flux, Q_n^D, and the convective flux, Q_n^A:

$$Q_n^T = Q_n^D + Q_n^A \qquad (5.20)$$

The dispersive boundary nodal flux is not known explicitly but must be calculated from equation (5.4). Hence, the dispersion flux, Q_n^D, for node n *can* be calculated as

$$Q_n^D = -[\epsilon S_{nm}^{j+1} + (1-\epsilon)S_{nm}^{j}]c_m^j - \epsilon f_n^{j+1} - (1-\epsilon)f_n^j - Q_{nn}^{j+\epsilon} \frac{c_n^{j+1} - c_n^j}{\Delta t} \qquad (5.21)$$

The convective flux is evaluated as

39

$$Q_n^A = Q_n c_n \tag{5.22}$$

where the fluid flux Q_n is known from the solution of the water flow equation.

5.3.4. *Implementation of Third-Type Boundary Conditions*

Equation (3.9) is rewritten as follows

$$\theta D_{ij} \frac{\partial c'}{\partial x_j} n_i = q_i n_i (c - c_0) \tag{5.23}$$

When substituted into the last term of (5.3), the boundary integral becomes

$$\sum_e \int_{\Gamma_N^e} \theta D_{ij} \frac{\partial c'}{\partial x_j} n_i \phi_n d\Gamma = Q_n c_n - Q_n c_{n0} \tag{5.24}$$

The first term on the right-hand side of (5.24) represents the convective flux. This term is incorporated into the coefficient matrix [S] of (5.4). The last term of (5.24) represents the total material flux, which is added to the known vector $\{f\}$.

At nodes where free outflow of water and its dissolved solutes takes place, the exit concentration c_0 is equal to the local (nodal) concentration c,. In this case the dispersive flux becomes zero and the total material flux through the boundary is evaluated as

$$Q_n^T = Q_n c_n \tag{5.25}$$

5.3.5. *Mass Balance Calculations*

The total amount of mass in the entire flow domain, or in a preselected subregion, is given by

$$M = \sum_e \int_{\Omega_e} \theta R c \, d\Omega = \sum_e V_e \frac{\theta_i R_i c_i + \theta_j R_j c_j + \theta_k R_k c_k + \theta_l R_l c_l}{4} \tag{5.26}$$

where $\theta_{i,j,k,l}$, $R_{i,j,k,l}$ and $c_{i,j,k,l}$ represent, respectively, water contents, retardation factors, and concentrations evaluated at the comer nodes of element e. The summation is taken over all elements within the specified region.

The cumulative amounts M^0 and M^1 of solute removed from the flow region by zero- and first-order reactions, respectively, are calculated as follows

$$M^0 = \int_0^t \sum_e \int_{\Omega_e} (\gamma_w \theta + \gamma_s \rho) \, d\Omega \, dt \qquad (5.27)$$

$$M^1 = \int_0^t \sum_e \int_{\Omega_e} (\mu_w \theta + \mu_s \rho k) c \, d\Omega \, dt \qquad (5.28)$$

whereas the cumulative amount M_r of solute taken up by plant roots is given by

$$M_r = \int_0^t \sum_{e_R} \int_{\Omega_e} S c_s \, d\Omega \, dt \qquad (5.29)$$

where e_R represents the elements making up the root zone.

Finally, when all boundary material fluxes, decay reactions, and root uptake mass fluxes have been computed, the following mass balance should hold, at least theoretically, for the flow domain as a whole:

$$M_t - M_0 = \int_0^t \sum_{n_\Gamma} Q_n^T \, dt + M^0 + M^1 - M_r \qquad (5.30)$$

where M, and M_0 are the amounts of solute in the flow region at times t and zero, respectively, as calculated with (5.26), and n_Γ represents nodes located along the boundary of the flow domain or at internal sinks and/or sources. However, since numerical solutions are always approximate, (5.30) will generally not be exact. The difference between the left- and right-hand sides of (5.30) represents the absolute error, ϵ_a^c, in the solute mass balance. Similarly as for water flow, the accuracy of the numerical solution for solute transport is evaluated by using the relative error,

41

ϵ_r^c [%], in the solute mass balance as follows

$$\epsilon_r^c = \frac{100\,|\,\epsilon_a^c\,|}{\max\left[\sum_e |M_t^e - M_0^e|,\ |M^0| + |M^1| + |M_r| + \int_0^t \sum_{n_\tau} |\,Q_n^T\,|\,dt\right]} \qquad (5.3\ 1)$$

where M_0^e and M_t^e are the amounts of solute in element e at times 0 and t, respectively. Note again that SWMS_3D does not relate the absolute error to the total amount of mass in the flow region. Instead, the program uses as a reference the maximum value of (1) the absolute change in element concentrations as summed over all elements, and (2) the sum of the absolute values of all cumulative solute fluxes across the flow boundaries including those resulting from sources and sinks in the flow domain.

5.3.6. *Prevention of Numerical Oscillations*

Numerical solutions of the transport equation often exhibit non-physical oscillatory behavior and/or excessive numerical dispersion near relatively sharp concentration fronts. These problems can be especially serious for convection-dominated transport characterized by small dispersivities. One way to partially circumvent numerical oscillations is to use upstream weighing as discussed in Section 5.3.2. Undesired oscillations can often be prevented also by selecting an appropriate combination of space and time discretizations. Two dimensionless numbers may be used to characterize the space and time discretizations. One of these is the grid Peclet number, Pe_i^e, which defines the predominant type of the solute transport (notably the ratio of the convective and dispersive transport terms) in relation to coarseness of the finite element grid:

$$Pe_i^e = \frac{q_i \Delta x_i}{\theta D_{ii}} \qquad (5.32)$$

where Δx, is the characteristic length of a finite element. The Peclet number increases when the convective part of the transport equation dominates the dispersive part, i.e., when a relatively steep concentration front is present. To achieve acceptable numerical results, the spatial discretization must be kept relatively fine to maintain a low Peclet number. Numerical oscillation

can be virtually eliminated when the local Peclet numbers do not exceed about 5. However, acceptably small oscillations may be obtained with local Peclet numbers as high as 10 *[Huyakorn and Pinder,* 1983].

A second dimensionless number which characterizes the relative extent of numerical oscillations is the Courant number, Cr_i^e. The Courant number is associated with the time discretization as follows

$$Cr_i^e = \frac{q_i \Delta t}{\theta R \Delta x_i} \tag{5.33}$$

Three stabilizing options are used in SWMS_3D to avoid oscillations in the numerical solution of the solute transport equation [*Šimůnek and Suarez,* 1993]. One option is upstream weighing (see Section 5.3.2), which effectively eliminates undesired oscillations at relatively high Peclet numbers. A second option for minimizing or eliminating numerical oscillations uses the following criterion developed by *Perrochet and Berod* [1993]

$$Pe \cdot Cr \leq \omega_s = 2 \tag{5.34}$$

where ω_s is the performance index [-]. This criterion indicates that convection-dominated transport problems having large *Pe* numbers can be safely simulated provided *Cr* is reduced according to (5.34) *[Perrochet and Berod,* 1993]. When small oscillations in the solution can be tolerated, ω_s can be increased to about 5 or 10.

A third stabilizing option implemented in SWMS_3D also utilizes criterion (5.33). However, instead of decreasing *Cr* to satisfy equation (5.33), this option introduces artificial dispersion to decrease the Peclet number. The amount of additional longitudinal dispersivity, $\overline{D}_L$ [L], is given by *[Perrochet and Berod,* 1993]

$$\overline{D}_L = \frac{|q| \Delta t}{\theta R \omega_s} - D_L - \frac{\theta D_d \tau}{|q|} \tag{5.35}$$

The maximum permitted time step is calculated using all three options, as well as the additional requirement that the Courant number must remain less than or equal to 1. The time step

calculated in this way is subsequently used as one of the time discretization rules (rule No. B) discussed in section 4.3.3.

6. PROBLEM DEFINITION

6.1. *Construction of Finite Element Mesh*

The finite element mesh is constructed by dividing the flow region into tetrahedral, hexahedral and/or triangular prismatic elements (Fig. 6.1) whose shapes are defined by the coordinates of the nodes that form the element comers. The program automatically subdivides hexahedrals and triangular prisms into tetrahedrals which are then treated as subelements (Fig. 6.1). Two different ways are possible in SWMS_3D to subdivide the hexahedrals into tetrahedrals, whereas six different possibilities exist for subdividing the triangular prisms into tetrahedrals (see Fig. 6.1). Since it is important to keep the proper orientation of comer nodes for each subelement, it is necessary to pay close attention on how the comer nodes of an element are written into the input file.

If two neighboring hexahedral elements are subdivided in the same way (e.g., options 2a or 2b in Figure 6.1), the newly formed edges on a common surface will cross each other, a feature which is not allowed. Two neighboring hexahedral elements should therefore always use both options 2a and 2b as shown in Figure 6.1, so that the newly formed edges on the common surface will coincide. Therefore, it is necessary to give not only the comer nodes which define an element, but also the code which specifies how a particular element is to be subdivided into subelements. It is necessary to always realize how the neighboring elements are going to be subdivided, and to input also the proper code specifying the subdivision. Having high flexibility in terms of possible subdivisions into subelements is important, especially for unstructured finite element meshes using triangular prisms. In order to overcome some of the problems related correct definition of the comer nodes and the subdivision codes in the input file, we have provided a separate finite element generator which may be used to generate the nodes and elements for a hexahedral domain.

The finite element dimensions always must be adjusted to a particular problem. They should be made relatively small in directions where large hydraulic gradients are expected. Regions with sharp gradients are usually located in the vicinity of the internal sources or sinks, or close to the soil surface where highly variable meteorological factors can cause fast changes

1

4

3

1

2

Element: 1, 2, 3, 4

2a

3

4

1

2

7

8

5

6
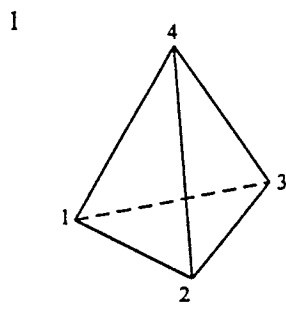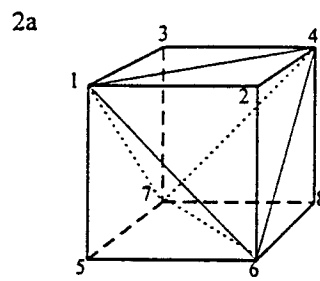
Element: 1, 2, 3, 4, 5, 6, 7, 8
Subdivision Code: 1
Subelements: 1, 4, 7, 3
1, 6, 4, 2
5, 6, 7, 1
7, 6, 8, 4
1, 6, 7, 4

2b

3

4

1

2

7

8

5

6
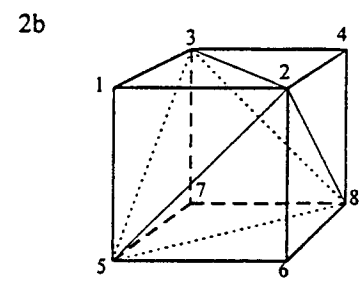
Element: 1, 2, 3, 4, 5, 6, 7, 8
Subdivision Code: 2
Subelements: 5, 2, 3, 1
5, 6, 8, 2
5, 8, 7, 3
5, 2, 8, 3
2, 8, 3, 4

3a

3

2

1

6

5

4
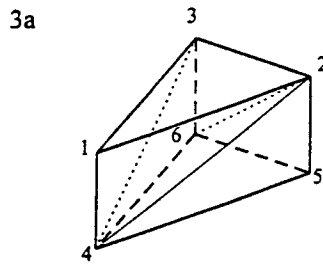
Element: 1, 2, 3, 4, 5, 6
Subdivision Code: 1
Subelements: 4, 2, 3, 1
4, 5, 6, 2
4, 5, 6, 2

3b

3

2

1

6

5

4
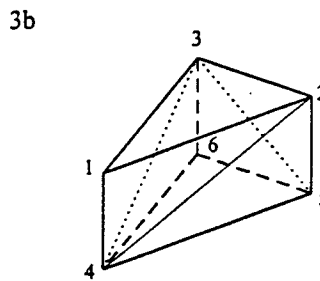
Element: 1, 2, 3, 4, 5, 6
Subdivision Code: 2
Subelements: 4, 2, 3, 1
4, 5, 3, 2
4, 5, 6, 3

3c

3

2

1

6

5

4
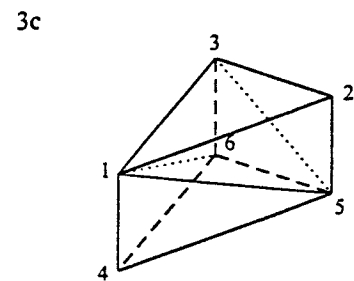
Element: 1, 2, 3, 4, 5, 6
Subdivision Code: 3
Subelements: 4, 5, 6, 1
1, 5, 6, 3
1, 5, 3, 2

3d

3

2

1

6

5

4
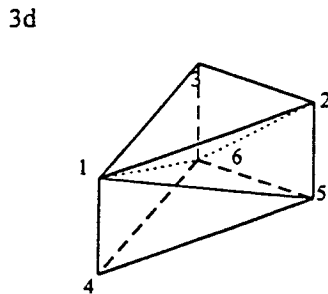
Element: 1, 2, 3, 4, 5, 6
Subdivision Code: 4
Subelements: 4, 5, 6, 1
1, 5, 6, 2
1, 2, 6, 3

3e

3

2

1

6

5

4
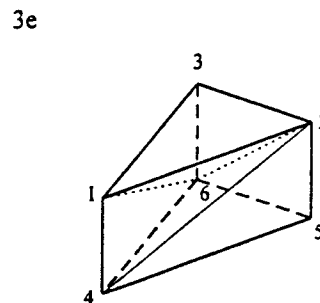
Element: 1, 2, 3, 4, 5, 6
Subbdivision Code: 5
Subelements: 4, 1, 6, 2
4, 2, 6, 1
1, 2, 6, 3

3f

3

2

1

6

5

4
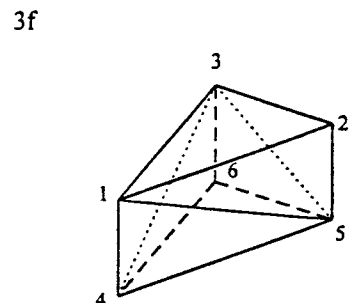
Element: 1, 2, 3, 4, 5, 6
Subdivision Code: 6
Subelements: 4, 5, 6, 3
1, 5, 3, 2
1, 4, 3, 5

Fig. 6.1. Finite elements and subelements used to discretize the 3-D domain: 1) tetrahedral, 2) hexahedral, 3) triangular prism.

in pressure head. Hence, we recommend to normally use relatively small elements at and near the soil surface. The size of elements can gradually increase with depth to reflect the generally much slower changes in pressure heads at deeper depths. The element dimensions should also depend upon the soil hydraulic properties. For example, coarse-textured soils having relatively high n-values and small a-values (see Eqs. (2.11) and (2.18)) generally require a finer discretization than fine-textured soils. We also recommend using elements having approximately equal sizes to decrease numerical errors. No special restrictions are necessary to facilitate the soil root zone.

6.2. *Coding of Soil Types and Subregions*

Soil Types - An integer code beginning with 1 and ending with *NMat (the* total number of soil materials) is assigned to each soil type in the flow region. The appropriate material code is subsequently assigned to each nodal point *n* of the finite element mesh.

Interior material interfaces do not coincide with element boundaries. When different material numbers are assigned to the comer nodes of a certain element, material properties of this element will be averaged automatically by the finite element algorithm. This procedure will somewhat smooth soil interfaces.

A set of soil hydraulic parameters and solute transport characteristics must be specified for each soil material. Also, the user must define for each element the principal components of the conductivity anisotropy tensor, as well as the angle between the local and global coordinate systems.

As explained in Section 2.3, one additional way of changing the unsaturated soil hydraulic properties in the flow domain is to introduce scaling factors associated with the water content, the pressure head and the hydraulic conductivity. The scaling factors are assigned to each nodal point *n* in the flow region.

Subregions - Water and solute mass balances are computed separately for each specified subregion. The subregions may or may not coincide with the material regions. Subregions are

characterized by an integer code which runs from 1 *to NLay (the* total number of subregions). A subregion code is assigned to each element in the flow domain.

6.3. *Coding of Boundary Conditions*

Flow boundary conditions were programmed in a fairly similar way as done in the UNSATl and UNSAT2 models of Neuman [1972] and *Neuman et al. [1974].* A boundary code, *Kode(n),* must be assigned to each node, *n.* If node n is to have a prescribed pressure head during a time step (Dirichlet boundary condition), *Kode(n)* must be set positive during that time step. If the volumetric flux of water entering or leaving the system at node n is prescribed during a time step (Neumann boundary condition), *Kode(n)* must be negative or zero.

Constant Boundary Conditions · The values of constant boundary conditions for a particular node, *n, are* given by the initial values of the pressure head, *h(n),* in case of Dirichlet boundary conditions, or by the initial values of the recharge/discharge flux, *Q(n),* in case of *Neumann* boundary conditions. Table 6.1 summarizes the use of the variables *Kode(n), Q(n)* and *h(n)* for various types of nodes.

Table 6.1. Initial settings of Kode(n), Q(n), and h(n) for constant boundary conditions.

Node Type	*Kode(n)*	*Q(n)*	*h(n)*
Internal; not sink/source	0	0.0	Initial Value
Internal; sink/source (Dirichlet condition)	1	0.0	Prescribed
Internal; sink/source (Neumann condition)	-1	Prescribed	Initial Value
Impermeable Boundary	0	0.0	Initial Value
Specified Head Boundary	1'	0.0	Prescribed
Specified Flux Boundary	-1[‡]	Prescribed	Initial Value

[†] 6 may also be used
[‡] -6 may also be used

48

Variable Boundary Conditions - Three types of variable boundary conditions can be imposed:

    1. Atmospheric boundary conditions for which $Kode(n)=\pm4,$

    2. Variable pressure head boundary conditions for which $Kode(n) = +3$, and

    3. Variable flux boundary conditions for which $Kode(n) = -3$.

These conditions can be specified along any part of the boundary. It is not possible to specify more than one time-dependent boundary condition for each type. Initial settings of the variables $Kode(n)$, $Q(n)$ and $h(n)$ for the time-dependent boundary conditions are given in Table 6.2.

Table *6.2.* Initial settings of Kode(n), $Q(n)$, and h(n) for variable boundary conditions.

Node Type	Kode(*n*)	Q(n)	h(n)
Atmospheric Boundary	- 4	0.0	Initial Value
Variable Head Boundary	+3	0.0	Initial Value
Variable Flux Boundary	- 3	0.0	Initial Value

Atmospheric boundary conditions are implemented when $Kode(n)=\pm4,$ in which case time-dependent input data for the precipitation, *Prec,* and evaporation, *rSoil,* rates must be specified in the input file ATMOSPH.IN. The potential fluid flux across the soil surface is determined by *rAtm= rSoil-Prec.* The actual surface flux is calculated internally by the program. Two limiting values of the surface pressure head must be provided: *hCritS* which specifies the maximum allowed pressure head at the soil surface (usually O.O), and *hCritA* which specifies the minimum allowed surface pressure head (defined from equilibrium conditions between soil water and atmospheric vapor). The program automatically switches the value of Kode(n) from -4 to +4 if one of these two limiting points is reached. Table 6.3 summarizes the use of the variables *rAtrn, hCritS* and *hCritA* during program execution. Width(n) in this table denotes the surface area of the boundary segment associated with node n.

Table 6.3. Definition of the variables Kode(n), Q(n) and h(n)
when an atmospheric boundary condition is applied.

Kode(n)	Q(n)	h(n)	Event
-4	-Width(n)*rAtm	Unknown	rAtm=rSoil-Prec
+4	Unknown	hCritA	Evaporation capacity is exceeded
+4	Unknown	hCritS	Infiltration capacity is exceeded

Variable head and flux boundary conditions along a certain part of the boundary are implemented when Kode(n)=+3 and -3, respectively. In that case, the input file ATMOSPH.IN must contain the prescribed time-dependent values of the pressure head, *ht*, or the flux, rt, imposed along the boundary. The values of *ht* or *rt are* assigned to particular nodes at specified times according to rules given in Table 6.4.

Table 6.4. Definition of the variables Kode(n), Q(n) and h(n)
when variable head or flux boundary conditions are applied.

Node Type	Kode(n)	Q(n)	h(n)
Variable Head Boundary	+3	Unknown	ht
Variable Flux Boundary	-3	-Width(n)*rt	Unknown

Water Uptake by Plant Roots - The program calculates the rate at which plants extract water from the soil root zone by evaluating the term D (equation (4.9)) in the finite element formulation. The code requires that *Kode(n)* be set equal to 0 or negative for all nodes in the root zone. Values of the potential transpiration rate, *rRoot,* must be specified at preselected times in the input file ATMOSPH.IN. Actual transpiration rates are calculated internally by the program as discussed in Section 2.2. The root uptake parameters are taken from input file

SELECTOR.IN. Values of the function Beta(n), which describes the potential water uptake distribution over the root zone (equation (2.5)), must be specified for each node in the flow domain (see the description of input Block H in Table 8.8 of Section 8). All parts of the flow region where Beta(n)>0 are treated as the soil root zone.

Deep Drainage from the Soil Profile - Vertical drainage, *q(h),* across the lower boundary of the soil profile is sometimes approximated by a flux which depends on the position of groundwater level (e.g., ***Hopmans and Stricker,*** 1989). If available, such a relationship can be implemented in the form of a variable flux boundary condition for which ***Kode(n)= -3.*** This boundary condition is implemented in SWMS_3D by setting the logical variable ***qGWLF*** in the input file ATMOSPH.IN equal to "true." The discharge rate ***Q(n)*** assigned to node n is determined in the program as Q(n)=- Width(n)*q(h) where ***h*** is the local value of the pressure head, and ***q(h)*** is given by

$$q(h) = -A_{qh}\exp(B_{qh}|h-GWL0L|) \tag{6.1}$$

where ***A,*** and B_{qh} ***are*** empirical parameters which must be specified in the input file ATMOSPH.IN, together with ***GWL0L*** which represents the reference position of the groundwater level (usually set equal to the z-coordinate of the soil surface).

Free Drainage - Unit vertical hydraulic gradient boundary conditions can be implemented in the form of a variable flux boundary condition for which ***Kode(n)= -3.*** This boundary condition is implemented in SWMS_3D by setting the logical variable ***FreeD*** in the input file SELECTOR.IN equal to "true.". The program determines the discharge rate ***Q(n)*** assigned to node ***n as Q(n)= -Width(n)*K(h),*** where ***h*** is the local value of the pressure head, and ***K(h)*** is the hydraulic conductivity corresponding to this pressure head.

Seepage Faces - The initial settings of the variables ***Kode(n), Q(n)*** and ***h(n)*** for nodes along a seepage face are summarized in Table 6.5. All potential seepage faces must be identified before starting the numerical simulation. This is done by providing a list of nodes along each

potential seepage face (see input Block E as defined in Table 8.5 of Section 8).

Table 6.5. Initial setting of Kode(n), Q(n), and h(n) for seepage faces.

Node Type	$Kode(n)$	$Q(n)$	$h(n)$
Seepage Face (initially saturated)	$+2$	0.0	0.0
Seepage Face (initially unsaturated)	-2	0.0	Initial Value

Drains - Table 6.6 summarizes the initial settings of the variables $Kode(n)$, $Q(n)$ and $h(n)$ for nodes representing drains. All drains must be identified before starting the numerical simulation. This is done by providing a list of nodes representing drains, together with a list of elements around each drain whose hydraulic conductivities are to be adjusted according to discussion in Section 4.3.7 (see also input Block F as defined in Table 8.6 of Section 8).

Table 6.6. Initial setting of Kode(n), Q(n), and h(n) for drains.

Node Type	$Kode(n)$	$Q(n)$	$h(n)$
Drain (initially saturated)	$+5$	0.0	0.0
Drain (initially unsaturated)	-5	0.0	Initial Value

Solute Transport Boundary Conditions. The type of boundary condition to be invoked for solute transport is specified by the input variable *KodCB*. A positive sign of this variable means that a first-type boundary condition will be used. When *KodCB* is negative, SWMS_3D selects a third-type boundary condition when the calculated water flux is directed into the region, or a second-type boundary condition when the water flux is zero or directed out of the region.

52

One exception to these rules occurs for atmospheric boundary conditions when $Kode(n)=\pm 4$ and $Q(n)<0$. SWMS_3D assumes that solutes cannot leave the flow region across atmospheric boundaries. The solute flux in this situation becomes zero, i.e., $c_0=0$ in equation (5.23). Cauchy and Neumann boundary conditions are automatically applied to internal sinks/sources depending upon the direction of water flow. The dependence (or independence) of the solute boundary conditions on time or the system is then still defined through the variable Kode(n) as discussed above.

Although SWMS_3D can implement frost-type boundary conditions, we recommend users to invoke third-type conditions where possible. This is because third-type conditions, in general, are physically more realistic and preserve solute mass in the simulated system (e.g., *van Genuchten and Parker* [*1984]; Leij et al. [1991]).*

For the user's convenience, Table 6.7 summarizes possible values of the different boundary codes and their association with specific water flow and solute transport boundary conditions.

6.4. Program Memory Requirements

One single parameter statement is used at the beginning of the code to define the problem dimensions. All major arrays in the program are adjusted automatically according to these dimensions. This feature makes it possible to change the dimensions of the problem to be simulated without having to recompile all program subroutines. Different problems can be investigated by changing the dimensions in the parameter statement at the beginning of the main program, and subsequently linking all previously compiled subroutines with the main program when creating an executable file. Table 6.8 lists the array dimensions which must be defined in the parameter statement.

Table 6.7. Summary of Boundary Coding.

	Boundary Type	Water Flow		Solute Transport	
		Kode	Input	KodCB	Input
Time-independent	Impermeable	0	initial h(n), Q(n)=0	NA	NA
	Constant head	1	prescribed h(n), Q(n)=0	≠0	cBound(*i*)
	Constant flux	-1	initial h(n), prescribed Q(n)	≠0 (inflow)	cBound(i)
	Source/sink (Dirichlet)	1	prescribed h(n), Q(n)=0	≠0 (Source)	*cBound*(11)
	Source/sink (Neumann)	-1	initial $h(n)$, prescribed $Q(n)$	≠0 (Source)	*cBound*(11)
	Seepage Face (saturated)	2	$h(n)$=0, $Q(n)$=0	0	-
	Seepage Face (unsaturated)	-2	initial $h(n)$, $Q(n)$=0	0	-
	Free drainage	-3	initial $h(n)$, $Q(n)$=0	0	-
	Drains (saturated)	5	$h(n)$=0, $Q(n)$=0	0	-
	Drains (unsaturated)	-5	initial h(n), Q(n)=0	0	-
Time-dependent	Changing head	3	$h(t)$, initial $h(n)$, $Q(n)$=0	≠0	$c_h(t)$
	Changing flux	-3	$q(t)$, initial $h(n)$, $Q(n)$=0	≠0 (inflow)	$c_r(t)$
	Atmospheric boundary	-4	**Prec, rSoil,** h_A, h_S, initial **h(n)**, Q(n)=0	**0**	**cPrec(t)**
	Root zone	0	**rRoot,** initial **h(n), Q(n)=0**	NA	cBound(12)
	Deep drainage	-3	**Aqh, Bqh, GWLOL,** initial h(n), Q(n)=0	0	-

i = 1, *2, ...)* 10

Table 6.8. List of array dimensions in SWMS_3D.

Dimension	Description
NumNPD	Maximum number of nodes in finite element mesh
NumElD	Maximum number of elements in finite element mesh
MBandD	Maximum dimension of the bandwidth of matrix A when Gaussian elimination is used. Maximum number of nodes adjacent to a particular node, including itself, when iterative matrix solvers are used.
NumBPD	Maximum number of boundary nodes for which $Kode(n) \neq 0$
NSeepD	Maximum number of seepage faces
NumSPD	Maximum number of nodes along a seepage face
NDrD	Maximum number of drains
NElDrD	Maximum number of elements surrounding a drain
NMatD	Maximum number of materials
NTabD	Maximum number of items in the table of hydraulic properties generated by the program for each soil material
NumKD	Maximum number of available code number values (equals 6 in present version)
NObsD	Maximum number of observation nodes for which values of the pressure head, the water content, and concentration are printed at each time level
MNorth	Maximum number of orthogonalizations performed when iterative solvers are used

6.5. Matrix Equation Solvers

Discretization of the governing partial differential equations for water flow (2.1) and solute transport (3.4) leads to the system of linear equations

$$[A]\{x\} = \{b\} \tag{6.2}$$

in which matrix [A] is symmetric for water flow and asymmetric for solute transport.

The original version of SWMS_2D [*Šimůnek et al.,* 1992] used Gaussian elimination to solve both systems of linear algebraic equations. The invoked solvers took advantage of the

banded nature of the coefficient matrices and, in the case of water flow, of the symmetric properties of the matrix. Such direct solution methods have several disadvantages as compared to iterative methods. Direct methods require a fixed number of operations (depending upon the size of the matrix) which increases approximately by the square of the number of nodes [Mendoza et. **al.,** 1991]. Iterative methods, on the other hand, require a variable number of repeated steps which increase at a much smaller rate (about 1.5) with the size of a problem **[Mendoza et al.,** 1991]. A similar reduction also holds for the memory requirement since iterative methods do not require the storage of non-zero matrix elements. Memory requirements, therefore, increase at a much smaller rate with the size of the problem when iterative solvers are used **[Mendoza et al.,** 1991]. Round-off errors also represent less of a problem for iterative methods as compared to direct methods. This is because round-off errors in iterative methods are self-correcting [Letniowski, 1989]. Finally, for time-dependent problems, a reasonable approximation of the solution (i.e., the solution at the previous time step) exists for iterative methods, but not for direct methods [Letniowski, 1989]. In general, direct methods are more appropriate for relatively small problems, while iterative methods are more suitable for larger problems.

Many iterative methods have been used in the past for handling large sparse matrix equations. These methods include Jacobi, Gauss-Seidel, alternating direction implicit (ADI), block successive over-relaxation (BSSOR), successive line over-relaxation (SLOR), and strongly implicit procedures (SIP), among others [Letniowski, 1989]. More powerful preconditioned accelerated iterative methods, such as the preconditioned conjugate gradient method (PCG) [Behie **and Vinsome,** 1982], were introduced more recently. **Sudicky and Huyakorn** [1991] gave three advantages of the PCG procedure as compared to other iterative methods: PCG can be readily applied to finite element methods with irregular grids, the method does not require iterative parameters, and PCG usually outperforms its iterative counterparts for situations involving relatively stiff matrix conditions.

The current version 1.0 of SWMS_3D implements both direct and iterative methods for solving the system of linear algebraic equations given by (6.2). Depending upon the size of matrix [A], we use either direct Gaussian elimination or the preconditioned conjugate gradient

method [Mendoza et al., 1991) for water flow and the ORTHOMIN (preconditioned conjugate gradient squared) procedure [Mendoza et *al.,* 1991] for solute transport. Gaussian elimination is used if either the bandwidth of matrix [A] is smaller than 20, or the total number of nodes is smaller than 500. The iterative methods used in SWMS_3D were adopted from the ORTHOFEM software package of *Mendoza et al. [* 1991].

The preconditioned conjugate gradient and ORTHOMIN methods consist of two essential parts: initial preconditioning, and iterative solution with either conjugate gradient or ORTHOMIN acceleration *[Mendoza et al.,* 1991]. Incomplete lower-upper (ILU) preconditioning is used in ORTHOFEM when matrix [A] is factorized into lower and upper triangular matrices by partial Gaussian elimination. The preconditioned matrix is subsequently repeatedly inverted using updated solution estimates to provide a new approximation of the solution. The orthogonalization-minimization acceleration technique is used to update the solution estimate. This technique insures that the search direction for each new solution is orthogonal to the previous approximate solution, and that either the norm of the residuals (for conjugate gradient acceleration *[Meijerink and van der Vorst, 1981])* or the sum of squares of the residuals (for ORTHOMIN [Behie *and Vinsome, 1982])* is minimized. More details about the two methods is given in the user's guide of ORTHOFEM *[Mendoza et al.,* 1991] or in *Letniowski [* 1989]. *Letniowski [1989] also* gives a comprehensive review of accelerated iterative methods, as well as of different preconditioning techniques.

7. EXAMPLE PROBLEMS

Four example problems are presented in this section. Examples 1 and 2 provide comparisons of the water flow part of SWMS_3D code with results from both the UNSAT2 code of *Neuman* [1974] and the SWATRE code of *Belmans et al.* [1983]. Both examples were also used in the documentation of SWMS_2D [*Šimůnek et al.,* 1992]. Example 3 serves to verify the accuracy of the solute transport part of SWMS_3D by comparing numerical results against those obtained with a three-dimensional analytical solution during steady-state groundwater flow. Example 4 shows numerical results for contaminant transport in an unconfined acquifer subjected to well pumping. The input and output files of the examples are listed at the end of Sections 8 and 9, respectively.

7.1. *Example 1 - Column Infiltration Test*

This example simulates a one-dimensional laboratory infiltration experiment discussed by Skuggs *et al.* [1970]. The example was used later by *Davis and Neuman* [1983] and *Šimůnek et al.* [1992] as a test problem for the UNSAT2 and SWMS_2D codes, respectively. Hence, the example provides a means of comparing results obtained with the SWMS_3D and UNSAT2 codes.

Figure 7.1 gives a graphical representation of the soil column and the finite element mesh used for the numerical simulations. The soil water retention and relative hydraulic conductivity functions of the sandy soil are presented in Figure 7.2. The soil was assumed to be homogenous and isotropic with a saturated hydraulic conductivity of 0.0433 cm/min. The initial pressure head of the soil was taken to be -150 cm. The column was subjected to ponded infiltration (a Dirichlet boundary condition) at the soil surface, resulting in one-dimensional vertical water flow. The open bottom boundary of the soil column was simulated by implementing a no-flow boundary condition during unsaturated flow (h<O), and a seepage face with h=O when the bottom boundary becomes saturated (this last condition was not reached during the simulation). The impervious sides of the column were simulated by imposing no-flow boundary conditions.

59
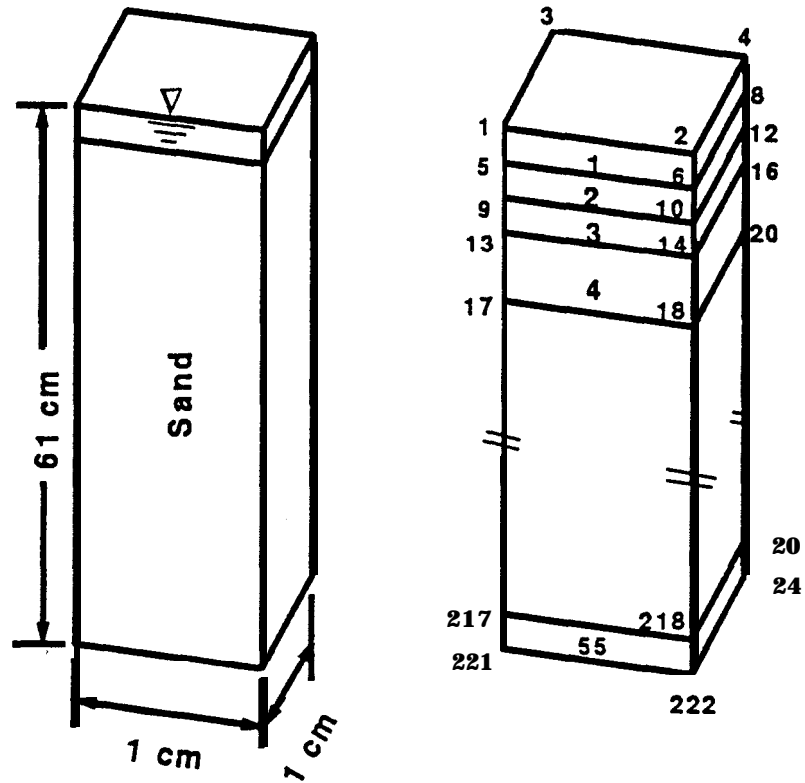
Fig. 7.1. Flow system and finite element mesh for example 1.

The simulation was carried out for 90 min, which corresponds to the total time duration of the experiment. Figure 7.3 shows the calculated instantaneous (q_0) and cumulative (I_0) infiltration rates simulated with SWMS_3D. Notice that the calculated results agreed closely with those obtained by *Davis and Neuman [1983]* using their UNSAT2 code. The results obtained with SWMS_3D code were essentially identical with those calculated with SWMS_2D.
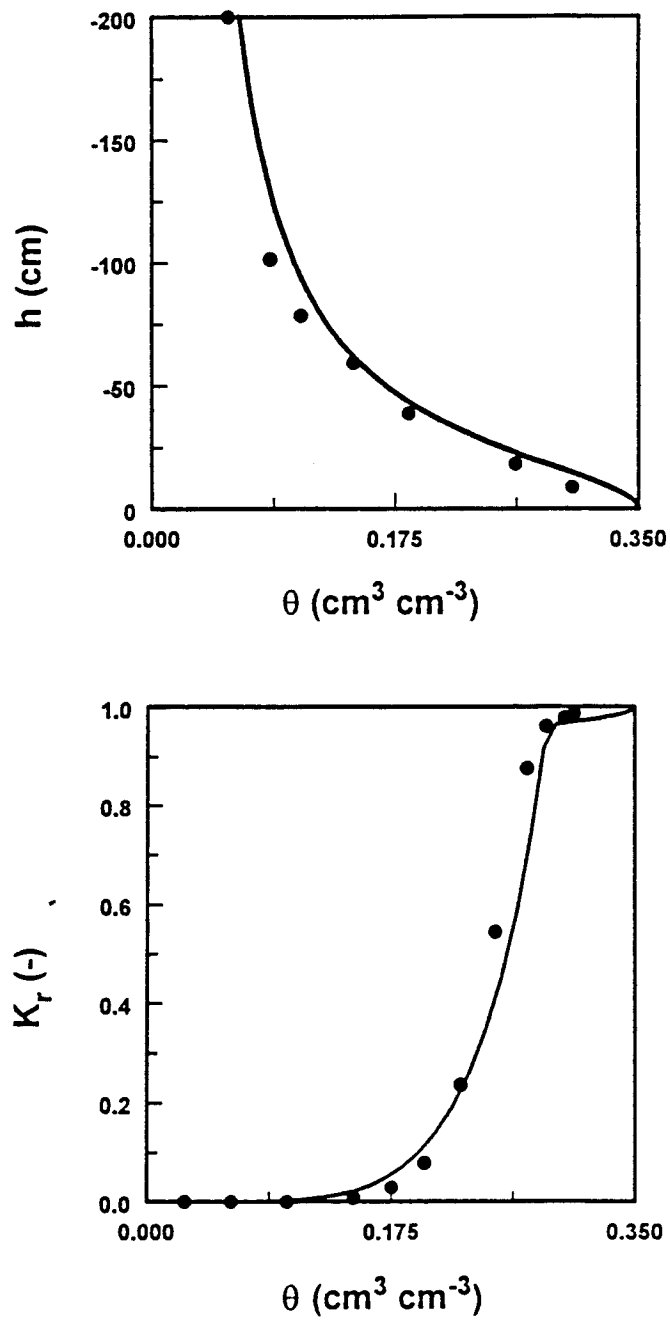
Fig. 7.2. Retention and relative hydraulic conductivity functions for example 1. The solid circles are UNSAT2 input data [*Davis and Neuman*, 1983].
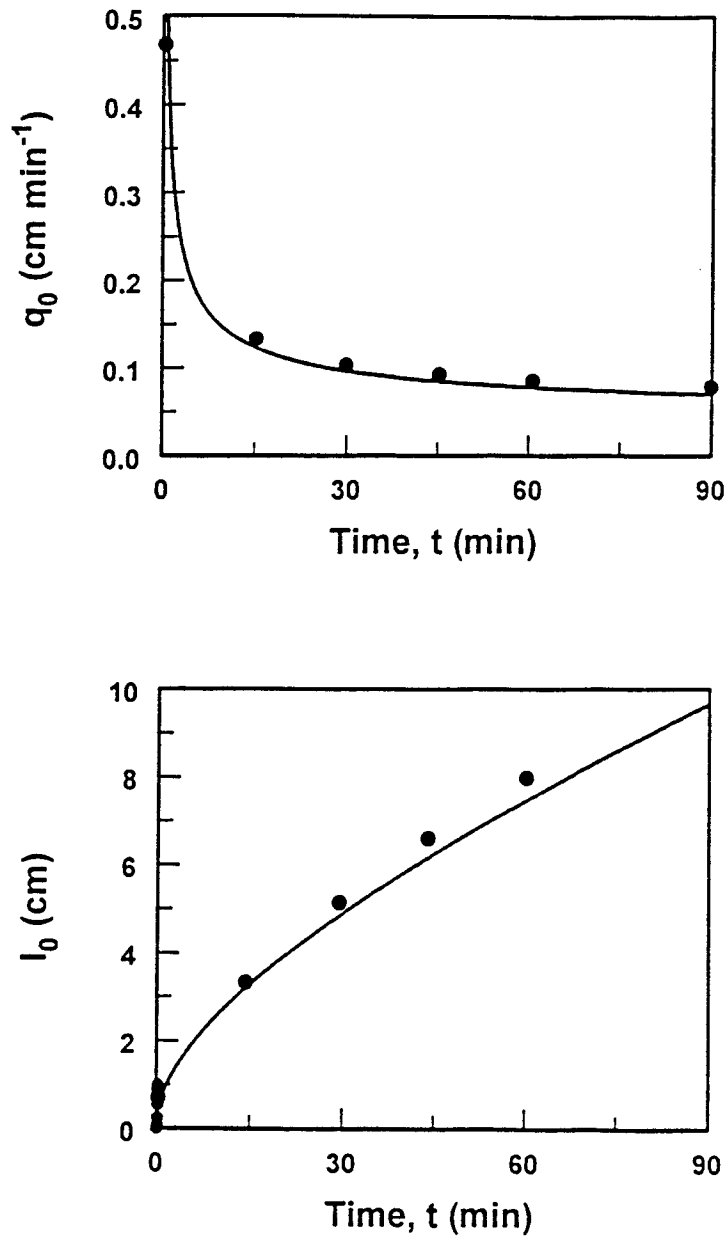
Fig. 7.3. Instantaneous, q_0, and cumulative, I_0, infiltration rates simulated with the SWMS_3D (solid lines) and UNSAT2 (solid circles) for example 1.

7.2. Example 2 - Water Flow in a Field Soil Profile Under Grass

This example considers one-dimensional water flow in a field profile of the Hupselse Beek watershed in the Netherlands. Atmospheric data and observed ground water levels provided the required boundary conditions for the numerical model. Calculations were performed for the period of April 1 to September 30 of the relatively dry year 1982. Simulation results obtained with SWMS 3D will be compared with those generated with the SWATRE computer program *[Feddes et al., 1978, Belmans et al., 1983].*

The soil profile (Fig. 7.4) consisted of two layers: a 40-cm thick A-horizon, and a B/C-horizon which extended to a depth of about 300 cm. The depth of the root zone was *30* cm. The mean scaled hydraulic functions of the two soil layers in the Hupselse Beek area [*Císlerová,* 1987; *Hopmans and Stricker, 1989] are* presented in Figure 7.5.
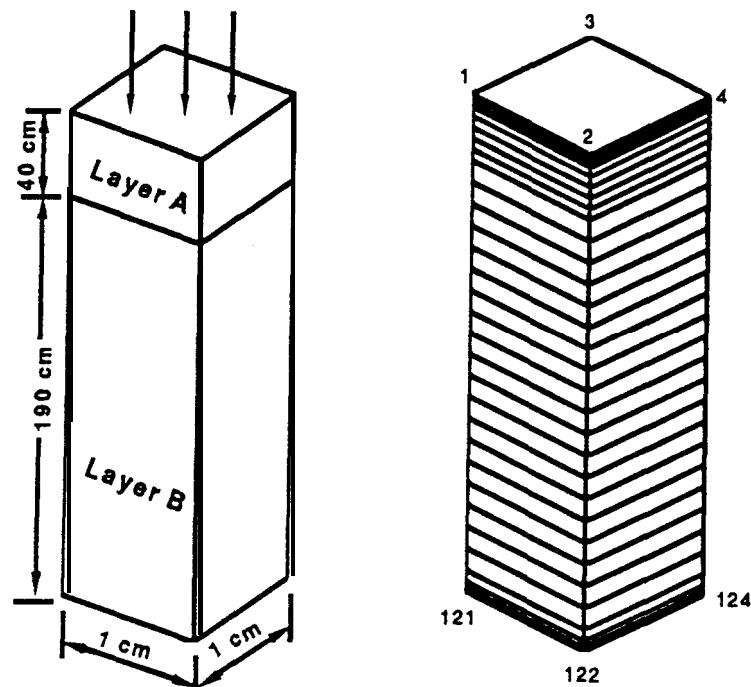
Fig. 7.4. Flow system and finite element mesh
for example 2.

The soil surface boundary conditions involved actual precipitation and potential transpiration rates for a grass cover. The surface fluxes were incorporated by using average daily rates distributed uniformly over each day. The bottom boundary condition consisted of a prescribed drainage flux - groundwater level relationship, $q(h)$, as given by equation (6.1). The groundwater level was initially set at 55 cm below the soil surface. The initial moisture profile was taken to be in equilibrium with the initial ground water level.

Figure 7.6 presents input values of the precipitation and potential transpiration rates. Calculated cumulative transpiration and cumulative drainage amounts as obtained with the SWMS_3D and SWATRE codes are shown in Figure 7.7. The pressure head at the soil surface and the arithmetic mean pressure head of the root zone during the simulated season are presented in Figure 7.8. Finally, Figure 7.9 shows variations in the calculated groundwater level with time. Again, the results obtained with SWMS_3D code are almost identical with those calculated with SWMS_2D.
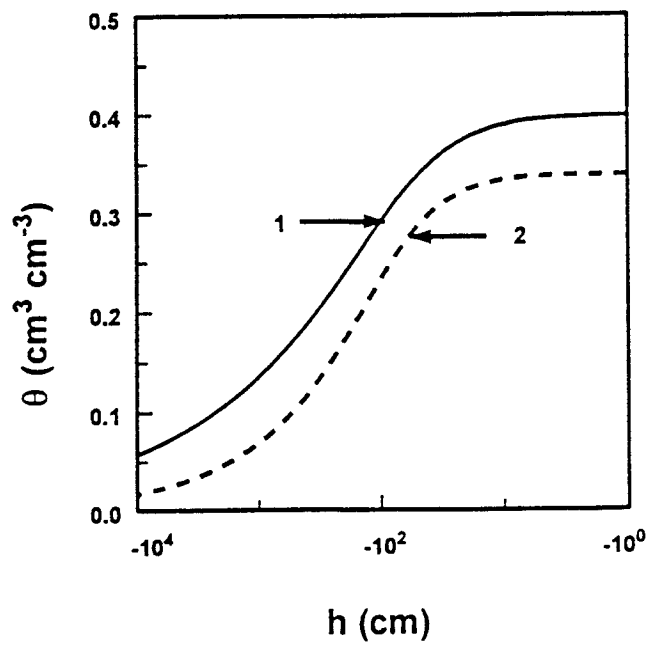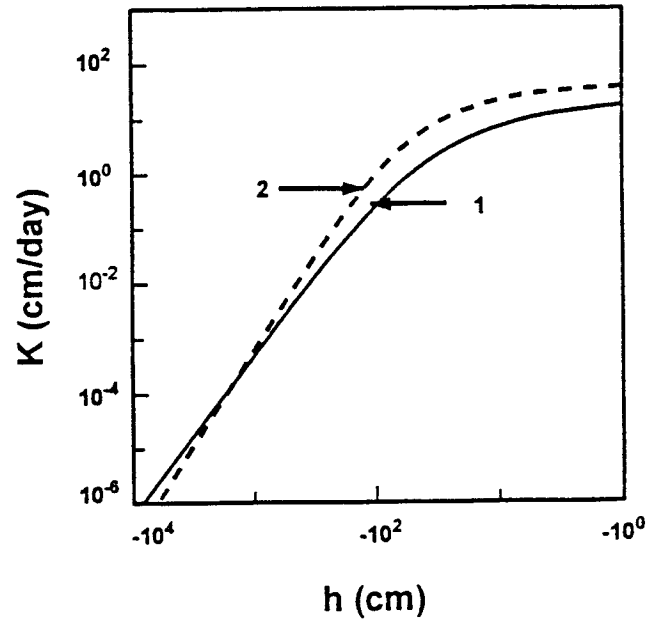
Fig. 7.5. Unsaturated hydraulic properties of the first and second soil layers for example 2.
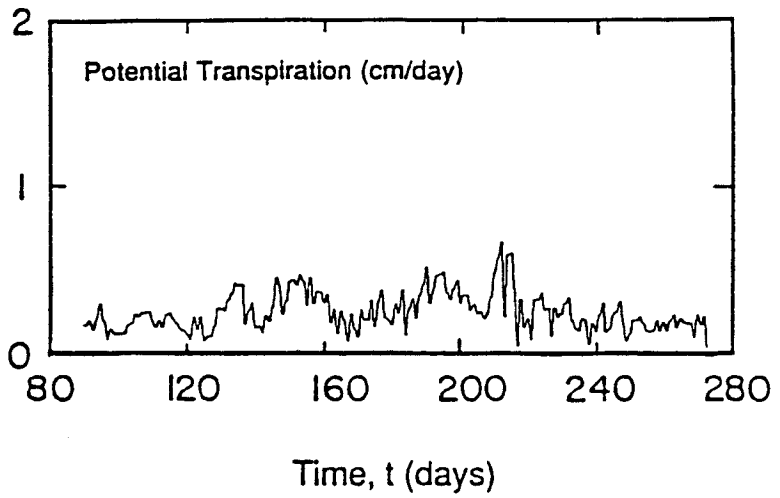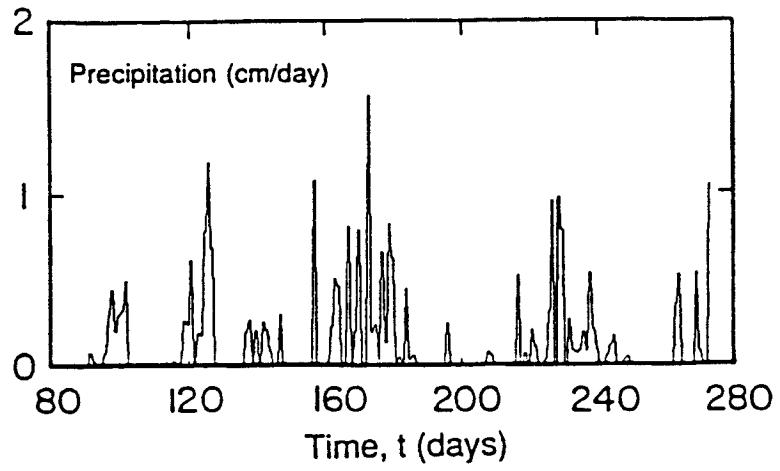
Fig. 7.6. Precipitation and potential transpiration rates for example 2.

66
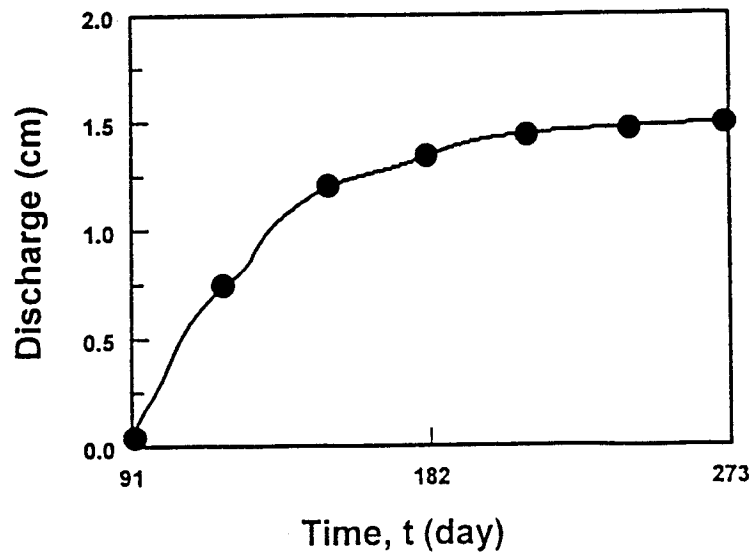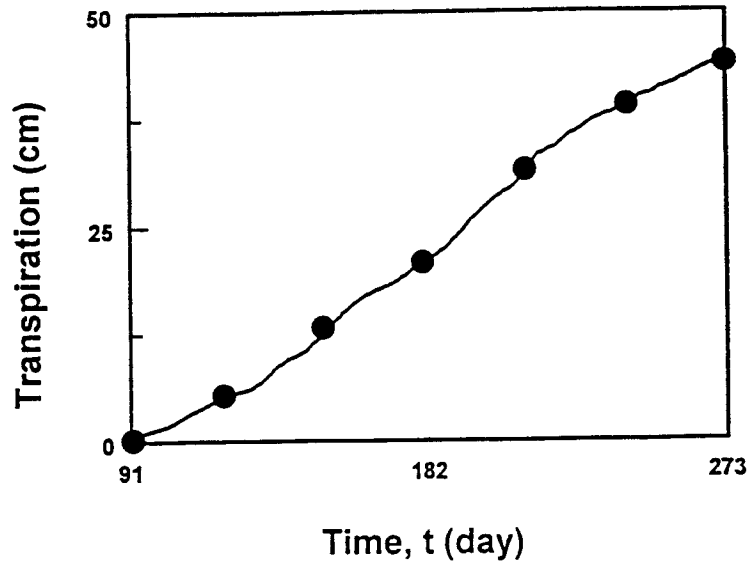
Fig. 7.7. Cumulative values for the actual transpiration and bottom discharge rates for example 2 as simulated with SWMS_3D (solid line) and SWATRE (solid circles).
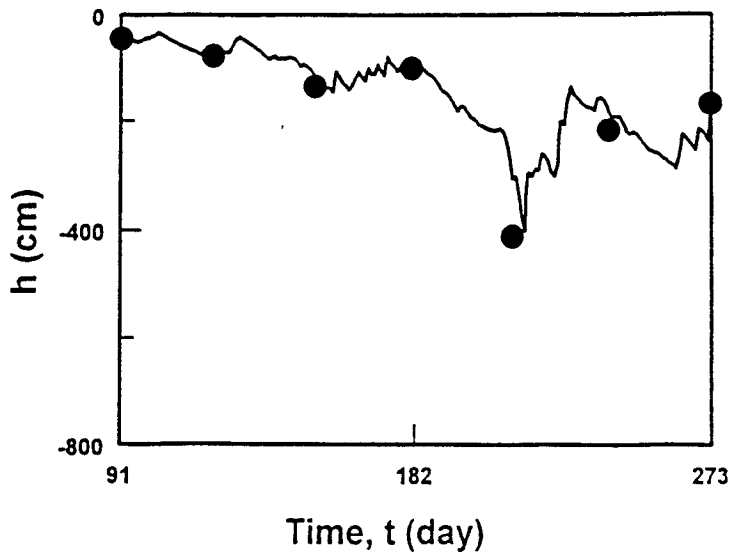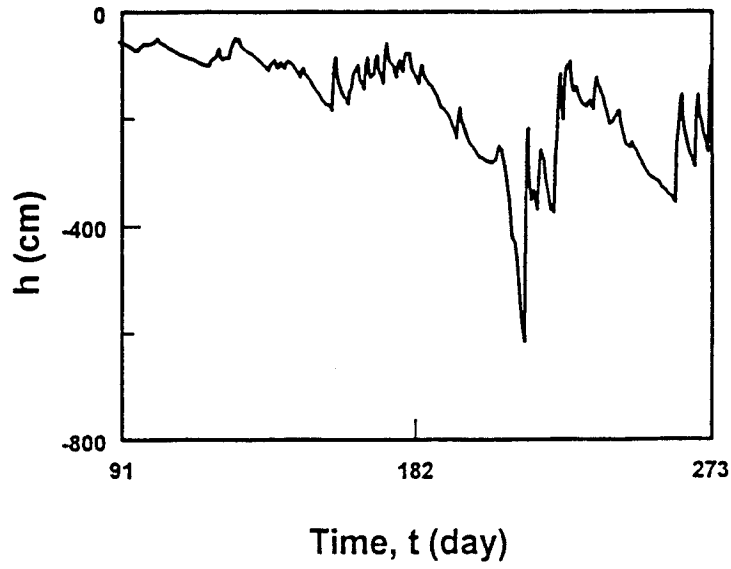
Fig. 7.8. Pressure head at the soil surface and mean pressure head of the root zone for example 2 as simulated with SWMS_3D (solid lines) and SWATRE (solid circles).
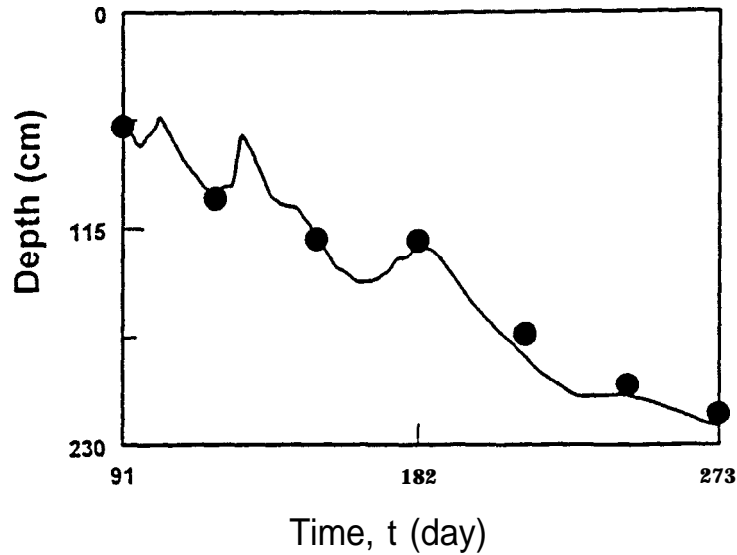
Fig. 7.9. Location of the groundwater table versus time for example 2 as simulated with the SWMS_3D (solid line) and SWATRE (solid circles) computer programs.

7.3. *Example 3 - Three-Dimensional Solute Transport*

This example was used to verify the mathematical accuracy of the solute transport part of SWMS_3D. *Leij et al. [1991]* published several analytical solutions for three-dimensional dispersion problems. One of these solutions holds for solute transport in a homogeneous, isotropic porous medium during steady-state unidirectional groundwater flow (Figure 7.10). The solute transport equation (3.4) for this situation reduces to

$$R\frac{\partial c}{\partial t} = D_T \frac{\partial^2 c}{\partial x^2} + D_T \frac{\partial^2 c}{\partial y^2} + D_L \frac{\partial^2 c}{\partial z^2} - v\frac{\partial c}{\partial z} - \mu c + \lambda \qquad (7.1)$$

where λ and μ are a zero- and first-order degradation constants, respectively; D_L and D_T are the longitudinal and transverse dispersion coefficients, respectively; v $(= q_z/\theta)$ is the average pore water velocity in the flow direction, and z is the spatial coordinate parallel to the direction of flow, while x and y are the spatial coordinates perpendicular to the flow direction. The initially

69

solute-free medium is subjected to a solute source, c_0, of unit concentration. The rectangular surface source has dimensions *2a* and 2b along the inlet boundary at $z=0$, and is located symmetrically about the coordinates $x=0$ and $y=0$ (Figure 7.10). The transport region of interest is the half-space ($z\geq0; -\infty\leq x\leq\infty, -\infty\leq y\leq\infty$). The boundary conditions may be written as:

$$c(x,y,0,t) = c_0 \qquad -a \leq x \leq a, \quad -b \leq y \leq b$$

$$c(x,y,0,t) = 0 \qquad other \ values \ of \ x, y$$

$$\lim_{z\to\infty} \frac{\partial c}{\partial z} = 0$$

$$\lim_{x\to\pm\infty} \frac{\partial c}{\partial x} = 0$$

$$\lim_{y\to\pm\infty} \frac{\partial c}{\partial y} = 0$$

(7.2)

The analytical solution of the above transport problem is [Leij *and Bradford, 1994]*

$$
\begin{aligned}
c(x,y,z,t) = \frac{c_0}{4} \int_{P(t)}^{t} & \left[\frac{Rz^2}{4\pi D_L \tau^3} \right]^{1/2} \exp\left[-\frac{\mu\tau}{R} - \frac{(Rz - v\tau)^2}{4RD_L\tau} \right] \\
& \left[erfc\left(\frac{x - a}{2(D_T\tau/R)^{1/2}} \right) - erfc\left(\frac{x + a}{2(D_T\tau/R)^{1/2}} \right) \right] \\
& \left[erfc\left(\frac{y - b}{2(D_T\tau/R)^{1/2}} \right) - erfc\left(\frac{y + b}{2(D_T\tau/R)^{1/2}} \right) \right] d\tau + \\
\frac{\lambda}{2R} \int_0^t \exp\left[-\frac{\mu\tau}{R} \right] & \left[erfc\left(\frac{v\tau - Rz}{2(RD_L\tau)^{1/2}} \right) - \exp\left(\frac{vz}{D_L} \right) erfc\left(\frac{Rz + v\tau}{2(RD_L\tau)^{1/2}} \right) \right] d\tau
\end{aligned}
$$

(7.3)

where P(t) = 0 if $t<t_0$ and P(t) $= t-t_0$ if $t>t_0$, and where t_0 is the duration of solute pulse. The input transport parameters for two simulations are listed in Table 7.1. The width of the source was assumed to be 100 m in both the *x* and y directions. Because of symmetry, calculations were carried out only for part of the transport domain where $x\geq0$, $y\geq0$ and $z\geq0$.

70
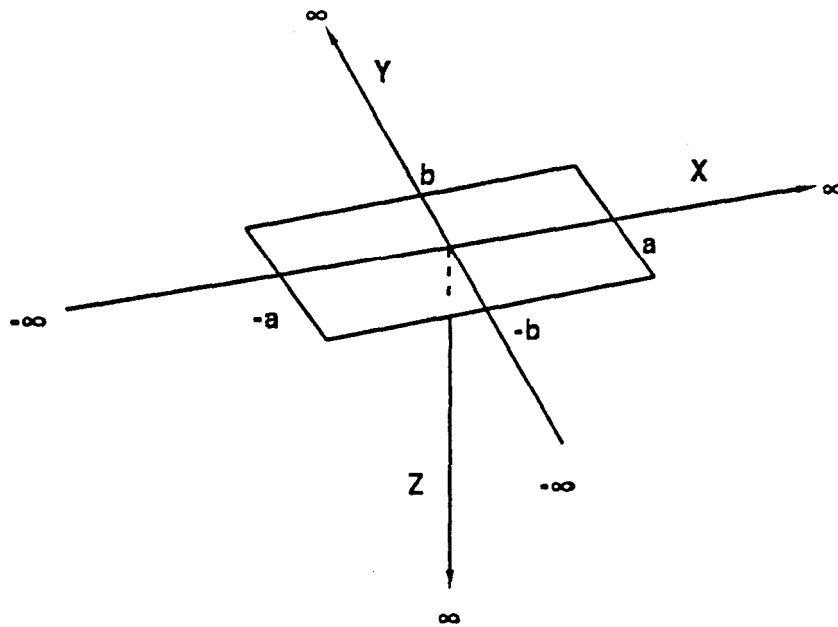
Fig. 7.10. Schematic of the transport system for example 3.

Table 7.1. Input parameters for example 3.

Parameter	Example 3a	Example 3b
v [m/day]	0.1	1.0
D_T [m^2/day]	1.0	0.5
D_L [m^2/day]	1.0	1.0
μ [day^{-1}]	0.0	0.01
R [-]	1.0	3.0
c_0 r-1	1.0	1.0

Figure 7.11 shows the calculated concentration front (taken at a concentration of 0.1) at selected times for the first set of transport parameters in Table 7.1. Notice the close agreement between the analytical and numerical results. Excellent agreement is also obtained for the calculated concentration distributions after 365 days at the end of the simulation (Fig. 7.12). Figures 7.13 and 7.14 show similar results for the second set of transport parameters listed in Table 7.1. All four figures were drawn assuming the y coordinate to be zero.
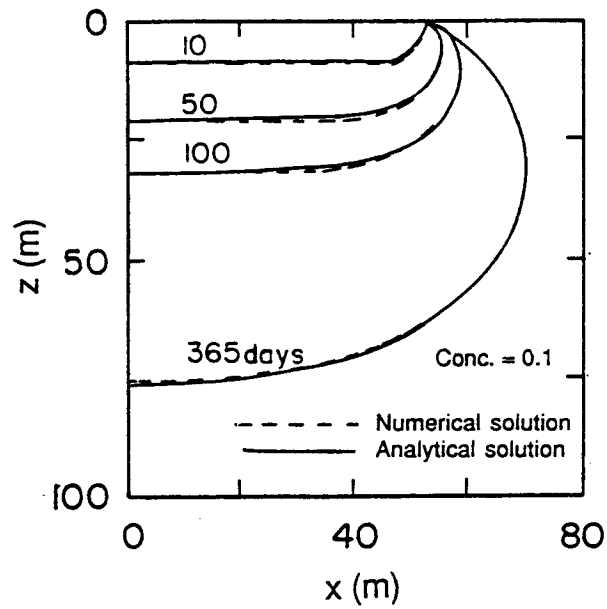
Fig. 7.11. Advancement of the concentration front (c=0.1) for example 3a as calculated with SWMS_3D (dotted lines) and the analytical solution (solid lines).
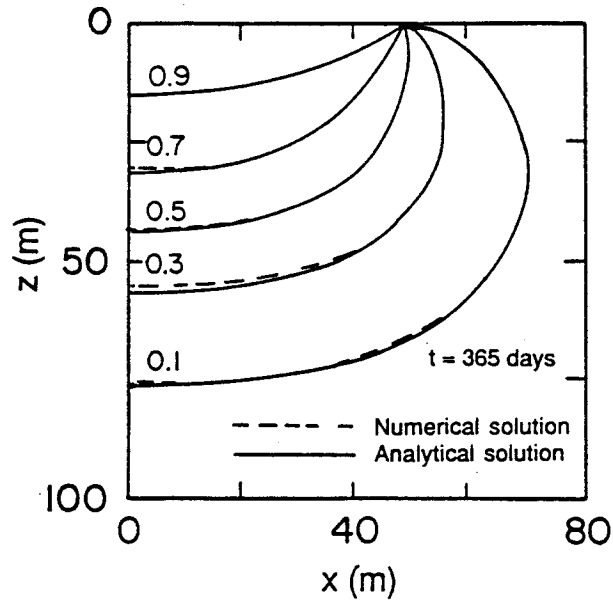
Fig. 7.12. Concentration profiles at the end of the simulation (t=365 days) for example 3a as calculated with SWMS_3D (dotted lines) and the analytical solution (solid lines).

72
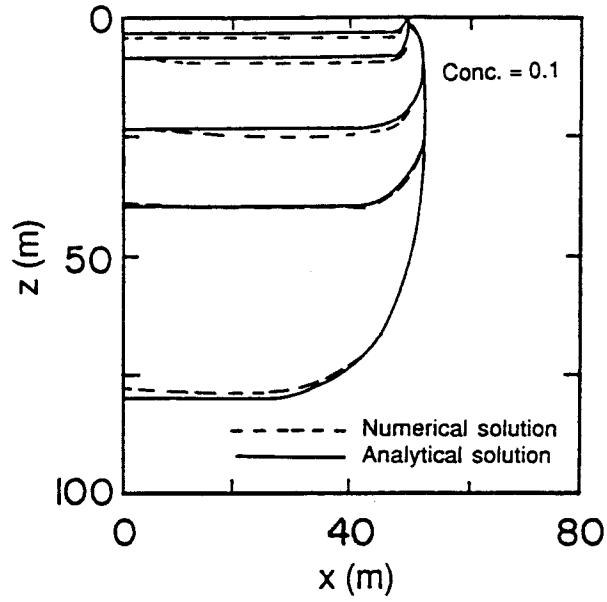
Fig. 7.13. Advancement of the concentration front (c=0.1) for example 3b as calculated with SWMS_3D (dotted lines) and the analytical solution (solid lines).
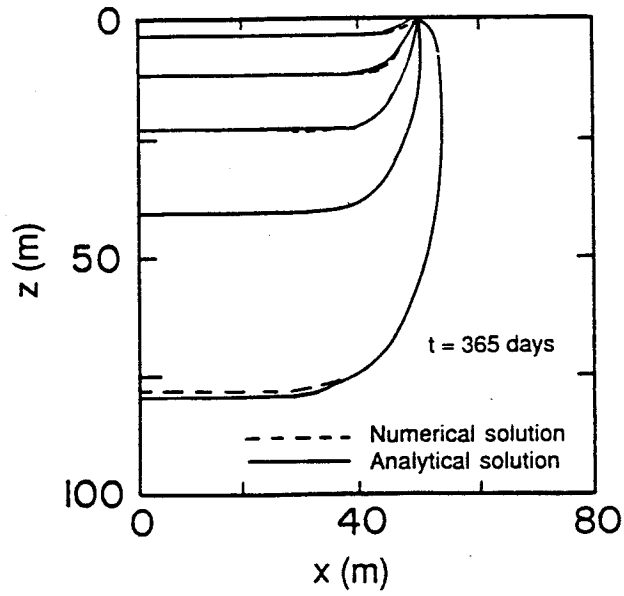
Fig. 7.14. Concentration profiles at the end of the simulation (t=365 days) for example 3b as calculated with SWMS_3D (dotted lines) and the analytical solution (solid lines).

7.4. Example 4 - Contaminant Transport From a Waste Disposal Site

This test problem concerns contaminant transport from a waste disposal site (or possibly a landfill) into a unconfined aquifer containing a pumping well downgradient of the disposal site as shown in Figure 7.15. Water was assumed to infiltrate from the disposal site into the unsaturated zone under zero-head ponded conditions. The concentration of the contaminant leaving the disposal site was taken to be 1 .O during the first 50 days, and zero afterwards. The waste disposal site itself had lateral dimensions of 10 x 40 m^2. Initially, the water table decreased from a height of 28 m above the base of the aquifer at the left-hand side (Figure 7.15) to 26 m on the right-hand side of the flow domain. The initial pressure head in the unsaturated zone was assumed to be at equilibrium with the initial water table, i.e., no vertical flow occurred. The transport experiment started when the water table in the fully penetrated well at x = 170 m $(y =$ 0) was suddenly lowered to a height of 18 m above the bottom of the unconfined aquifer. We assumed that at that same time *(t = 0)* infiltration started to occur from the disposal site. Prescribed hydraulic head conditions $h + z = 28$ m and $h + z = 26$ m were imposed along the left-hand (x = 0) and right-hand $(x = 260$ m) side boundaries (-50 $\leq$ y $\leq$ 50 m). A prescribed hydraulic head condition of $h + z = 18$ m was used to represent the well along a vertical below the water table (z $\leq$ 18) at x = 170 m and y = 0 m, while a seepage face was defined at that location along the vertical above the water table $(z > 18)$. No-flow conditions were assumed along all other boundaries, including the soil interface. Hydraulic and transport parameters used in the analysis are listed in Table 7.2. We selected the retention hydraulic parameters for a coarse-textured soil with a relatively high saturated hydraulic conductivity, K_s, in order to test the SWMS_3D code for a comparatively difficult numerical problem.

Because of symmetry about the y axis, only half of the flow region was simulated. The solution domain defined by $0 \leq x \leq 260$, $0 \leq y \leq 50$, and $0 \leq z \leq 38$ m was discretized into a rectangular grid comprised of 10560 elements and 12144 nodes (Figure 7.16). Nodal spacings were made relatively small in regions near the disposal site and near the pumping well where the highest head gradients and flow velocities were expected. The variably saturated flow problem was solved using SWMS_3D assuming an iteration head tolerance of 0.01 m and a water content

Plan-View

Cross-Section
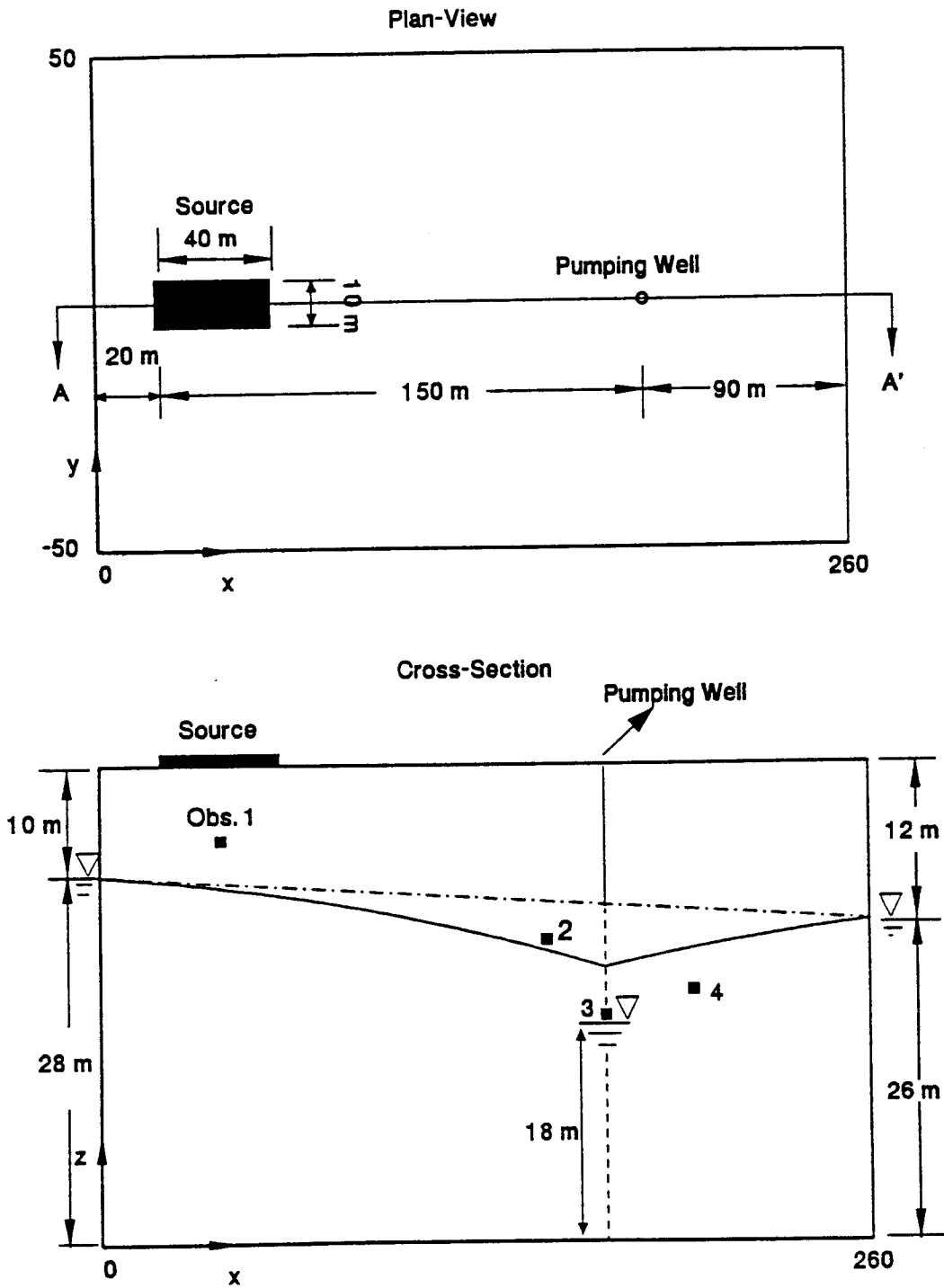
Fig. 7.15. Geometry and boundary conditions for example 4 simulating three-dimensional flow and contaminant transport in a pumped variably-saturated aquifer.

75

Table 7.2. Input parameters for example 4.

Hydraulic Parameters		Transport Parameters	
$\theta_s = \theta_m = \theta_k$	0.450	ρ [kg/m³]	1400
$\theta_r = \theta_a$	0.05	D_d [m²/day]	0.01
$K_s = K_k$ [m/day]	5.0	D_L [m]	1.0
α [I/m]	4.1	D_T [m]	0.25
n [-]	2.0	k [m³/kg]	0.0
		μ_w [l/day]	0.0
		μ_s [l/day]	0.0
		γ_w [1/day]	0.0
		γ_s [l/day]	0.0
		c_0	1.0

tolerance of 0.0001.

Computed water table elevations are plotted in Figure 7.17a and 7.17b along longitudinal ($y=0$) and transverse ($x=170$ m) planes through the pumping well, respectively. The results show a relatively strong direct interaction between the infiltrating water and the saturated zone after only a short period of time; water flow reached approximately steady state about 1.5 days after the experiment started. The velocity field and streamlines in a longitudinal section through the pumping well are presented in Figure 7.18. Note that the length of the seepage face along the well was determined to be approximately 5 meters. The calculated well discharge rate for the fixed water table ($z = 18$ m) was calculated to be 39.6 m³/day. A concentration contour plot (c = 0.1) is presented in Figure 7.19. This figure shows that contaminant transport was strongly affected by well pumping. Note that although the contaminant source was located 10 m above the initial groundwater table, and 150 m upgradient of the pumping well, the solute reached the pumping well after only 200 days of pumping. Figure 7.20 gives a two-dimensional view of calculated concentration distributions at several times in a horizontal plane ($z = 20$ m).

76

Finally, Figure 7.21 presents solute breakthrough curves observed at observation node 1 ($x = 40$ m, $z = 32$ m), node 2 ($x = 150$ m, $z = 24$ m), node 3 ($x = 170$ m, $z = 18$ m), and node 4 ($x = 200$ m, $z = 20$ m). These observation nodes are all on a vertical cross-section ($y = 0$) as shown in Figure 7.15b. Notice that the breakthrough curves differ considerably in shape and especially peak concentrations. Although the breakthrough curve at observation node 1 immediately below the disposal site was very steep, no numerical oscillations were observed here. This shows that SWMS_3D is able to solve the present solute transport problem involving sharp concentration distributions without generating non-physical oscillations. However, the efficiency of the numerical simulation for this example was limited by the need for relatively small time steps so as to satisfy the grid Courant criterion (Section 5.3.6). Although water flow had reached approximately steady-state within less than 2 days, the time step for the solute transport problem was only 0.073 day because of relatively large flow velocities near the well.
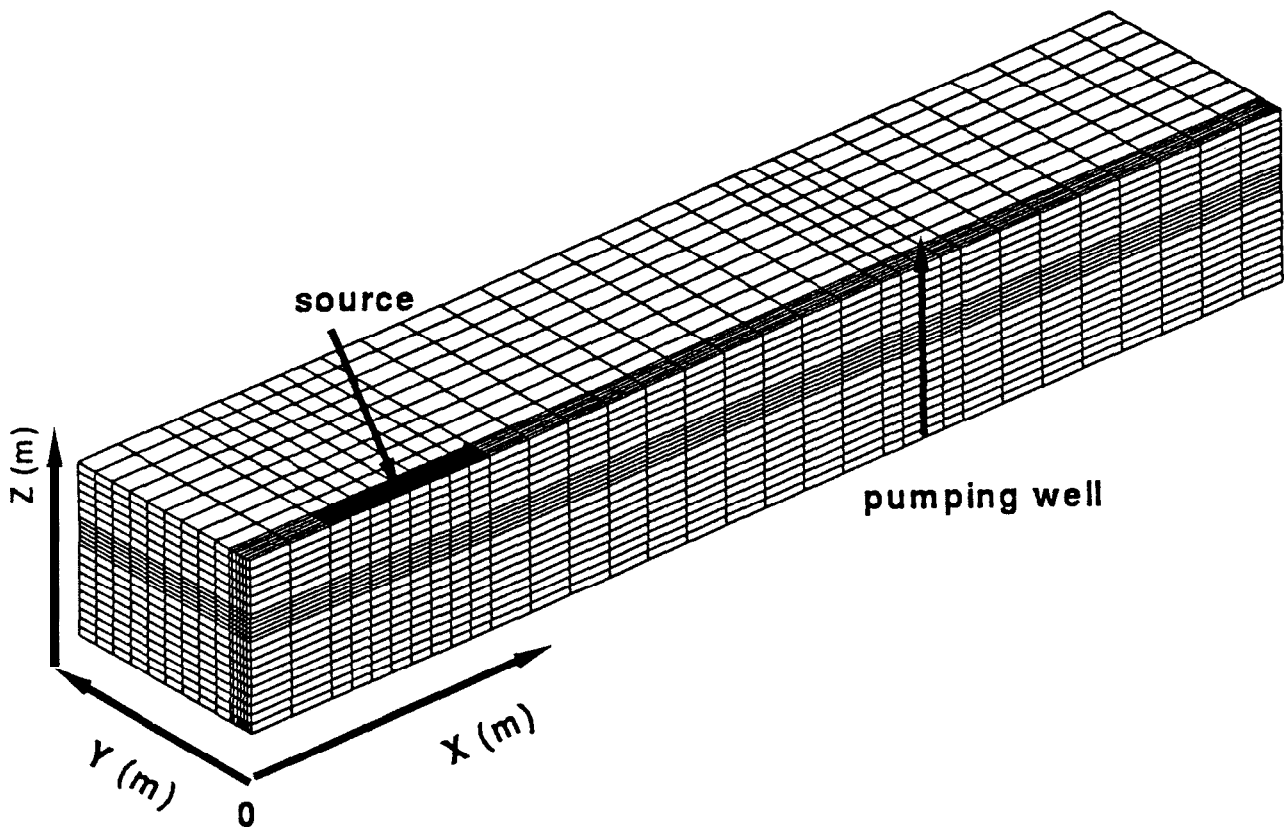
Fig. 7.16. Finite element mesh for example 4.
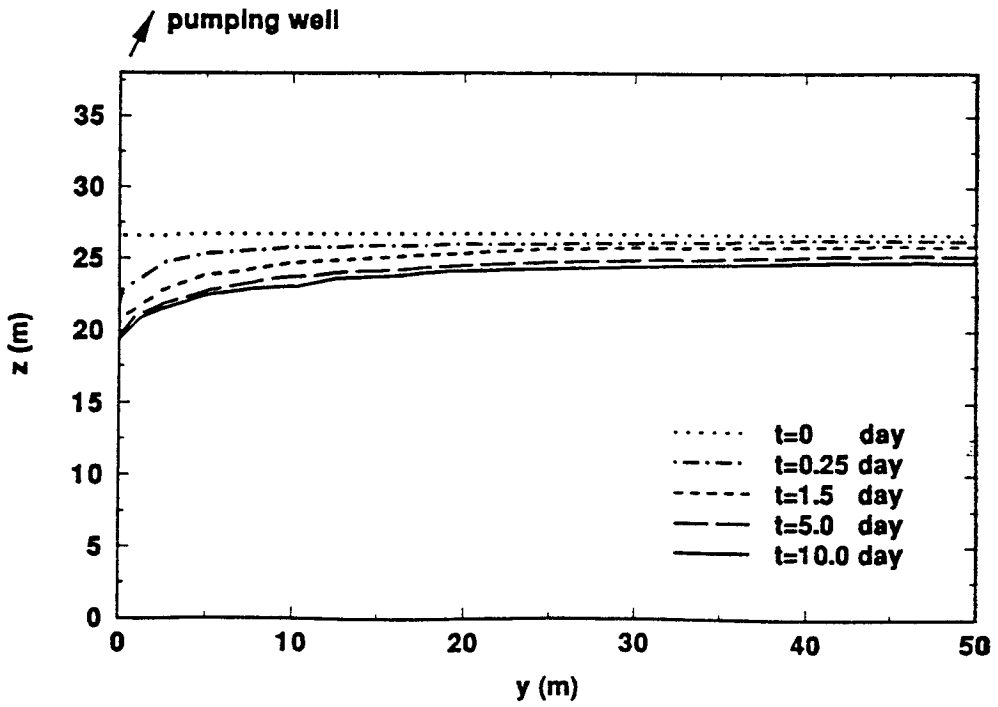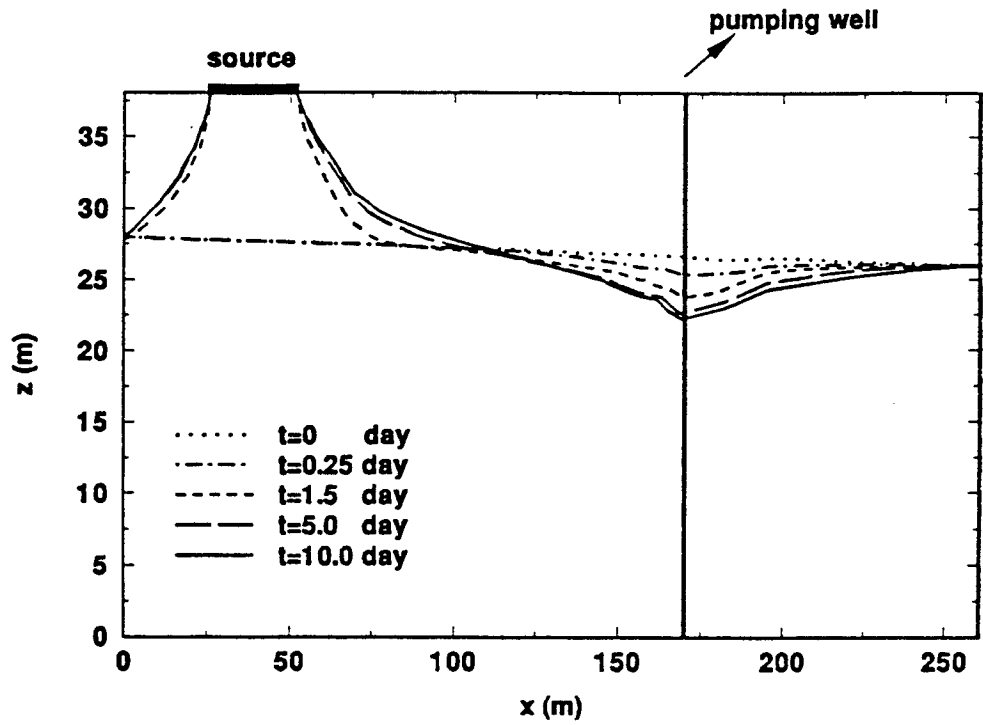
Fig. 7.17. Calculated (a) longitudinal (y=0) and (b) transverse (x=170 m) elevations of the groundwater table.
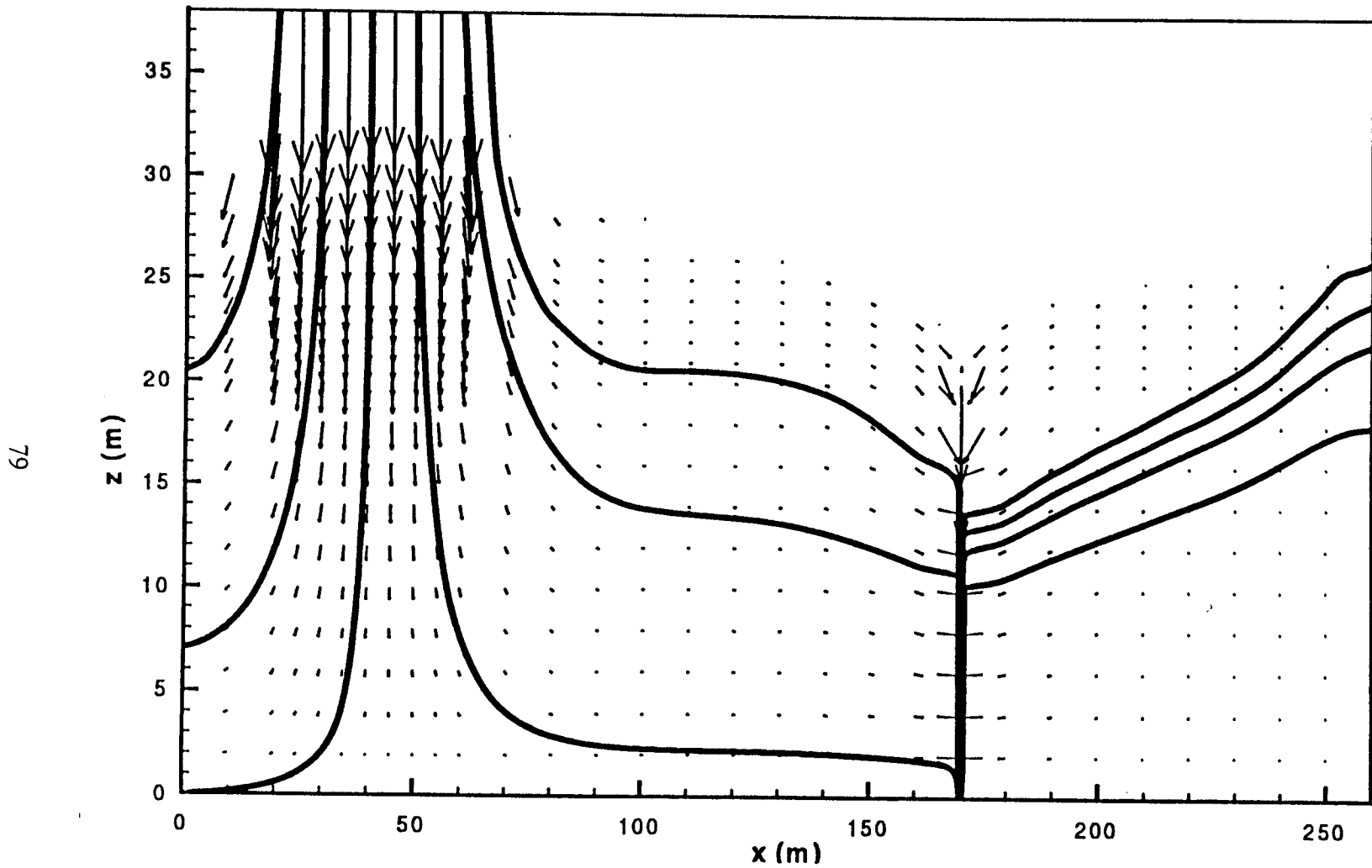
Fig. 7.18. Computed velocity field and streamlines at t = 10 days.
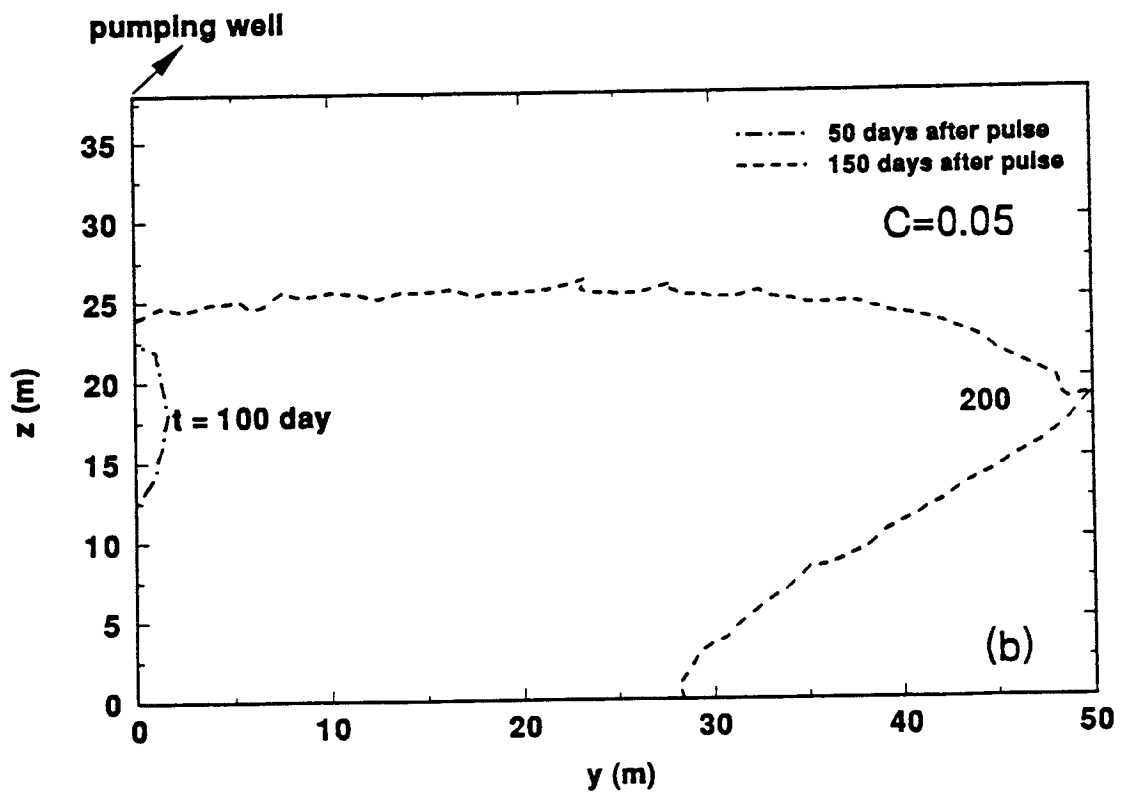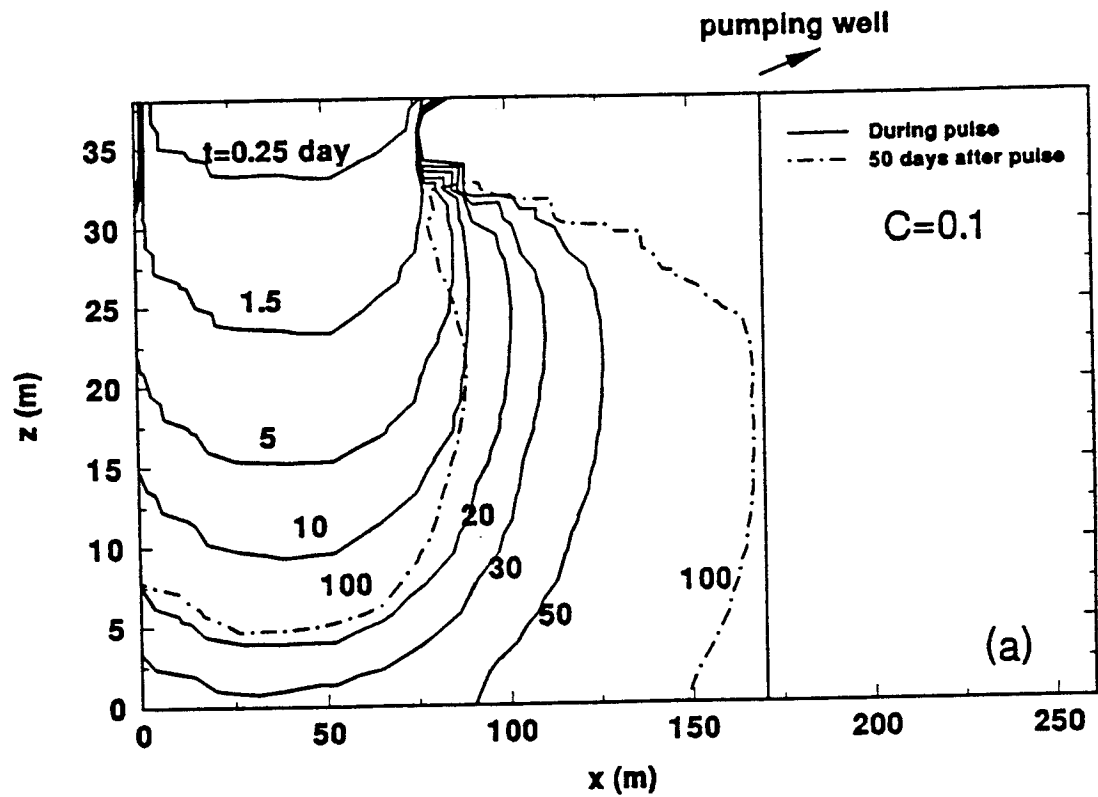
Fig. 7.19. Concentration contour plots for (a) $c = 0.1$ in a longitudinal cross-section ($y = 0$), and (b) c = 0.05 in a transverse cross-section ($x = 170$ m).
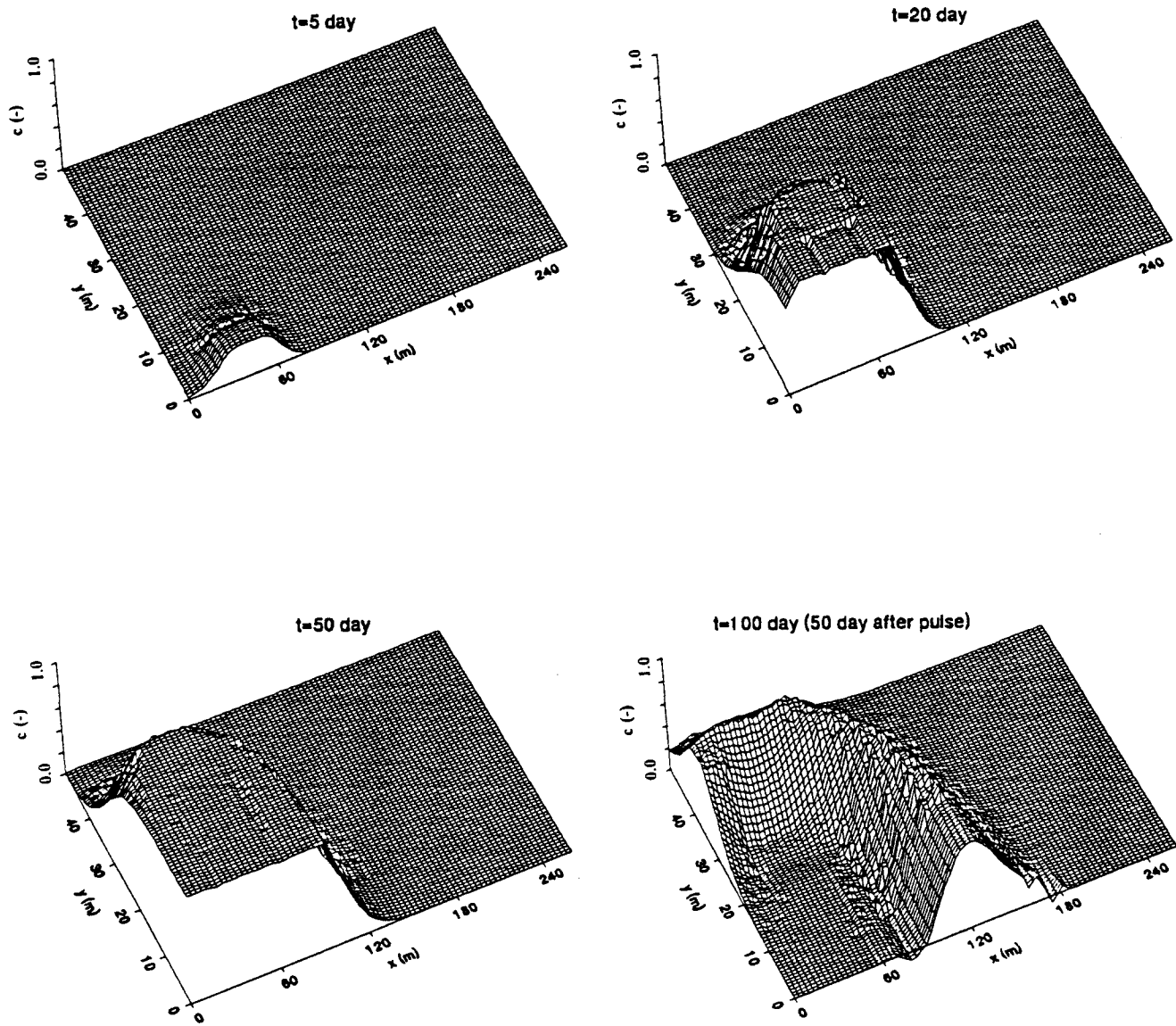
Fig. 7.20. Concentration distributions in a horizontal plane located at $z = 20$ m
for $t = 10$, 50, 100, and 200 days.
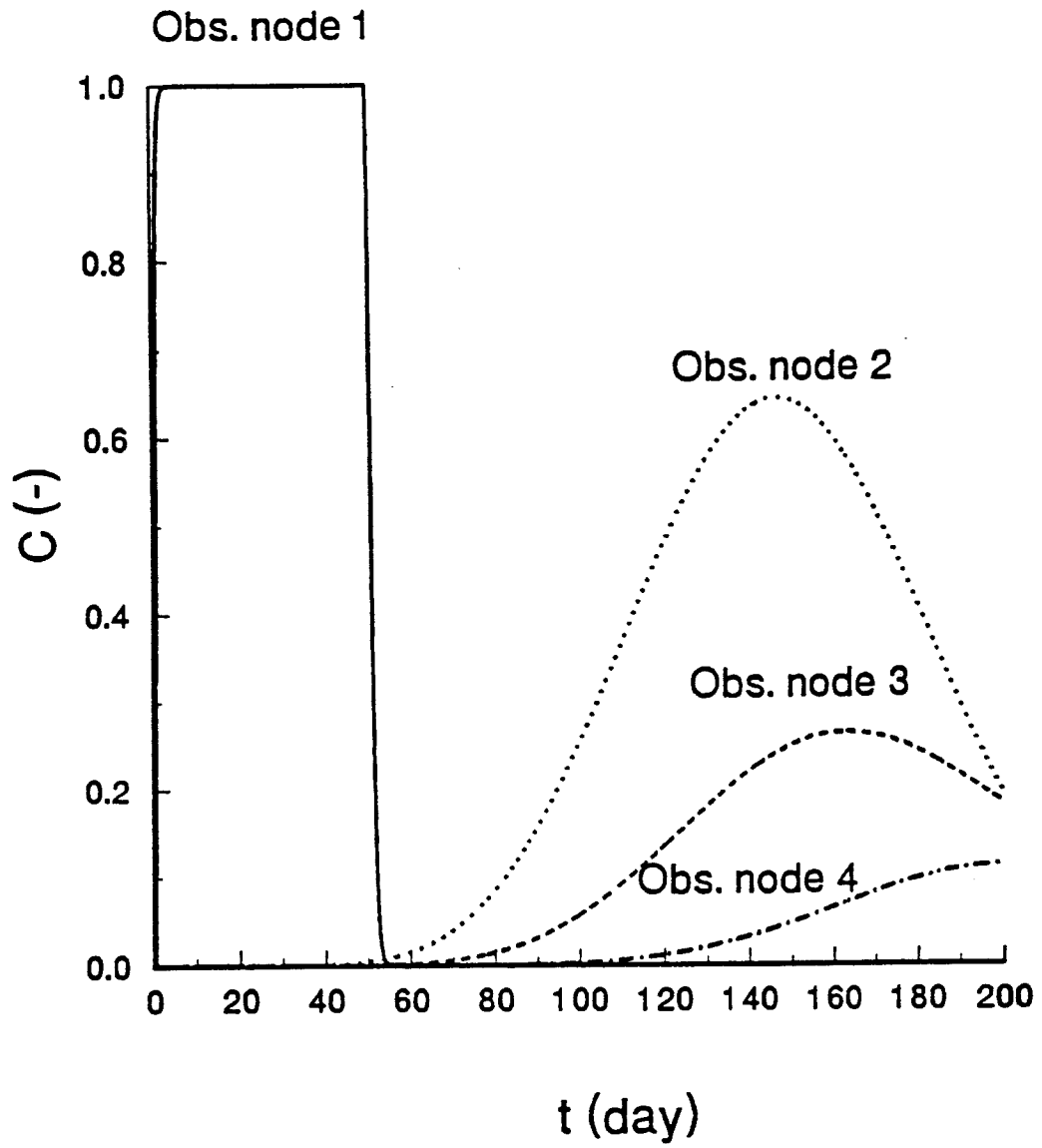
Fig. 7.21. Breakthrough curves at observation node 1 ($x = 40$ m, $z = 32$ m), node 2 ($x = 150$ m, z =24 m), node 3 ($x = 170$ m, $z = 18$ m), and node 4 ($x = 200$ m, $z = 20$ m).

8. INPUT DATA

The input data for SWMS_3D are given in three separate input files. These input files consist of one or more input blocks identified by the letters from A through K. The input files and blocks must be arranged as follows:

> SELECTOR.IN
> > A. Basic Information
> > B. Material Information
> > C. Time Information
> > D. Root Water Uptake Information
> > E. Seepage Information
> > F. Drainage Information
> > G. Solute Transport Information
>
> **GRID.IN**
> > H. Nodal Information
> > I. Element Information
> > J. Boundary Geometry Information
>
> ATMOSPH.IN
> > K. Atmospheric Information

The various input blocks are described in detail in Section 8.1, while Section 8.2 lists the actual input files for examples 1 through 4 discussed in Section 7. The output files for these examples are discussed in Section 9.

8.1. *Description of Data Input Blocks*

Tables 8.1 through 8.11 describe the data required for each input block. All data are read in using list-directed formatting (free format). Comment lines are provided at the beginning of, and within, each input block to facilitate, among other things, proper identification of the function of the block and the input variables. The comment lines are ignored during program execution; hence, they may be left blank but should not be omitted. All input files must be placed in the directory SWMS_3D.IN. The program assumes that all input data are specified in a consistent set of units for mass M, length L, and time T.

Most of the information in Tables 8.1 through 8.11 should be self-explanatory. Table 8.8 (Block H) is used to define, among other things, the nodal coordinates and initial conditions for the pressure head and the concentration. One short-cut may be used when generating the nodal coordinates. The short-cut is possible when two nodes (e.g., N, and N_2), not adjacent to each other, are located along a transverse line such that N_2 is greater than N_1+1. The program will automatically generate nodes between N_1 and N_2, provided all of the following conditions are met simultaneously: (1) all nodes along the transverse line between nodes N_1 and N_2 are spaced at equal intervals, (2) values of the input variables hNew(n), Beta(n), Axz(n), Bxz(n), Dxz(n), and Conc(n) vary linearly between nodes N, and N_2, and (3) values of Kode(n), Q(n) and MatNum(n) are the same for all n = N,, N_1+1,..., N_2-1 (see Table 8.8).

A similar short-cut is possible when generating the elements in Block I (Table 8.9). Consider two elements, E_1 and E_2, between two transverse lines such that E_2 is greater than $E_,$. The program requires input data only for element E_1 (i.e., data for elements E_1+1 through E_2 may be omitted), provided the following two conditions are met simultaneously: (1) all elements between E_1 and E_2 **are** hexahedrals, including E_1 and E_2, and (2) all elements, **$E_,,....$, $E_,$, are** assigned the same values of $Cos11(e), Cos22(e), Cos33(e), Cos12(e), Cos13(e), Cos23(e), ConA1(e), ConA2(e), ConA3(e)$, and $LayNum(e)$ as defined in Table 8.9.

To overcome problems with definition of finite elements and their comer nodes in input file GRID.IN, we have provided a separate finite element generator GENER3 which generates the nodes and elements for a hexahedral domain. Table 8.12 shows how the input file for the finite element mesh generator GENER3 is constructed. The resulting file GRID.IN can be modified using any word- or data-processing software.

Table 8.1. Block A - Basic information.

Record	Type	Variable	Description
1,2	-	_	Comment lines.
3	Char	*Hed*	Heading.
4	_		Comment line.
5	Char	*L Unit*	Length unit (e.g., 'cm').
5	- Char	*TUnit*	Time unit (e.g., 'min').
5	Char	*MUnit*	Mass unit for concentration (e.g., 'g', 'mol', '-').
6			Comment line.
7	Integer	*MaxIt*	Maximum number of iterations allowed during any time step (usually 20).
7	Real	*TolTh*	Absolute water content tolerance for nodes in the unsaturated part of the flow region [-] (its recommended value is 0.0001). *TolTh* represents the maximum desired absolute change in the value of the water content, θ, between two successive iterations during a particular time step.
7	Real	*TolH*	Absolute pressure head tolerance for nodes in the saturated part of the flow region [L] (its recommended value is 0.1 cm). *TofH* represents the maximum desired absolute change in the value of the pressure head, *h*, between two successive iterations during a particular time step.
8			Comment line.
9	Logical	*lWat*	Set this logical variable equal to **.true.** when transient water flow is considered. Set this logical variable equal to **.false.** when steady-state water flow is to be calculated.
9	Logical	*lChem*	Set this logical variable equal to .true. if solute transport is to be considered.
9	Logical	*CheckF*	Set this logical variable equal to .true. if the grid input data are to be printed for checking.
9	Logical	*ShortF*	**.true.** if information is to be printed only at preselected times, but not at each time step (T-level information, see Section 9. l), **.false.** if information is to be printed at each time step.
9	Logical	*FluxF*	**.true.** if detailed information about the element fluxes and discharge/recharge rates is to be printed.
9	Logical	*AtmInf*	.true. if atmospheric boundary conditions are supplied via the input file ATMOSPH.IN, **.false.** if the file ATMOSPH.IN is not provided (i.e., in case of time independent boundary conditions).
9	Logical	*SeepF*	**.true.** if one or more seepage faces is to be considered.

Table 8.1. (continued)

Record	Type	Variable	Description
9	Logical	*FreeD*	Set this logical variable equal to **.true.** if a unit vertical hydraulic gradient boundary condition (free drainage) is used at the bottom boundary. Otherwise set equal to **.false.** .
9	Logical	*DrainF*	Set this logical variable equal to **.true.** if a dram is to be simulated by means of boundary condition. Otherwise set equal to **.false.** . Section 4.3.7 explains how tile drains can be represented as boundary conditions in a regular finite element mes

Table 8.2. Block B - Material information.

Record	Type	Variable	Description
I,2	-		Comment lines.
3	Integer	*NMat*	Number of soil materials. Materials are identified by the material number, *MatNum,* specified in Block H.
3	Integer	**NLay**	Number of subregions for which separate water balances are being computed. Subregions are identified by the subregion number, *LayNum,* specified in Block I.
3	Real	ha	Absolute value of the upper limit [L] of the pressure head interval below which a table of hydraulic properties will be generated internally for each material (h_a must be greater than 0.0; e.g. 0.001 cm) (see Section 4.3.11).
	Real	hb	Absolute value of the lower limit [L] of the pressure head interval for which a table of hydraulic properties will be generated internally for each material (e.g. 1000 m). One may assign to h_b, *the* highest (absolute) expected pressure head to be expected during a simulation. If the absolute value of the pressure head during program execution lies outside of the interval $[h_a, h_b]$, then appropriate values for the hydraulic properties are computed directly from the hydraulic functions (i.e., without interpolation in the table).
3	Integer	*NPar*	Number of parameters specified for each material (i.e., 9 in case of the modified van Genuchten model). If the original van Genuchten model is *to* be used, *then* set $\theta_a = \theta_r$, $\theta_m = \theta_k = \theta_s$ and $K_k = K_s$ *(see* Section 2.3 for the description of unsaturated soil hydraulic properties).
4	-		Comment line.
5	Real	*Par(1,M)*	Parameter θ_r for material M [-].
5	Real	*Par(2,M)*	Parameter θ_s for material M [-].
5	Real	*Par(3,M)*	Parameter θ_a for material M [-].
5	Real	*Par(4,M)*	Parameter θ_m for material M [-].
5	Real	*Par(5,M)*	Parameter α for material M [L^{-1}].
5	Real	*Par(6,M)*	Parameter n for material M [-].
5	Real	*Par(7,M)*	Parameter K_s for material M [LT'].
5	Real	*Par(8,M)*	Parameter K_k for material M [LT^{-1}].
5	Real	*Par(9,M)*	Parameter θ_k for material M [-].
			Record 5 information is provided for each material M (from 1 to *NMat).*

Table 8.3. Block C - Time information.

Record	Type	Variable	Description
I,2	-		Comment lines.
3	Real	*dt*	Initial time increment, Δt [T]. Initial time step should be estimated in dependence on the problem solved. For problems with high pressure gradients (e.g. infiltration into an initially dry soil), Δt should be relatively small.
3	Real	*dtMin*	Minimum permitted time increment, At, [T].
3	Real	*dtMax*	Maximum permitted time increment, At_ [T].
3	Real	*dMul*	If the number of required iterations at a particular time step is less than or equal to 3, then At for the next time step is multiplied by a dimensionless number *dMul* ≥ 1 .O (its value is recommended not to exceed 1.3).
3	Real	*dMul2*	If the number of required iterations at a particular time step is greater than or equal to 7, then At for the next time step is multiplied by *dMul2* ≤ 1.0 (e.g. *0.33).*
3	Integer	*MPL*	Number of specified print-times at which detailed information about the pressure head, water content, concentration, flux, and the soil water and solute balances will be printed.
4			Comment line.
5	Real	*TPrint(1)*	First specified print-time [T].
5	Real	*TPrint(2)*	Second specified print-time [T].
.			
.			
5	Real	*TPrint(MPL)*	Last specified print-time [T].

Table 8.4. Block D - Root water uptake information.+

Record	Type	Variable	Description
1,2		-	Comment lines.
3	Real	PO	Value of the pressure head, h_1 (Fig. 2.1), below which roots start to extract water from the soil.
3	Real	P2H	Value of the limiting pressure head, h,, below which the roots cannot extract water at the maximum rate (assuming a potential transpiration rate of *r2H).*
3	Real	P2L	As above, but for a potential transpiration rate of *r2L.*
3	Real	P3	Value of the pressure head, h_4, below which root water uptake ceases (usually equal to the wilting point).
3	Real	*r2H*	Potential transpiration rate $[LT^{-1}]$ (currently set at 0.5 cm/day).
3	Real	*r2L*	Potential transpiration rate $[LT^{-1}]$ (currently set at 0.1 cm/day).

The above input parameters permit one to make the variabie h_3 a function of the potential transpiration rate, T_p (h_3 presumably decreases at higher transpiration rates). SWMS_3D currently implements the same linear interpolation scheme as used in several versions of the SWATRE code (e.g., *Wesseling and Brandyk, 1985). The* scheme is based on the following interpolation:

$$h, = P2H + \frac{P2L - P2H}{r2H - r2L}(r2H - T_p) \qquad \textit{for } r2L < T_p < r2H$$

$$h, = P2L \qquad \text{for } T_a \leq \textit{r2L}$$
$$h, = P2H \qquad \textit{for } T_a \geq \textit{r2H}$$

Record	Type	Variable	Description
4		-	Comment line.
5	Real	*POptm(*1)	Value of the pressure head, h_2, below which roots start to extract water at the maximum possible rate (material number 1).
5	Real	*POptm(2)*	As above (material number 2).
5	ReaI	*POptm(NMat)*	As above (for material number *NMat).*

[+] Block D is not read in if the logical variable *SinkF* (Block K) is set equal to .false.

Table 8.5. Block E - Seepage face information.[†]

Record	Type	Variable	Description
1,2	-		Comment lines.
3	Integer	*NSeep*	Number of seepage faces expected to develop.
4			Comment line.
5	Integer	*NSP(1)*	Number of nodes on the first seepage face.
5	Integer	NSP(2)	Number of nodes on the second seepage face.
.	.	.	
.	.	.	
5	Integer	*NSP(NSeep)*	Number of nodes on the last seepage face.
6			Comment line.
7	Integer	*NP(l,1)*	Sequential global number of the first node on the first seepage face.
7	Integer	*NP(1,2)*	Sequential global number of the second node on the first seepage face.
7	Integer	*NP(1,NSP(1))*	Sequential global number of the last node on the first seepage face.
			Record 7 information is provided for each seepage face.

[†] Block E is not read in if the logical variable *SeepF* (Block A) is set equal to .false. .

Table 8.6. Block F - Drainage information.'

Record	Type	Variable	Description
1,2		_	Comment lines.
3	Integer	**NDr**	Number of drains. See Section 4.3.7 for a discussion on how tile drains can be represented as boundary conditions in a regular finite element mesh.
3	Real	**DrCorr**	Additional reduction in the correction factor C_d (See Section 4.3.7).
4			Comment line.
5	Integer	**ND(l)**	Number of nodes representing the first drain.
5	Integer	**ND(2)**	Number of nodes representing the second drain.
.			
5	Integer	**ND(NDr)**	Number of nodes representing the last drain.
6		_	Comment line.
7	Integer	**NElD(1)**	Number of elements surrounding the first drain in a plane perpendicular to the drain.
7	Integer	**NElD(2)**	Number of elements surrounding the second drain in a plane perpendicular to the drain.
7	Integer	**NElD(NDr)**	Number of elements surrounding the last drain in a plane perpendicular to the drain.
8			Comment line.
9	Real	EfDim(1,1)	Effective diameter of the first drain (see Section 4.3.7).
9	Real	EfDim(2,l)	Dimension of the square in finite element mesh in a plane perpendicular to a drain, representing the first drain (see Section 4.3.7).
			Record 9 information is provided for each drain.
10			Comment line.
11	Integer	KNoDr(1,1)	Global number of the first node representing the first drain.
11	Integer	KNoDr(1,2)	Global number of the second node representing the first drain.
11	Integer	**KNoDr(1 ,ND(1))**	Global number of the last node representing the first drain.
			Record 11 information is provided for each drain.
12			Comment line.
13	Integer	KElDr(l,I)	Global number of the first element surrounding the first drain.
13	Integer	**KElDr(1,2)**	Global number of the second element surrounding the first drain.
I3	Integer	**KElDr(l,NElD(1))**	Global number of the last element surrounding the first drain.
			Record 13 information is provided for each drain.

† Block F is not read in if the logical variable **DrainF** (Block A) is set equal to .false. .

Table 8.7. Block G - Solute transport information.+

Record	Type	Variable	Description
1,2		–	Comment lines.
3	Real	**Epsi**	Temporal weighing coefficient. =O.O for an explicit scheme. =0.5 for a Crank-Nicholson implicit scheme. =1.0 for a fully implicit scheme.
3	- Logical	**lUpW**	**.true.** if upstream weighing formulation is to be used. **.false.** if the original Galerkin formulation is to be used.
3	Logical	**1ArtD**	**.true.** if artificial dispersion is to be added in order to fulfill the stability criterion **PeCr (see** Section 5.3.6). **.false.** otherwise.
3	Real	**PeCr**	Stability criterion (see Section 5.3.6). Set equal to zero when *lUpW* is equal to **.true..**
4		–	Comment line.
5	Real	**ChPar(** 1 ,M)	Bulk density of material M, ρ [ML^{-3}].
5	Real	**ChPar(2,M)**	Ionic or molecular diffusion coefficient in free water, D_d [L^{2}T^{-1}].
5	Real	**ChPar(3,M)**	Longitudinal dispersivity for material type M, D_L [L].
5	Real	**ChPar(4,M)**	Transverse dispersivity for material type M, D_T [L].
5	Real	**ChPar(5,M)**	Freundlich isotherm coefficient for material type M, k [M^{-1}L^3].
5	Real	**ChPar(6,M)**	First-order rate constant for dissolved phase, material type M, μ_w [T^{-1}].
5	Real	**ChPar(7,M)**	First-order rate constant for solid phase, material type M, μ_s [T^{-1}].
5	Real	**ChPar(8,M)**	Zero-order rate constant for dissolved phase, material type M, γ_w [ML^{-3}T^{-1}].
5	Real	**ChPar(9,M)**	Zero-order rate constant for solid phase, material type M, γ_s [T^{-1}].
			Record 5 information is provided for each material M (from 1 to **NMat).**
6		–	Comment line.
7	Integer	**KodCB(** 1)	Code specifying the type of boundary condition for solute transport applied to a particular node. Positive (+ 1) and negative (- l) signs indicate that first-, or second- or third- (depending upon the calculated water flux Q) type boundary condition are implemented, respectively. **KodCB(l) = 0** for all outflow boundary nodes. In case of time-independent boundary conditions (*Kode*(i)=±1, or ±6 - **See** Block H), **KodCB(1)** also refers to the field **cBound** for the value of the solute transport boundary condition. The value of **cBound(abs(KodCB(** 1))) specifies the boundary condition for node **KXB(1)** (the first of a set of sequentially numbered boundary nodes for which **Kode(N)** is not equal to zero). Permissible values are ±1,±2,...,±9,±10.
7	Integer	**KodCB(2)**	Same as above for the second boundary node.
.			
.			
7	Integer	**KodCB(NumBP)**	**Same as** above for the last boundary node.
8			Comment line.

Table 8.7. (continued)

Record	Type	Variable	Description
9	Real	cBound(1)	Concentration [ML"] for nodes with a time-independent boundary condition ($Kode(i)$=±1, or ±6) for which $KodCB(n)$=±1 is specified. Set *cBound(1)* equal to zero if no time-independent boundary condition and no $KodCB(n)$=±1 is specified.
9	Real	*cBound(2)*	Concentration $[ML^{-3}]$ for nodes with a time-independent boundary condition ($Kode(i)$=±1, or ±6) for which $KodCB(n)$=±2 is specified. Set *cBound(2)* equal to zero if no time-independent boundary condition and no $KodCB(n)$=±2 is specified.
9	Real	*cBound(10)*	Concentration [ML"] for nodes with a time-independent boundary condition ($Kode(i)$=±1, or ±6) for which $KodCB(n)$=±10 is specified. Set *cBound(I0)* equal to zero if no time-independent boundary condition and no $KodCB(n)$=±10 is specified.
9	Real	*cBound(11)*	If internal sources are specified, then *cBound(l1)* is **used** for the concentration of fluid injected into the flow region through internal sources [ML"]. Set equal to zero if no internal sources are specified.
9	Real	*cBound(12)*	If water uptake is specified, then *cBound(12)* is used for the concentration of fluid removed from the flow region by root water uptake [ML"]. Set equal to zero if root solute uptake is not specified.
10	-	-	Comment line.
11	Real	*Pulse*	Time duration of the concentration pulse for constant head or inflow flux boundary and source nodes [T]. The current version of SWMS_3D assumes that the time durations of concentration pulses imposed on different boundary segments are the same.

[†] Block G is not needed when the logical variable lChem in Block A is set equal to .false..

A summary of possible codes for solute transport boundary conditions is given in Table 6.7.

Table 8.8. Block H - Nodal information.'

Record	Type	Variable	Description
1,2	–		Comment lines.
3	Integer	*NumNP*	Number of nodal points.
3	Integer	*NumEl*	Number of elements (tetrahedrals, hexahedrals and/or triangular prisms).
3	Integer	*IJ*	Maximum number of nodes on any transverse line. Set equal to zero if IJ> 10.
3	Integer	*NumBP*	Number of boundary nodes for which *Kode(n)* is not equal to 0.
3	Integer	*NObs*	Number of observationnodes for which values of the pressure head, water content, and concentration (for *IChem=.true.) are* printed at each time level.
4			Comment line.
5	Integer	*n*	Nodal number.
5	Integer	*Kode(n)*	Code specifying the type of boundary condition applied to a particular node. Permissible values are $0,\pm1,\pm2,\pm3,\pm4,...,\pm6$ *(NumKD) (see* Section 6.3).
5	Real	*x(n)*	x-coordinate of node n [L] (a horizontal coordinate).
5	Real	*y(n)*	y-coordinate of node n [L] (a horizontal coordinate).
5	Real	*z(n)*	z-coordinate of node *n [L] (z* is the vertical coordinate).
5	Real	*hNew(n)*	Initial value of the pressure head at node *n* [L]. If IWat=.false. in Block A, then *hNew(n)* represents the initial guess of the pressure head for steady state conditions.
5	Real	*Conc(n)*	Initial value of the concentration at node n [ML"] (set = 0 if lChem=.false.).
5	Real	Q(n)	Prescribed recharge/discharge rate at node n $[L^3 T^{-1}]$. Q(n) is negative when directed out of the system. When no value for Q(n) is needed, set Q(n) equal to zero.
5	Integer	*MatNum(n)*	Index for material whose hydraulic and transport properties are assigned to node *n*.
5	Real	*Beta(n)*	Value of the root water uptake distribution, *b(x, y, z),* in the soil root zone at node n. Set *Beta(n)* equal to zero if node *n* lies outside the root zone. See Section 2.2 for detailes.
5	Real	*Axz(n)*	Nodal value of the dimensionless scaling factor α_h associated with the pressure head. See Section 2.4 for detailes.
5	Real	*Bxz(n)*	Nodal value of the dimensionless scaling factor α_K associated with the saturated hydraulic conductivity. See Section 2.4 for detailes.
5	Real	*Dxz(n)*	Nodal value of the dimensionless scaling factor α_θ associated with the water content. See Section 2.4 for detailes.

Table 8.8. (continued)

Record	Type	Variable	Description
			In general, record 5 information is required for each node n, starting with n= 1and continuing sequentially until $n=NumNP$. Record 5 information for certain nodes may be skipped if several conditions are satisfied (see beginning of this section).

[†] This block can be generated for hexahedral flow region by program GENER3 (See Table 8.12).

Table 8.9. Block I - Element information.+

Record	Type	Variable	Description
1,2	-		Comment lines.
3	Integer	e	Element number.
3	Integer	KX(e, 1)	Global nodal number of the first comer node i.
3	Integer	KX(e,2)	Global nodal number of the second comer node j.
3	Integer	KX(e,3)	Global nodal number of the third comer node k.
3	Integer	KX(e,4)	Global nodal number of the forth comer node 1.
3	Integer	KX(e,5)	Global nodal number of the fifth comer node *m*.
3	Integer	KX(e,6)	Global nodal number of the sixth comer node n.
3	Integer	KX(e,7)	Global nodal number of the seventh comer node o.
3	Integer	KX(e,8)	Global nodal number of the eighth comer node p. Indices *i, j, k, l, m, n, o* and p, refer to the comer nodes of an element e taken in a certain orientation as described in Section 6.1. KX(e,5) for tetrahedral and KX(e,7) for triangular prismatic elements must be equal to zero.
3	Integer	KX(e,9)	Code specifying the subdivision of hexahedral and triangular prismatic elements yinto tetrahedrals (See Chapter 6.1 and Figure 6.1).
3	Real	**ConA** l(e)	First principal component, K_1^A, of the dimensionless tensor $\mathbf{K}^A$ describing the local anisotropy of the hydraulic conductivity assigned to element e.
3	Real	**ConA2(e)**	Second principal component, K_2^A of $\mathbf{K}^A$.
3	Real	**ConA3(e)**	Third principal component, K_3^A of $\mathbf{K}^A$.
3	Real	Cosl l(e)	Cosine of the angle between the first principal conductivity direction, X, and the x-coordinate axis.
3	Real	**Cos22(e)**	Same for the second principal conductivity direction, Y, and the y-coordinate axis.
3	Real	**Cos33(e)**	Same for the third principal conductivity direction, Z, and the z-coordinate axis.
3	Real	Cos12(e)	Same for the first principal conductivity direction, X, and the y-coordinate axis.
3	Real	Cosl3(e)	Same for the first principal conductivity direction, X, and the z-coordinate axis.
3	Real	Cos23(e)	Same for the second principal conductivity direction, Y, and the z-coordinate axis.
3	Integer	LayNum(e)	Subregion number assigned to element e.
			In general, record 3 information is required for each element e, starting with e= 1 and continuing sequentially until *e=NumEl,* Record 3 information for certain elements may be skipped if several conditions are satisfied (see beginning of this section).

+ This block for a hexahedral flow region can be generated with program GENER3 (See Table 8.12).

Table 8.10. Block J - Boundary geometry information.[+]

Record	Type	Variable	Description
1,2			Comment lines.
3	Integer KXB(1)		Global node number of the first of a set of sequentially numbered boundary nodes for which Kode(n) is not equal to zero.
3	Integer	KXB(2)	As above for the second boundary node.
.			
3	Integer	*KXB(NumBP)*	As above for the last boundary node.
4			Comment line.
5	Real	*Width(* 1)	Surface area of the boundary $[L^2]$ associated with boundary node *KXB(1).* *Width(n)* includes *one* quarter of the boundary surface area of each element connected to node *KXB(n)* along the boundary. The type of boundary condition assigned to *KXB(n)* is determined by the value of *Kode(n)* If a unit vertical hydraulic gradient or a deep drainage boundary condition is specified at node n, then *Width(n)* represents only the horizontal component of the boundary.
5	Real	*Width(2)*	As above for node KXB(2).
5	Real	*Width(NumBP)*	As above for node *KXB(NumBP).*
6	-	-	Comment line.
7	Real	*d e n*	Area of soil surface associated with transpiration $[L^2]$. Set *rLen* equal to zero for problems without transpiration.
8			Comment line.
9	Integer *Node(1)*		Global node number of the first observation node for which values of the pressure head, water content, and concentration (for *IChem=.true.)* are printed at each time level.
9	Integer *Node(2)*		*Same as* above for the second observation node.
.			
.			
9	Integer *Node(NObs)*		*Same* as above for the last observation node.

[†]   This block for a hexahedral flow region can be generated with program GENER3 (See Table 8.12).

Table 8.11. Block K - Atmospheric information.+

Record	Type	Variable	Description
1,2,3,4	-	-	Comment lines.
5	Logical	*SinkF*	Set this variable equal to .true. if water extraction from the root zone is imposed.
5	Logical	*qGWLF*	Set this variable equal to .true. if the discharge-groundwater level relationship *q(GWL)* given by equation (6.1) is used as the bottom boundary condition; G *WL=h-G WLOL,* where *h* is the pressure head at the boundary.
6		_	Comment line.
7	Real	G *WLOL*	Reference position of groundwater table (usually the z-coordinate of the soil surface).
7	Real	Aqh	Value of the parameter A, $[LT^{-1}]$ *in* the q(GWL)-relationship (equation (6.1)); set to zero if *qGWLF=.false.*
7	Real	Bqh	Value of the parameter B_{qh} $[L^{-1}]$ in the q(GWL)-relationship (equation (6.1)); set to zero if *qGWLF =*.false.
8			Comment line.
9	Real	*tInit*	Starting time [T] of the simulation.
9	Integer	*MaxAl*	Number of atmospheric data records.
10		_	Comment line.
11	Real	*hCritS*	Maximum allowed pressure head at the soil surface [L].
12		-	Comment line.
13	Real	*tAtm(i)*	Time for which the *i-th* data record is provided [T].
13	Real	*Prec(i)*	Precipitation $[LT^{-1}]$ (in absolute value).
13	Real	*cPrec(i)*	Solute concentration of rainfall water $[ML^{-3}]$ (set = 0 if lChem=.false.).
13	Real	*rSoil(i)*	Potential evaporation rate $[LT^{-1}]$ (in absolute value).
13	Real	*rRoot(i)*	Potential transpiration rate $[LT^{-1}]$ (in absolute value).
13	Real	*hCritA(i)*	Absolute value of the minimum allowed pressure head at the soil surface [L].
13	Real	*rG WL(i)*	Time-dependent prescribed flux (positive when water leaves the flow region) for nodes where *Kode(n)= -3.* Set to zero when no *Kode(n)=-3* boundary condition is specified.
13	Real	*GWL(i)*	Time-dependent prescribed head for nodes where *Kode(n)=3,* i.e., groundwater level [L] (usually negative). Set to zero when no *Kode(n)=3* is specified. The prescribed value of the pressure head is *h=GWL+GWLOL.*

Table 8.11. (continued)

Record	Type	Variable	Description
13	Real	*crt(i)*	Time-dependent concentration for the third-type boundary condition at the changing inflow flux boundary [ML^{-3}] where *Kode*(*n*)=±3 and KodCB(n)<0; set to zero otherwise.
13	Real	*cht(i)*	Time-dependent concentration [ML^{-3}] for the first-type boundary condition prescribed for nodes for which *Kode*(*n*)=±3 and *KodCB(n)>0.* Set to zero otherwise.
			The total number of atmospheric data records is *MaxAl* (i=1,2, ..,*MaxAl).*

[†] Block K is not read if the logical variable AtmInf(Block A) is set equal to .false.

Table 8.12. Block L - Input file 'GENER3.IN' for finite element mesh generator.

Record	Type	Variable	Description
1,2	-		Comment lines.
3	Real	ConA 1	First principal component, K_1^A, of the dimensionless tensor $\mathbf{K}^A$ which describes the local anisotropy of the hydraulic conductivity assigned to all elements.
3	Real	ConA2	Second principal component, K_2^A of $\mathbf{K}^A$.
3	Real	ConA3	Third principal component, K_3^A of $\mathbf{K}^A$.
3	Real	Cosll	Cosine of the angle between the first principal conductivity direction, X, and the x-coordinate axis.
3	Real	cos22	Same for the second principal conductivity direction, Y, and the y-coordinate axis.
3	Real	cos33	Same for the third principal conductivity direction, Z, and the z-coordinate axis.
3	Real	cos12	Same for the first principal conductivity direction, X, and the y-coordinate axis.
3	Real	cos13	Same for the first principal conductivity direction, X, and the z-coordinate axis.
3	Real	Cos23	Same for the second principal conductivity direction, Y, and the z-coordinate axis.
4	-		Comment lines.
5	Integer	**NLinZ**	Number of nodal points in the direction of the vertical axis z.
5	Integer	**NColX**	Number of nodal points in the direction of the horizontal axis x.
5	Integer	**NColY**	Number of nodal points in the direction of the horizontal axis y.
6			Comment lines.
7	Real	**xCol**	x-coordinate of the front left bottom node [L].
7	Real	**ycol**	y-coordinate of the front left bottom node [L].
7	Real	**zLin**	z-coordinate of the front left bottom node [L].
8,9			Comment lines.
10	Real	**dx(i)**	Array of Ax increments [L], $i = I, 2,..., (NColX-I)$ input subsequently from left to right.
11			Comment lines.
12	Real	**dy(i)**	Array of Ay increments [L], $i = 1, 2,..., (NColY-1)$. Input subsequently from front to back.
13		-	Comment lines.
14	Real	**dz(i)**	Array of Δz increments [L], $i = 1, 2,..., (NLinZ-1)$. Input subsequently from top to bottom.
15,16		-	Comment lines.
17	Integer	**n**	Number of the horizontal layers starting at the upper boundary and continuing down to the bottom.
17	Integer	**Kode(n)**	Code specifying the type of boundary condition applied to nodes of a particular

100

Table 8.12. (continued)

Record	Type	Variable	Description
17	Real	*hOld(n)*	Initial value of the pressure head assigned to nodes of a particular horizontal layer n [L].
17	Real	*Conc(n)*	Initial value of the concentration assigned to nodes of a particular horizontal layer *n [ML"]*.
17	Real	*Q(n)*	Prescribed recharge/dischargerate assigned to node n, $[L^3T^{-1}]$. Q(n) is negative when directed out of the system. When no value for Q(n) is needed, set Q(n) equal to zero.
17	Int	*LayNum(n)*	Subregion number assigned to nodes of a particular horizontal layer *n*.
17	Real	*Beta(n)*	Value of the water uptake distribution, b(x,y,z), in the soil root zone assigned to nodes of a particular horizontal layer n [L"]. Set *Beta(n)* equal to zero if horizontal layer n lies entirely outside the root zone.
17	Real	Axz(n)	Nodal value of the dimensionless scaling factor α_h associated with the pressure head assigned to nodes of a particular horizontal layer n.
17	Real	*Bxz(n)*	Nodal value of the dimensionless scaling factor α_K associated with the saturated hydraulic conductivity assigned to nodes of a particular horizontal layer n.
17	Real	*Dxz(n)*	Nodal value of the dimensionless scaling factor α_θ associated with the water content assigned to nodes of a particular horizontal layer *n*.
			In general, record 17 information is required for each horizontal layer n, starting with n= 1 and continuing sequentially until *n=NLinZ*. Record 17 information for certain horizontal layers may be skipped if several conditions are satisfied (see beginning of this section).

8.2. Example Input Files

Table 8.13. Input data for example ↑ (input file 'SELECTOR.IN').

```
*** BLOCK A: BASIC INFORMATION • ****************************************
Heading
'Example 1 · Column Test'
LUnit   TUnit   MUnit                  (units are obligatory for all input data)
'cm'    'sec'   '-'
MaxIt   TolTh   TolH (max. number of iterations and precis. tolerances)
  20    .0001    .1
LWat    LChem   CheckF  ShortF  FluxF  AtmInF  SeepF  FreeD  DrainF
  t       f       f       t      t       f      t      f      f
• ** BLOCK 8: MATERIAL INFORMATION  ****************************************
NMat    NLay    hTabl   hTabN   NPar
  1      1      .001    200.     9
thr     ths     tha     thm     Alfa    n      Ks      Kk      thk
.02    -350    .02     .350    .0410  1.964  .000722 .000695 .2875
*** BLOCK C: TIME INFORMATION  *****************************************
dt      dtMin   dtMax   DMul    DMul2   MPL
 1.     -01     60.     1.1     .33      6
TPrint(1),TPrint(2),...,TPrint(MPL)                 (print-time array)
 60 900 1800 2700 3600 5400
*** BLOCK E: SEEPAGE INFORMATION (only if SeepF =.true.) **************
NSeep                                      (number of seepage faces)
 1
NSP(1),NSP(2) ,.......,NSP(NSeep)          (number of nodes in each s.f.)
 4
NP(i,1),NP(i,2),.....,NP(i,NSP(i))     (nodal number array of i-th s.f.)
 221 222 223 224
*** END OF INPUT FILE 'SELECTOR.IN'  ***************************************
```

Table 8.14. Input data for example 1 (input file 'GENER3.IN').

```
*** INPUT FILE 'GENER3.IN' **********************************************
Aniz1  Aniz2  Aniz3 Cos11 Cos22 Cos33 Cos12 Cos13 Cos23     (Anis. Inf.)
  1.     1.     1.   1.    1.    1.    0.    0.    0.
NLinZ  NColX  NColY   (Number of nodal points in a particular direction)
  56     2      2
xCol(1)yCol(1)z(NLin)       (x,y,z-coordinates of front left bottom node)
  0      0      0
*** SPACE INCREMENTS ****************************************************
dx-array (number of items is NColX-1):
  1
dy-array (number of items is NColY-1):
  1
dz-array (number of items is NLinZ-1):
  4*.25  2*.5  39*1  10*2
*** LINE ATTRIBUTES ****************************************************
LineNumber  Code  hInit   Conc  Q    MatNum  Beta  Axz  Bxz  Dxz
    1         1    .75     1.   0.      1      0.    1.   1.   1.
    2         0    -150    0.   0.      1      0.    1.   1.   1.
   55         0    -150    0.   0.      1      0.    1.   1.   1.
   56        -2    -150    0.   0.      1      0.    1.   1.   1.
*** END OF INPUT FILE 'GENER3.IN' **************************************
```

103

Table 8.15. Input data for example 1 (input file 'GRID.IN').[†]

```
*** BLOCK H: NODAL INFORMATION *******************************************************
  NumNP    NumEl      IJ    NumBP     NObs
   224       55        4       8        0
   n Code      x         y         z        h          Conc        Q         M    B     Axz   Bxz   Dxz
   1    1     .00       .00      61.00   .7500E+00   .1000E+01   .0000E+00   1   .00  1.00  1.00  1.00
   2    1    1.00       .00      61.00   .7500E+00   .1000E+01   .0000E+00   1   .00  1.00  1.00  1.00
   3    1     .00      1.00      61.00   .7500E+00   .1000E+01   .0000E+00   1   .00  1.00  1.00  1.00
   4    1    1.00      1.00      61.00   .7500E+00   .1000E+01   .0000E+00   1   .00  1.00  1.00  1.00
   5    0     .00       .00      60.75  -.1500E+03   .0000E+00   .0000E+00   1   .00  1.00  1.00  1.00
   6    0    1.00       .00      60.75  -.1500E+03   .0000E+00   .0000E+00   1   .00  1.00  1.00  1.00
   7    0     .00      1.00      60.75  -.1500E+03   .0000E+00   .0000E+00   1   .00  1.00  1.00  1.00
   8    0    1.00      1.00      60.75  -.1500E+03   .0000E+00   .0000E+00   1   .00  1.00  1.00  1.00
   9    0     .00       .00      60.50  -.1500E+03   .0000E+00   .0000E+00   1   .00  1.00  1.00  1.00
  10    0    1.00       .00      60.50  -.1500E+03   .0000E+00   .0000E+00   1   .00  1.00  1.00  1.00
  11    0     .00      1.00      60.50  -.1500E+03   .0000E+00   .0000E+00   1   .00  1.00  1.00  1.00
  12    0    1.00      1.00      60.50  -.1500E+03   .0000E+00   .0000E+00   1   .00  1.00  1.00  1.00
  13    0     .00       .00      60.25  -.1500E+03   .0000E+00   .0000E+00   1   .00  1.00  1.00  1.00
  14    0    1.00       .00      60.25  -.1500E+03   .0000E+00   .0000E+00   1   .00  1.00  1.00  1.00
                  .        .         .        .           .           .
                  .        .         .        .           .           .
                  .        .         .        .           .           .
 215    0     .00      1.00       4.00  -.1500E+03   .0000E+00   .0000E+00   1   .00  1.00  1.00  1.00
 216    0    1.00      1.00       4.00  -.1500E+03   .0000E+00   .0000E+00   1   .00  1.00  1.00  1.00
 217    0     .00       .00       2.00  -.1500E+03   .0000E+00   .0000E+00   1   .00  1.00  1.00  1.00
 218    0    1.00       .00       2.00  -.1500E+03   .0000E+00   .0000E+00   1   .00  1.00  1.00  1.00
 219    0     .00      1.00       2.00  -.1500E+03   .0000E+00   .0000E+00   1   .00  1.00  1.00  1.00
 220    0    1.00      1.00       2.00  -.1500E+03   .0000E+00   .0000E+00   1   .00  1.00  1.00  1.00
 221   -2     .00       .00        .00  -.1500E+03   .0000E+00   .0000E+00   1   .00  1.00  1.00  1.00
 222   -2    1.00       .00        .00  -.1500E+03   .0000E+00   .0000E+00   1   .00  1.00  1.00  1.00
 223   -2     .00      1.00        .00  -.1500E+03   .0000E+00   .0000E+00   1   .00  1.00  1.00  1.00
 224   -2    1.00      1.00        .00  -.1500E+03   .0000E+00   .0000E+00   1   .00  1.00  1.00  1.00
*** BLOCK I: ELEMENT INFORMATION *****************************************************
   e    i    j    k    l    m    n    o    p   Sub  Aniz1  Aniz2  Aniz3  --- CosAngle----  LayNum
   1    1    2    3    4    5    6    7    8    1   1.00   1.00   1.00   1  1  1  0  0  0     1
   2    5    6    7    8    9   10   11   12    2   1.00   1.00   1.00   1  1  1  0  0  0     1
   3    9   10   11   12   13   14   15   16    1   1.00   1.00   1.00   1  1  1  0  0  0     1
   4   13   14   15   16   17   18   19   20    2   1.00   1.00   1.00   1  1  1  0  0  0     1
   5   17   18   19   20   21   22   23   24    1   1.00   1.00   1.00   1  1  1  0  0  0     1
   6   21   22   23   24   25   26   27   28    2   1.00   1.00   1.00   1  1  1  0  0  0     1
   7   25   26   27   28   29   30   31   32    1   1.00   1.00   1.00   1  1  1  0  0  0     1
   8   29   30   31   32   33   34   35   36    2   1.00   1.00   1.00   1  1  1  0  0  0     1
   9   33   34   35   36   37   38   39   40    1   1.00   1.00   1.00   1  1  1  0  0  0     1
  10   37   38   39   40   41   42   43   44    2   1.00   1.00   1.00   1  1  1  0  0  0     1
            .         .         .
            .         .         .
            .         .         .
  48  189  190  191  192  193  194  195  196    2   1.00   1.00   1.00   1  1  1  0  0  0     1
  49  193  194  195  196  197  198  199  200    1   1.00   1.00   1.00   1  1  1  0  0  0     1
  50  197  198  199  200  201  202  203  204    2   1.00   1.00   1.00   1  1  1  0  0  0     1
  51  201  202  203  204  205  206  207  208    1   1.00   1.00   1.00   1  1  1  0  0  0     1
  52  205  206  207  208  209  210  211  212    2   1.00   1.00   1.00   1  1  1  0  0  0     1
  53  209  210  211  212  213  214  215  216    1   1.00   1.00   1.00   1  1  1  0  0  0     1
  54  213  214  215  216  217  218  219  220    2   1.00   1.00   1.00   1  1  1  0  0  0     1
  55  217  218  219  220  221  222  223  224    1   1.00   1.00   1.00   1  1  1  0  0  0     1
*** BLOCK J : BOUNDARY INFORMATION ***************************************************
Node number array:
       1        2        3        4      221      222      223      224
Width array:
    .33333   .16667   .16667   .33333   .16667   .33333   .33333   .16667
Length:
    0.00
***** End of file Grid.In ************************************************************
```

[†] This file was generated using code GENER3.

Table 8.16. Input data for example 2 (input file 'SELECTOR.IN').

```
*** BLOCK A: BASIC INFORMATION • ****************************************
Heading
'Example 2 - Grass Field Problem (Hupselse Beek 1982)'
LUnit TUnit MUnit (indicated units are obligatory for all input data)
'cm'    'day'    '-'
MaxIt   TolTh   TolH (max. number of iterations and precis. tolerances)
 20     .0001   0.1
1Wat    1Chem   CheckF  ShortF  FluxF   AtmInF  Seepf   FreeD   DrainF
 t       f       f       t       t       t       f       f       f
*** BLOCK B: MATERIAL INFORMATION ***************************************
NMat    NLay    hTabl   hTabN   NPar
 2       2      .001    1000.    9
thr     ths     tha     thm     Alfa    n       Ks      Kk      thk
.0001   .399    .0001   .399    .0174   1.3757  29.75   29.75   .399
.0001   .339    .0001   .339    .0139   1.6024  45.34   45.34   .339
*** BLOCK C: TIME INFORMATION ******************************************
dt      dtMin   dtMax   DMul    DMul2   MPL
 .02    1e-10   0.50    1.3     .3      6
TPrint(1),TPrint(2),...,TPrint(MPL)                    (print-time array)
 120  151  181  212  243  273
*** BLOCK D: SINK INFORMATION ******************************************
P0      P2H     P2L     P3      r2H     r2L
-10.    -200.   -800.   -8000.  0.5     0.1
POptm(1),POptm(2),...,POptm(NMat)
-25.    -25.
• ** END OF INPUT FILE 'SELECTOR.IN '  ****************************
```

Table 8.17. Input data for example 2 (input fil 'ATMOSPH.IN').

```
*** BLOCK K: ATMOSPHERIC INFORMATION   **********************************
*** Hupselse Beek 1982                  ****************************
***********************************************************************
SinkF   qGWLF
  t       t
GWLOL   Aqh     Bqh                          (if qGWLF=f then Aqh=Bqh=0)
 230    -.1687  -.02674
tInit   MaxAL                       (MaxAL = number of atmospheric data-records)
 90.     183
hCritS                              (max. allowed pressure head at the soil surface)
 1e30
```

tAtm	Prec	cPrec	rSoil	rRoot	hCritA	rt	ht	crt	cht
91	0	0	0	0.16	1000000	0	0	0	0
92	0.07	0	0	0.18	1000000	0	0	0	0
93	0.02	0	0	0.13	1000000	0	0	0	0
94	0	0	0	0.20	1000000	0	0	0	0
95	0	0	0	0.28	1000000	0	0	0	0
96	0.07	0	0	0.18	1000000	0	0	0	0
97	0.29	0	0	0.08	1000000	0	0	0	0
98	0.44	0	0	0.14	1000000	0	0	0	0
99	0.20	0	0	0.11	1000000	0	0	0	0
100	0.29	0	0	0.11	1000000	0	0	0	0
1 0 1	0.32	0	0	0.11	1000000	0	0	0	0
102	0.49	0	0	0.11	1000000	0	0	0	0
103	0.01	0	0	0.16	1000000	0	0	0	0
104	0	0	0	0.17	1000000	0	0	0	0
105	0	0	0	0.22	1000000	0	0	0	0
106	0	0	0	0.21	1000000	0	0	0	0
107	0	0	0	0.23	1000000	0	0	0	0
108	0	0	0	0.23	1000000	0	0	0	0
109	0	0	0	0.24	1000000	0	0	0	0
110	0	0	0	0.18	1000000	0	0	0	0
111	0	0	0	0.15	1000000	0	0	0	0
112	0	0	0	0.19	1000000	0	0	0	0
113	0.01	0	0	0.15	1000000	0	0	0	0
114	0.01	0	0	0.22	1000000	0	0	0	0
115	0	0	0	0.23	1000000	0	0	0	0
116	0.02	0	0	0.20	1000000	0	0	0	0
117	0	0	0	0.17	1000000	0	0	0	0
118	0.02	0	0	0.14	1000000	0	0	0	0
119	0.26	0	0	0.13	1000000	0	0	0	0
120	0.24	0	0	0.11	1000000	0	0	0	0
.	.								
256	0	0	0	'0.13	1000000	0	0	0	0
257	0	0	0	0.14	1000000	0	0	0	0
258	0	0	0	0.20	1000000	0	0	0	0
259	0	0	0	0.14	1000000	0	0	0	0
260	0	0	0	0.19	1000000	0	0	0	0
261	0	0	0	0.14	1000000	0	0	0	0
262	0	0	0	0.20	1000000	0	0	0	0
263	0.35	0	0	0.23	1000000	0	0	0	0
264	0.52	0	0	0.16	1000000	0	0	0	0
265	0	0	0	0.21	1000000	0	0	0	0
266	0	0	0	0.19	1000000	0	0	0	0
267	0	0	0	0.18	1000000	0	0	0	0
268	0	0	0	0.18	1000000	0	0	0	0
269	0.53	0	0	0.09	1000000	0	0	0	0
270	0.07	0	0	0.23	1000000	0	0	0	0
271	0	0	0	0.17	1000000	0	0	0	0
272	0	0	0	0.22	1000000	0	0	0	0
273	1.04	0	0	0	1000000	0	0	0	0

```
*** END OF INPUT FILE 'ATMOSPH.IN'  *********************************
```

Table 8.18. Input data for example 2 (input file ' GENER3 . IN').

```
*** INPUT FILE 'GENER3.IN'  **********************************************
Aniz1 Aniz2 Aniz3 Cos11 Cos22 Cos33 Cos12 Cos13 Cos23      (Anis.  Inf.)
  1.    1.    1.    1.    1.    1.    0.    0.    0.
NLinZ   NColX NColY   (Number of nodal points in a particular direction)
  33      2     2
xCol(l)yCol(l)z(NLin)           (x,y,z-coordinates  of  front  left  bottom node)
  0       0      0
*** SPACE INCREMENTS ***********************************************
dx-array (number of items is NColX-1):
  1
dy-array (number of items is NColY-1):
  1
dz-array (number of items is NLinZ-1):
 2*1  2*2   4 4*5 19*10 5 3 2*1
*** LINE ATTRIBUTES ***********************************************
LineNumber   Code   hInit   Conc   Q   MatNum  Beta   A x z  Bxz  Dxz
    1         -4    -55.     0.    0.    1      0.    1.    1.    1.
    2          0    -54.     0.    0.    1      0.    1.    1.    1.
    3          0    -53.     0.    0.    1      1.    I.    1.    1.
    4          0    -51.     0.    0.    1      1.    1.    1.    1.
    5          0    -49.     0.    0.    1      1.    1.    1.    1.
    6          0    -45.     0.    0.    1      1.    1.    1.    I.
    7          0    -40.     0.    0.    1      1.    1.    1.    1.
    8          0    -35.     0.    0.    1      1.    I.    1.    1.
    9          0    -30.     0.    0.    1      1.    1.    1.    1.
   10          0    -25.     0.    0.    1      1.    1.    1.    1.
   11          0    -15.     0.    0.    1      0.    1.    1.    1.
   12          0     -5.     0.    0.    2      0.    1.    1.    I.
   13          0      5.     0.    0.    2      0.    I.    1.    1.
   14          0     15.     0.    0.    2      0.    1.    1.    1.
   15          0     25.     0.    0.    2      0.    1.    1.    I.
   16          0     35.     0.    0.    2      0.    1.    1.    1.
   17          0     45.     0.    0.    2      0.    1.    1.    1.
   18          0     55.     0.    0.    2      0.    1.    1.    1.
   19          0     65.     0.    0.    2      0.    1.    1.    1.
   20          0     75.     0.    0.    2      0.    1.    1.    1.
   21          0     85.     0.    0.    2      0.    1.    1.    1.
   22          0     95.     0.    0.    2      0.    1.    I.    1.
   23          0    105.     0.    0.    2      0.    1.    1.    1.
   24          0    115.     0.    0.    2      0.    1.    1.    1.
   25          0    125.     0.    0.    2      0.    1.    1.    1.
   26          0    135.     0.    0.    2      0.    1.    1.    1.
   27          0    145.     0.    0.    2      0.    1.    1.    1.
   28          0    155.     0.    0.    2      0.    1.    1.    1.
   29          0    165.     0.    0.    2      0.    1.    1.    1.
   30          0    170.     0.    0.    2      0.    I.    1.    1.
   31          0    173.     0.    0.    2      0.    1.    1.    1.
   32          0    174.     0.    0.    2      0.    1.    1.    1.
   33         -3    175.     0.    0.    2      0.    1.    1.    1.
*** END OF INPUT FILE 'GENER3.IN' **************************************
```

Table 8.19. Input data for example 2 (input file 'GRID.IN').[†]

```
*** BLOCK H: NODAL INFORMATION ******************************************************
  NumNP    NwnEl      IJ    NumBP    NObs
   132       32        4       8       0
    n  Code       x          y          z          h          Conc          Q          M    B     Axz    Bxz    Dxz
    1   -4       .00        .00      230.00    -.5500E+02    .0000E+00    .0000E+00    1   .00   1.00   1.00   1.00
    2   -4      1.00       -00      230.00    -.5500E+02    .0000E+00    .0000E+00    1   .00   1.00   1.00   1.00
    3   -4       .00       1.00     230.00    -.5500E+02    .0000E+00    .0000E+00    1   .00   1.00   1.00   1.00
    4   -4      1.00       1.00     230.00    -.5500E+02    .0000E+00    .0000E+00    1   .00   1.00   1.00   1.00
    5    0       .00        .00      229.00    -.5400E+02    .0000E+00    .0000E+00    1   .00   1.00   1.00   1.00
    6    0      1.00        .00      229.00    -.5400E+02    .0000E+00    .0000E+00    1   .00   1.00   1.00   1.00
    7    0       .00       1.00     229.00    -.5400E+02    .0000E+00    .0000E+00    1   .00   1.00   1.00   1.00
    8    0      1.00       1.00     229.00    -.5400E+02    .0000E+00    .0000E+00    1   .00   1.00   1.00   1.00
    9    0       .00        .00      228.00    -.5300E+02    .0000E+00    .0000E+00    1  1.00   1.00   1.00   1.00
   10    0      1.00        .00      228.00    -.5300E+02    .0000E+00    .0000E+00    1  1.00   1.00   1.00   1.00
   11    0       .00       1.00     228.00    -.5300E+02    .0000E+00    .0000E+00    1  1.00   1.00   1.00   1.00
   12    0      1.00       1.00     228.00    -.5300E+02    .0000E+00    .0000E+00    1  1.00   1.00   1.00   1.00
   13    0       .00        .00      226.00    -.5100E+02    .0000E+00    .0000E+00    1  1.00   1.00   1.00   1.00
   14    0      1.00        .00      226.00    -.5100E+02    .0000E+00    .0000E+00    1  1.00   1.00   1.00   1.00
   15    0       .00       1.00     226.00    -.5100E+02    .0000E+00    .0000E+00    1  1.00   1.00   1.00   1.00
   16    0      1.00       1.00     226.00    -.5100E+02    .0000E+00    .0000E+00    1  1.00   1.00   1.00   1.00
   17    0       .00        .00      224.00    -.4900E+02    .0000E+00    .0000E+00    1  1.00   1.00   1.00   1.00
   18    0      1.00        .00      224.00    -.4900E+02    .0000E+00    .0000E+00    1  1.00   1.00   1.00   1.00
   19    0       .00       1.00     224.00    -.4900E+02    .0000E+00    .0000E+00    1  1.00   1.00   1.00   1.00
   20    0      1.00       1.00     224.00    -.4900E+02    .0000E+00    .0000E+00    1  1.00   1.00   1.00   1.00
                     .
                                    .
  127    0       .00      '1.00      1.00     .1740E+03    .0000E+00    .0000E+00    2   .00   1.00   1.00   1.00
  128    0      1.00       1.00      1.00     .1740E+03    .0000E+00    .0000E+00    2   .00   1.00   1.00   1.00
  129   -3       .00        .00       .00     .1750E+03    .0000E+00    .0000E+00    2   .oo   1.00   1.00   1.00
  130   -3      1.00        .00       .00     .1750E+03    .0000E+00    .0000E+00    2   .oo   1.00   1.00   1.00
  131   -3       .00       1.00       .00     .1750E+03    .0000E+00    .0000E+00    2   .00   1.00   1.00   1.00
  132   -3      1.00       1.00       .00     .1750E+03    .0000E+00    .0000E+00    2   .oo   1.00   1.00   1.00
 ** BLOCK 1: ELEMENT INFORMATION ******************************************************
    e    i     j     k     l     m     n     o     p    Sub  Anizl  Aniz2  Aniz3 --- CosAngle---- LayNum
    1    1     2     3     4     5     6     7     8     1   1.00   1.00   1.00  1  1  1  0  0  0     1
    2    5     6     7     8     9    10    11    12     2   1.00   1.00   1.00  1  1  1  0  0  0     1
    3    9    10    11    12    13    14    15    16     1   1.00   1.00   1.00  1  1  1  0  0  0     1
    4   13    14    15    16    17    18    19    20     2   1.00   1.00   1.00  1  1  1  0  0  0     1
    5   17    18    19    20    21    22    23    24     1   1.00   1.00   1.00  1  1  1  0  0  0     1
    6   21    22    23    24    25    26    27    28     2   1.00   1.00   1.00  1  1  1  0  0  0     1
    7   25    26    27    28    29    30    31    32     1   1.00   1.00   1.00  1  1  1  0  0  0     1
    8   29    30    31    32    33    34    35    36     2   1.00   1.00   1.00  1  1  1  0  0  0     1
    9   33    34    35    36    37    38    39    40     1   1.00   1.00   1.00  1  1  1  0  0  0     1
   10   37    38    39    40    41    42    43    44     2   1.00   1.00   1.00  1  1  1  0  0  0     1

   25   97    98    99   100   101   102   103   104     1   1.00   1.00   1.00  1  1  1  0  0  0     2
   26  101   102   103   104   105   106   107   108     2   1.00   1.00   1.00  1  1  1  0  0  0     2
   27  105   106   107   108   109   110   111   112     1   1.00   1.00   1.00  1  1  1  0  0  0     2
   28  109   110   111   112   113   114   115   116     2   1.00   1.00   1.00  1  1  1  0  0  0     2
   29  113   114   115   116   117   118   119   120     1   1.00   1.00   1.00  1  1  1  0  0  0     2
   30  117   118   119   120   121   122   123   124     2   1.00   1.00   1.00  1  1  1  0  0  0     2
   31  121   122   123   124   125   126   127   128     1   1.00   1.00   1.00  1  1  1  0  0  0     2
   32  125   126   127   128   129   130   131   132     2   1.00   1.00   1.00  1  1  1  0  0  0     2
*** BLOCK J : BOUNDARY INFORMATION ******************************************************
 Node number array:
      1        2        3        4       129      130      131      132
 Width array:
   .33333   .16667   .16667   .33333   .16667   .33333   .33333   .16667
 Length:
    1.00
***** End of file Grid.In ******************************************************
```

[†] This file was generated with code GENER3.

Table 8.20. Input data for example 3b (input file 'SELECTOR.IN').

```
*** BLOCK A: BASIC INFORMATION ****************************************
Heading
'Example 3b - Comparison with the 3-D analytical solution'
LUnit TUnit MUnit (indicated units are obligatory for all input data)
'm'     'days'  '-'
MaxIt   TolTh   TolH (max. number of iterations and precis.  tolerances)
  20    .0001   .1
LWat    LChem   CheckF  ShortF  FluxF AtmInF SeepF  FreeD  DrainF
f       t       f       t       f     f      t      f      f
*** BLOCK B: MATERIAL INFORMATION ********************************
NMat    NLay    hTab1   hTabN   NPar
  1     1       .001    200.    9
thr     ths     tha     thm     Alfa    n       Ks      Kk      thk
.02     .30     -.02    .30     .0410   1.964   0.3     0.3     .30
*** BLOCK C: TIME INFORMATION ********************************
dt      dtMin   dtMax   DMul    DMul2   MPL
1.0     .0001   100.    1.3     .33     3
TPrint(1),TPrint(2),...,TPrint(MPL)                    (print-time array)
 50 100 365
*** BLOCK E: SEEPAGE INFORMATION (only if SeepF =.true.) **************
NSeep                                          (number of seepage faces)
   7
NSP(1),NSP(2),.......,NSP(NSeep)              (number of nodes in each s.f.)
 225
NP(i,1),NP(i,2),......, NP(i,NSP(i))         (nodal number array of i-th s.f.)
4501 4502 4503 4504 4505 4506 4507 4508 4509 4510
4511 4512 4513 4514 4515 4516 4517 4584519 4520
4521 4522 4523 4524 4525 4526 4527 4528 4529 4530
4531 4532 4533 4534 4535 4534 4537 4538 4539 4540
4541 4542 4543 4544 4545 4546 4547 4548 4549 4550
4551 4552 4553 4554 4555 4556 4557 4558 4559 4560
4561 4562 4563 4564 4565 4566 4567 4568 4569 4570
4571 4572 4573 4574 4575 4576 4577 4578 4579 4580
4581 4582 4583 4584 4585 4586 4587 4588 4589 4590


4701 470; 4703 4704 4705 4706 4707 4708 4709 4710
4711 4712 4713 4714 4715 4716 4717 4718 4719 4720
4721 4722 4723 4724 4725
* ** BLOCK E: SOLUTE TRANSPORT INFORMATION * ****************************
Epsi    LUPW    LArtD   PeCr
 0.5    f       f       10
BuLk.d. Difus.  Disper.  Adsorp. SinkL1   Sinks1   SinkL0   SinkS0
1500    0.0     1.0 0.5  0.0004  -0.01    -0.01    0.0      0.0
KodCB(1),KodCB(2),......,KodCB(NumBP)
-1 -1 -1 -1 -1 -1 -1 -2 -2 -2 -2 -2 -2 -2 -2
-1 -1 -1 -1 -1 -1 -1 -2 -2 -2 -2 -2 -2 -2 -2
-1 -1 -1 -1 -1 -1 -1 -2 -2 -2 -2 -2 -2 -2 -2
-1 -1 -1 -1 -1 -1 -1 -2 -2 -2 -2 -2 -2 -2 -2
-1 -1 -1 -1 -1 -1 -1 -2 -2 -2 -2 -2 -2 -2 -2
-1 -1 -1 -1 -1 -1 -1 -2 -2 -2 -2 -2 -2 -2 -2
-1 -1 -1 -1 -1 -1 -1 -2 -2 -2 -2 -2 -2 -2 -2
-2 -2 -2 -2 -2 -2 -2 -2 -2 -2 -2 -2 -2 -2 -2
-2 -2 -2 -2 -2 -2 -2 -2 -2 -2 -2 -2 -2 -2 -2


-2 -2 -2 -2 -2 -2 -2 -2 -2 -2 -2  -2 -2 -2 -2
-2 -2 -2 -2 -2 -2 -2 -2 -2 -2 -2 -2 -2 -2 -2
-2 -2 -2 -2 -2 -2 -2 -2 -2 -2 -2 -2 -2 -2 -2
cBound(1..12)
 1. 0. 0. 0. 0. 0. 0. 0. 0. 0. 0. 0.
tPulse
 366
*** END OF INPUT FILE 'SELECTOR.IN' * ********************************
```

Table 8.21. Input data for example 3 (input file 'GENER3.IN').

```
*** INPUT FILE 'GENER3.IN' ************************************************
Aniz1  Aniz2  Aniz3  Cos11 Cos22 Cos33 Cos12 Cos13 Cos23      (Anis. Inf.)
 1.     1.     1.     1.    1.    1.    0.    0.    0.
NLinZ  NColX  NColY   (Number of nodal points in a particular direction)
 21     15     15
xCol(1)yCol(1)z(NLin)        (x,y,z-coordinates of front left bottom node)
 0      0     -200
*** SPACE INCREMENTS ************************************************
dx-array (number of items is NColX-1):
 4*10 5 4 2 4 5 7 8 10 15 20
dy-array (number of items is NColY-1):
 4*10 5 4 2 4 5 7 8 10 15 20
dz-array (number of items is NLinZ-1):
 12*5 4*10 4*25
*** LINE ATTRIBUTES ************************************************
LineNumber  Code  hInit  Conc  Q   MatNum  Beta  Axz  Bxz  Dxz
    1         1      0     0.   0.     1      0.    1.   1.   1.
    2         0      0     0.   0.     1      0.    1.   1.   1.
   20         0      0     0.   0.     1      0.    1.   1.   1.
   21         2      0     0.   0.     1      0.    1.   1.   1.
*** END OF INPUT FILE 'GENER3.IN' ************************************************
```

110

Table 8.22. Input data for example 3 (input file 'GRID.IN').[†]

```
*** BLOCK H: NODAL INFORMATION ********************************************************
   NumNP    NumEl      IJ    NumBP     NObs
   4725     3920      225     450        0
```

n	Code	x	Y	z	h	Conc	q	M	B	Axz	Bxz	Dxz
1	1	.00	.00	.00	.0000E+00	.0000E+00	.0000E+00	1	.00 1.00	1.00	1.00
2	1	10.00	.00	.00	.0000E+00	.0000E+00	.0000E+00	1	-.00	1.00	1.00	1.00
3	1	20.00	.00	.00	.0000E+00	.0000E+0o	.0000E+00	1	.oo	1.00	1.00	1.00
4	1	30.00	.oo	.00	.0000E+00	.0000E+00	.0000E+00	1	.oo	1.00	1.00	1.00
5	1	40.00	.00	.oo	.0000E+00	.0000E+00	.0000E+00	1	.00	1.00	1.00	1.00
6	1	45.00	.oo	.oo	.0000E+0o	.0000E+00	.0000E+00	1	.oo	1.00	1.00	1.00
7	1	49.00	.oo	.oo	.0000E+00	.0000E+00	.0000E+00	1	.oo	1.00	1.00	1.00
8	1	51.00	.00	.oo	.0000E+00	.0000E+00	.0000E+00	1	-.00	1.00	1.00	1.00
9	1	55.00	-.00	.oo	.0000E+00	.0000E+00	.0000E+00	1	.oo	1.00	1.00	1.00
4720	'2	60:00	120.00	-200.00	.0000E+00	.0000E+00	0000E+00	1	.oo	1.00	1.00	1.00
4721	2	67.00	120.00	-200.00	.0000E+00	.0000E+00	.0000E+00	1	.oo	1.00	1.00	1.00
4722	2	75.00	120.00	-200.00	.0000E+00	.0000E+00	.0000E+00	1	.oo	1.00	1.00	1.00
4723	2	85.00	120.00	-200.00	.0000E+00	.0000E+00	.0000E+00	1	.oo	1.00	1.00	1.00
4724	2	100.00	120.00	-200.00	.0000E+00	.0000E+00	.0000E+00	1	.oo	1.00	1.00	1.00
4725	2	120.00	120.00	-200.00	.0000E+00	.0000E+00	.0000E+00	1	.oo	1.00	1.00	1.00

```
*** BLOCK 1: ELEMENT INFORMATION **********************************************************
```

e	i	j	k	l	m	n	o	p	Sub	Anizl	Aniz2	Aniz3	--- CosAngle ---	LayNum
1	1	2	16	17	226	227	241	242	1	1.00	1.00	1.00	1 1 1 0 0 0	1
2	2	3	17	18	227	228	242	243	2	1.00	1.00	1.00	1 1 1 0 0 0	1
3	3	4	18	19	228	229	243	244	1	1.00	1.00	1.00	1 1 1 0 0 0	1
4	4	5	19	20	229	230	244	245	2	1.00	1.00	1.00	1 1 1 0 0 0	1
5	5	6	20	21	230	231	245	246	1	1.00	1.00	1.00	1 1 1 0 0 0	1
6	6	7	21	22	231	232	246	247	2	1.00	1.00	1.00	1 1 1 0 0 0	1
7	7	8	22	23	232	233	247	248	1	1.00	1.00	1.00	1 1 1 0 0 0	1
3917	4481	4482'	4496	4497	4766	4707	4721	4722	1	1.00	1.00	1.00	1 1 1 0 0 0	1
3918	4482	4483	4497	4498	4707	4708	4722	4723	2	1.00	1.00	1.00	1 1 1 0 0 0	1
3919	4483	4484	4498	4499	4708	4709	4723	4724	1	1.00	1.00	1.00	1 1 1 0 0 0	1
3920	4484	4485	4499	4500	4709	4710	4724	4725	2	1.00	1.00	1.00	1 1 1 0 0 0	1

```
*** BLOCK J : BOUNDARY INFORMATION *************************************************************
Node number array:
       1          2          3          4          5          6          7          a
       9         10         11         12         13         14         15         16

    4662       4'693      '4694       4695      4696'       4697       4698       4699
    4700       4701       4702       4703       4704       4705       4706       4707
    4708       4709       4710       4711       4712       4713       4714       4715
    4716       4717       4718       4719       4720       4721       4722       4723
    4724       4725
Width array:
   33.33333    33.33333    66.66666    33.33333    50.00000    15.00000    20.00000    10.00000
   30.00000    20.00000    50.00000    30.00000    83.33334    58.33333    66.66666    33.33333

   75.00000   208.33330   145.83330   166.66670    58.33333   233.33330   116.66670   233.33330
   87.50000   105.00000    35.00000    70.00000    52.50000   140.00000    87.50000   210.00000
  145.83330   408.33330   116.66670    66.66666    66.66666   133.33330    66.66666   100.00000
   30.00000    40.00000    20.00000    60.00000    40.00000   100.00000    60.00000   166.66670
  116.66670   133.33330
Length:
      0.00
• **** End of file Grid.In ***********************************************************************
```

[†] This file was generated using code GENER3.

Table 8.23. Input data for example 4 (input file 'SELECTORIN').

```
*** BLOCK A:  BASIC INFORMATION **************************************
Heading
'Example 4 · Contaminant Transport from a Waste Disposal Site'
LUnit  TUnit  MUnit  BUnit      (units are obligatory for all input data)
'm'    'day'  '-'    '-'
MaxIt  TolTh  TolH         (maximum number of iterations and tolerances)
 20    .0001  0.01
LWat      LChem    ChecF    ShortF  FluxF  AtmInF  SeepF  FreeD  DrainF
●             t       f        t       t      f       t      f      f
    :* BLOCK B: MATERIAL INFORMATION ***********************************
NMat     NLay    hTab1   hTabN   NPar
 1        1      .001    200.     9
thr      ths     tha     thm     Alfa   n      Ks     Kk     thk
.05      .45     .05     .45     4.1    2.0    5.0    5.0    .4500
· ** BLOCK C: TIME INFORMATION · ************************************
dt       dtMin   dtMax   DMUI    DMul2   MPL
 0.001   .0001   0.1      1.1     .33     9
TPrint(1),TPrint(2),...,TPrint(MPL)              (print-time array)
 0.25 1.5 5 10 20 30 50 100 200
· ** BLOCK E: SEEPAGE INFORMATION (only if SeepF =.true.) *************
NSeep                                    (number of seepage faces)
  1
NSP(1),NSP(2) ,.......,NSP(NSeep)        (number of nodes in each s.f.)
  7
NP(i,1),NP(i,2) ,.....,  NP(i,NSP(i))    (nodal number array of i-th s.f.)
  3191 3719 4247 4775 5303 5831 6359
*** BLOCK G: SOLUTE TRANSPORT INFORMATION*********************
Epsi    LUPW    LArtD   PeCr
 0.5     f       t       2.
Bulk.d.  Difus.      Disper.   Adsorp.   SinkLl  Sinks1  SinkLO  SinkSO
1.400    0.01        1.0       0.25      0.0     0.0     0.0     0.0     0.0
KodCB(1),KodCE(2),.....,KodCB(NunBP)
54*-1    577*-2
cBound(1..12)
 1. 0. 0. 0. 0. 0. 0. 0. 0. 0. 0. 0.
 tPulse
  50
· ** END OF INPUT FILE 'SELECTOR.IN'          ****************************
```

Table 8.24. Input data for example 4 (input file 'GENER3.IN').

```
*** INPUT FILE 'GENER3.IN' ***********************************************
Aniz1  Aniz2  Aniz3  Cos11 Cos22 Cos33 Cos12 Cos13 Cos23      (Anis. Inf.)
  1.     1.     1.    1.    1.    1.    0.    0.    0.
NLinZ  NColX  NColY   (Number of nodal points in a particular direction)
  23     33     16
xCol(1)yCol(1)z(NLin)        (x,y,z-coordinates of front left bottom node)
  0      0      0
*** SPACE INCREMENTS **************************************************
dx-array (number of items is NColX-1):
  2*10. 8*5. 10*10. 4*5. 8*10.
dy-array (number of items is NColY-1):
  6*1. 4. 8*5.
dz-array (number of items is NLinZ-1):
  6*2. 6*1. 10*2.
*** LINE ATTRIBUTES ***************************************************
LineNumber  Code  hInit   Conc  Q    MatNum  Beta  Axz  Bxz  Dxz
    1          0   -150    0.   0.      1      0.    1.   1.   1.
    23         0   -150    0.   0.      1      0.    1.   1.   1.
*** END OF INPUT FILE 'GENER3.IN' ************************************
```

113

Table 8.25. Input data for example 4 (input file 'GRID.IN').[†]

```
*** BLOCK H: NODAL INFORMATION ****************************************************************
    NumNP    NumEl    IJ    NumBP    NObs
    12144    10560    528     631      4
     n  Code       x          y         z        h          Conc          Q        M    B     Axz   Bxr   Dxz
     1    0       .00        .00     38.00   -.1000E+02   .0000E+00   .0000E+00   1   .00   1.00  1.00  1.00
     2    0     10.00        .00     38.00   -.1008E+02   .0000E+00   .0000E+00   1  -.00   1.00  1.00  1.00
     3    1     20.00        .00     38.00    .0000E+00   .0000E+00   .0000E+00   1  -.00   1.00  1.00  1.00
     4    1     25.00        .00     38.00    .0000E+00   .0000E+00   .0000E+00   1   .00   1.00  1.00  1.00
     5    1     30.00        .00     38.00    .0000E+00   .0000E+00   .0000E+00   1   .00   1.00  1.00  1.00
     6    1     35.00        .00     38.00    .0000E+00   .0000E+00   .0000E+00   1   .00   1.00  1.00  1.00
     7    1     40.00        .00     38.00    .0000E+00   .0000E+00   .0000E+00   1   .oo   1.00  1.00  1.00
     8    1     45.00        .00     38.00    .0000E+00   .0000E+00   .0000E+00   1   .oo   1.00  1.00  1.00
     9    1     50.00        .00     38.00    .0000E+00   .0000E+00   .0000E+00   1  -.00   1.00  1.00  1.00
    10    1     55.00        .00     38.00    .0000E+00   .0000E+00   .0000E+00   1  -.00   1.00  1.00  1.00
    11    1     60.00        .00     38.00    .0000E+00   .0000E+00   .0000E+00   1  -.00   1.00  1.00  1.00
    12    0     70.00        .D0     38.00   -.1054E+02   .0000E+00   .0000E+00   1  -.00   1.00  1.00  1.00
    13    0     80.00        .oo     38.00   -.1062E+02   .0000E+00   .0000E+00   1   .00   1.00  1.00  1.00
    14    0     90.00        .oo     38.00   -.1069E+02   .0000E+00   .0000E+00   1   .oo   1.00  1.00  1.00
    15    0    100.00        .00     38.00   -.1077E+02   .0000E+00   .0000E+00   1   .oo   1.00  1.00  1.00
    16    0    110.00        .oo     38.00   -.1085E+02   .0000E+00   .0000E+00   1   .00   1.00  1.00  1.00
    17    0    120.00        .oo     38.00   -.1092E+02   .0000E+00   .0000E+00   1   .00   1.00  1.00  1.00


 12141    0    230.00      50.00       .00    .2623E+02   .0000E+00   .0000E+00   1   .00   1.00' 1.00  1.00
 12142    0    240.00      50.00       .oo    .2615E+02   .0000E+00   .0000E+00   1   .oo   1.00  1.00  1.00
 12143    0    250.00      50.00       .oo    .2608E+02   .0000E+00   .0000E+00   1   .oo   1.00  1.00  1.00
 12144    1    260.00      50.00       .00    .2600E+02   .0000E+00   .0000E+00   1  -.00   1.00  1.00  1.00
*** BLOCK I:  ELEMENT INFORMATION ****************************************************************
     e    i    J    k     m    n     o     p  Sub Aniz1  Aniz2  Aniz3 ------ CosAngle ------- Lay
     1    1    2    34    3:   529   530   562   563  1  1.00  1.00  1.00  1.0 1.0 1.0  .o   .o   .o   1
     2    2    3    35    36   530   531   563   564  2  1.00  1.00  1.00  1.0 1.0 1.0  .o   .o   .o   1
     3    3    4    37    37   531   532   564   565  i  1.00  1.00  1.00  1.0 1.0 1.0  .o   .o  .o-   1
     4    4    5    38    38   532   533   565   566  2  1.00  1.00  1.00  1.0 1.0 1.0  .o   .o   .o   1
     5    5    6          39   533   534   566   567  1  1.00  1.00  1.00  1.0 1.0 1.0  .0   .0   .0   1


 10558 11580 11581 11613 11614 12108 12109 12141 12142  1 -1.00  1.00  1.00' 1.0 1.0 1.0  .0   .o   .o   1
 10559 11581 11582 11614 11615 12109 12110 12142 12143  2  1.00  1.00  1.00  1.0 1.0 1.0  .0   .o   .o   1
 10560 11582 11583 11615 11616 12110 12111 12143 12144  1  1.00  1.00  1.00  1.0 1.0 1.0  .o   .0   .o   1
. ** BLOCK J :  BOUNDARY INFORMATION ****************************************************************
 Node number array:
            3           4           5           6           7           8           9          10
           11          36          37          38          39          40          41          42
           43          44          69          70          71          72          73          74


        1-1913       11911       11946   ·   11947   ·  11979       11980       12012       12013
         12045       12046       12078       12079       12111       12112       12144
 Uidth array:
       5.00000     1.66667     3.33333      .83333     3.33333     1.66667     3.33333     1.66667
       5.00000     5.00000     6.66667     3.33333     3.33333     3.33333     6.66667     3.33333
       6.66667     5.00000    10.00000     3.33333     6.66667     1.66667     6.66667     3.33333


       6.66667     3.3333;     3.33333     6.66667     d.66667     3.33333     3.33333     6.66667
       6.66667     3.33333     3.33333     6.66667     6.66667     1.66667     1.66667
 Length:
      .00
 Observation nodes
 1591 4244 6363 6887
. **** End of file Grid.In ****************************************************************
```

[†] This file was generated using code GENER3 with subsequent editing of boundary conditions.

9. OUTPUT DATA

The program output consists of 17 output files organized into 3 groups:

       T-level   information
             H_MEAN.OUT
             V_MEAN.OUT
             CUMQ.OUT
             RUN_INF.OUT
             SOLUTE.OUT
             OBSNOD.OUT

       P-level   information
             H.OUT
             TH.OUT
             CONC.OUT
             Q.OUT
             VX.OUT
             VY.OUT
             VZ.OUT
             BOUNDARY.OUT
             BALANCE.OUT

       A-level   information
             A_LEVEL.OUT

In addition, some of the input data are printed to file CHECKOUT. All output files are directed to subdirectory SWMS_3D.OUT, which must be created by the user prior to program execution. The various output files are described in detail in Section 9.1. Section 9.2 lists selected output files for examples 1 through 3 (see Section 7). The input files for these examples were discussed in Section 8.2.

9.1. *Description of Data Output Files*

The file CHECKOUT contains a complete description of the finite element mesh, the boundary code of each node, and the hydraulic and transport properties of each soil material. Finite element mesh data are printed only when the logical variable *CheckF* in input Block A

(Table 9.1) is set equal to .true..

  T-level information - This group of output files contains information which is printed at the end of each time step. Printing can be suppressed by setting the logical variable *ShortF* in input Block A equal to true.; the information is then printed only at selected print times. Output files printed at the T-level are described in Tables 9.1 through 9.5. Output file OBSNOD.OUT contains information about the transient changes in pressure head, water content, and solute concentration at specified observation nodes.

  P-level information - P-level information is printed only at prescribed print times. The following output files are printed at the P-level:

H.OUT	Nodal values of the pressure head
TH.OUT	Nodal values of the water content
CONC.OUT	Nodal values of the concentration
Q.OUT	Discharge/recharge rates assigned to boundary or internal sink/ source nodes
VX.OUT	Nodal vaiues of the x-components of the Darcian flux vector
VY.OUT	Nodal values of the y-components of the Darcian flux vector
VZ.OUT	Nodal values of the z-components of the Darcian flux vector
BOUNDARY.OUT	This file contains information about each boundary node, n, for which $Kode(n) \neq 0$, including the discharge/recharge rate, $Q(n)$, the boundary flux, $q(n)$, the pressure head $h(n)$, the water content $\theta(n)$, and the concentration $Conc(n)$.
BALANCE.OUT	This file gives the total amount of water and solute inside each specified subregion, the inflow/outflow rates to/from that subregion, together with the mean pressure head (hMean) and the mean concentration (cMean) over each subregion (see Table 9.6). Absolute and relative errors in the water and solute mass balances are also printed to this file.

  The output files H.OUT, TH.OUT, CONC.OUT, Q.OUT, VX.OUT, VY.OUT and VZ.OUT provide printed tables of the specific variables. To better identify the output, each printed line starts with the nodal number and spatial coordinates of the first node on that line for which information is printed. Users can easily reprogram the original subroutines to restructure the output for their specific needs.

A-level information - A-level information is printed each time a time-dependent boundary condition is specified. The information is directed to output file A_LEVEL.OUT (Table 9.7).

Table 9.1. H_MEAN.OUT - mean pressure heads.

---

hAtm   Mean value of the pressure head calculated over a set of nodes for which $Kode(n)=\pm4$ (i.e., along part of a boundary controlled by atmospheric conditions) [L].

hRoot   Mean value of the pressure head over a region for which Beta(n)>0 (i.e., within the root zone) [L].

hKode3   Mean value of the pressure head calculated over a set of nodes for which $Kode(n)=\pm3$ (i.e., along part of a boundary where the groundwater level, the bottom flux, or other time-dependent pressure head and/or flux is imposed) [L].

hKode1   Mean value of the pressure head calculated over a set of nodes for which $Kode(n)=\pm1$ (i.e., along part of a boundary where time-independent pressure heads and/or fluxes are imposed) [L].

hSeep   Mean value of the pressure head calculated over a set of nodes for which $Kode(n)=\pm2$ (i.e., along seepage faces) [L].

hKode5   Mean value of the pressure head calculated over a set of nodes for which $Kode(n)=\pm5$ [L].

hKodeN   Mean value of the pressure head calculated over a set of nodes for which $Kode(n)=\pm NumKD$ [L].

Table 9.2. V_MEAN.OUT - mean and total water fluxes.+

rAtm	Potential surface flux per unit atmospheric boundary (*Kode(n)*=±4) $[LT^{-1}]$.
rRoot	Potential transpiration rate, T_p $[LT^{-1}]$.
vAtm	Mean value of actual surface flux per unit atmospheric boundary (*Kode(n)*=±4) $[LT^{-1}]$.
vRoot	Actual transpiration rate, T_a $[LT^{-1}]$.
vKode3	Total value of the bottom or other flux across part of a boundary where the groundwater level, the bottom flux, or other time-dependent pressure head and/or flux is imposed (*Kode(n)*=±3) $[L^3T^{-1}]$.
vKode 1	Total value of the boundary flux accros part of a boundary where time-independent pressure heads and/or fluxes are imposed, including internal sinks/sources (*Kode(n)*=±1) $[L^3T^{-1}]$.
vSeep	Total value of the boundary flux across a potential seepage face (*Kode(n)*=±2) $[L^3T^{-1}]$.
vKode5	Total value of the flux across a boundary containing nodes for which *Kode(n)*=±5 $[L^3T^{-1}]$.
vKodeN	Total value of the flux across a boundary containing nodes for which *Kode(n)*=±*NumKD* $[L^3T^{-1}]$.

† Boundary fluxes are positive when water is removed from the system.

Table 9.3. CUM_Q.OUT - total cumulative water fluxes.'

CumQAP	Cumulative total potential surface flux across the atmospheric boundary $(Kode(n)=\pm4)[L^3]$.
CumQRP	Cumulative total potential transpiration rate $[L^3]$.
CumQA	Cumulative total actual surface flux across the atmospheric boundary $(Kode(n)=\pm4)[L^3]$.
CumQR	Cumulative total actual transpiration rate $[L^3]$.
CumQ3	Cumulative total value of the bottom or other boundary flux across part of a boundary where the groundwater level, the bottom flux, or other time-dependent pressure head and/or flux is imposed $(Kode(n)=\pm3)$ $[L^3]$.
CumQl	Cumulative total value of the flux across part of a boundary along which time-independent pressure heads and/or fluxes are imposed, including internal sinks/sources $(Kode(n)=\pm1)[L^3]$.
CumQS	Cumulative total value of the flux across a potential seepage faces $(Kode(n)=\pm2)[L^3]$.
CumQ5	Cumulative total value of the flux across a boundary containing nodes for which $Kode(n)=\pm5[L^3]$.
CumQN	Cumulative total value of the flux across a boundary containing nodes for which $Kode(n)= \pm NumKD$ $[L^3]$.

[†] Boundary fluxes are positive when water is removed from the system.

Table 9.4. RUN_INF.OUT - time and iteration information.

TLevel	Time-level (current time-step number) [-].
Time	Time, t, at current time-level [T].
dt	Time step, At [T].
Iter	Number of iterations [-].
ItCum	Cumulative number of iterations [-].
Peclet	Maximum local Peclet number [-].
Courant	Maximum local Courant number [-].
PeCrMax	Maximum local product of Peclet and Courant numbers [-].

Table 9.5. SOLUTE.OUT - actual and cumulative concentration fluxes.

CumCh0	Cumulative amount of solute removed from the flow region by zero-order reactions (positive when removed from the system) [M].
CumCh 1	Cumulative amount of solute removed from the flow region by first-order reactions [M].
CumChR	Cumulative amount of solute removed from the flow region by root water uptake S [M].
ChemS1	Cumulative solute flux across part of a boundary along which time-independent pressure heads and/or fluxes are imposed, including internal sink/sources $(Kode(n)=\pm1)$ [M].
ChemS2	Cumulative solute flux across a potential seepage faces $(Kode(n)=\pm2)$ [M].
ChemS3	Cumulative solute flux across part of a boundary along which the groundwater level, the bottom flux, or other time-dependent pressure head and/or flux is imposed $(Kode(n)=\pm3)$ [M].
ChemS4	Cumulative total solute flux across the atmospheric boundary $(Kode(n)=\pm4)$ [M].
ChemS5	Cumulative total solute flux across an internal or external boundary containing nodes for which $Kode(n)=\pm5$ [M].
ChemSN	Cumulative total solute flux across an internal or external boundary containing nodes for which $Kode(n)=\pm NumKD$ [M].
qc1	Total solute flux across part of a boundary along which time-independent pressure heads and/or fluxes are imposed $(Kode(n)=\pm1)$ [MT'].
qc2	Total solute flux across a potential seepage face $(Kode(n)=\pm2)$ [MT'].
qc3	Total solute flux calculatedacross a boundary containing nodes for which $Kode(n)=\pm3$ (i.e., along part of a boundary where the groundwater level, the bottom flux, or other tune-dependent pressure head and/or flux is specified) [MT'].
qc4	Total solute flux across the atmospheric boundary $(Kode(n)=\pm4)$ [MT'].
qc5	Total solute flux across an internal or external boundary containing nodes for which $Kode(n)=\pm5$ {MT-'].
qcN	Total solute flux across an internal or external boundary containing nodes for which $Kode(n)=\pm NumKD$ [MT'].

Table 9.6. BALANCE.OUT - mass balance variables.

Area	Volume of the entire flow domain or a specified subregion $[L^3]$.
Volume	Volume of water in the entire flow domain or a specified subregion [L'].
InFlow	Inflow/Outflow to/from the entire flow domain or a specified subregion $[L^3T^{-1}]$.
hMean	Mean pressure head in the entire flow domain or a specified subregion [L].
Conc Vol	Amount of solute in the entire flow domain or a specified subregion [M].
cMean	Mean concentration in the entire flow domain or a specified subregion $[ML^{-3}]$.
WatBalT	Absolute error in the water mass balance of the entire flow domain [L'].
WatBalR	Relative error in the water mass balance of the entire flow domain [%].
CncBalT	Absolute error in the solute mass balance of the entire flow domain [M].
CncBalR	Relative error in the solute mass balance of the entire flow domain [%].

Table 9.7. A_LEVEL.OUT - mean pressure heads and total cumulative fluxes.[†]

CumQAP   Cumulative total potential flux across the atmospheric boundary (*Kode(n)*=±4) [L'].

CumQRP   Cumulative total potential transpiration rate [L^3].

CumQA   Cumulative total actual flux across the atmospheric boundary (*Kode*(*n*)=±4) [L'].

CumQR   Cumulative total actual transpiration rate [L'].

CumQ3   Cumulative total bottom or other flux across a boundary along which the groundwater level, the bottom flux, or other time-dependent pressure head and/or flux is imposed (*Kode*(*n*)=±3) [L^3].

hAtm   Mean value of the pressure head calculated over a set of nodes for which *Kode*(*n*)=±4 [L].

hRoot   Mean value of the pressure head over a region for which *Beta(n)>0* (i.e., the root zone) [L].

hKode3   Mean value of the pressure head over a set of nodes for which *Kode*(*n*)=±3 [L].

[†] Boundary fluxes are positive when water is removed from the system.

Table 9.8. Output data for example 1 (part of output file 'H.OUT').

line	***	5400.0000	• **			
n	x(n)	Y(n)	z(n)	h(n)	h(n+l) . . .	
1	.0	.0	61.0	.8	.8	.8	.8
5	.0	.0	60.8	.6	.6	.6	.6
9	.0	.0	60.5	.4	.4	.4	.4
13	.0	.0	60.3	.3	.3	.3	.3
17	.0	.0	60.0	.1	.1	.1	.1
21	.0	.0	59.5	-.2	-.2	-.2	-.2
25	.0	.0	59.0	-.5	-.5	-.5	-.5
29	.0	.0	58.0	-1.2	-1.2	-1.2	-1.2
33	.0	.0	57.0	-1.8	-1.8	-1.8	-1.8
37	.0	.0	56.0	-2.4	-2.4	-2.4	-2.4
41	.0	.0	55.0	-3.1	-3.1	-3.1	-3.1
45	.0	.0	54.0	-3.7	-3.7	-3.7	-3.7
49	.0	.0	53.0	-4.4	-4.4	-4.4	-4.4
53	.0	.0	52.0	-5.0	-5.0	-5.0	-5.0
57	.0	.0	51.0	-5.7	-5.7	-5.7	-5.7
61	.0	.0	50.0	-6.3	-6.3	-6.3	-6.3
65	.0	.0	49.0	-7.0	-7.0	-7.0	-7.0
69	.0	.0	48.0	-7.6	-7.6	-7.6	-7.6
73	.0	.0	47.0	-8.2	-8.2	-8.2	-8.2
77	.0	.0	46.0	-8.9	-8.9	-8.9	-8.9
81	.0	.0	45.0	-9.5	-9.5	-9.5	-9.5
85	.0	.0	44.0	-10.1	-10.1	-10.1	-10.1
89	-0	.0	43.0	-10.7	-10.7	-10.7	-10.7
93	.0	.0	42.0	-11.4	-11.4	-11.4	-11.4
97	.0	.0	47.0	-12.0	-12.0	-12.0	-12.0
101	.0	.0	40.0	-12.6	-12.6	-12.6	-12.6
105	.0	.0	39.0	-13.1	-13.1	-13.1	-13.1
109	.0	.0	38.0	-13.7	-13.7	-13.7	-13.7
113	.0	.0	37.0	-14.3	-14.3	-14.3	-14.3
117	.0	.0	36.0	-14.9	-14.9	-14.9	-14.9
121	.0	.0	35.0	-15.4	-15.4	-15.4	-15.4
125	.0	.0	34.0	-15.9	-15.9	-15.9	-15.9
129	.0	.0	33.0	-16.5	-16.5	-16.5	-16.5
133	.0	.0	32.0	-17.0	-17.0	-17.0	-17.0
137	.0	.0	31.0	-17.5	-17.5	-17.5	-17.5
141	.0	.0	30.0	-18.1	-18.1	-18.1	-18.1
145	.0	.0	29.0	-18.8	-18.8	-18.8	-18.8
149	.0	.0	28.0	-19.5	-19.5	-19.5	-19.5
153	.0	.0	27.0	-20.3	-20.3	-20.3	-20.3
157	.0	.0	26.0	-21.3	-21.2	-21.2	-21.3
161	.0	.0	25.0	-22.4	-22.4	-22.4	-22.4
165	.0	.0	24.0	-23.8	-23.8	-23.8	-23.8
169	.0	.0	23.0	-25.5	-25.6	-25.6	-25.5
173	.0	.0	22.0	-27.8	-27.7	-27.7	-27.8
177	.0	.0	21.0	-30.7	-30.8	-30.8	-30.7
181	.0	.0	20.0	-34.9	-34.7	-34.7	-34.9
185	.0	.0	18.0	-48.5	-49.0	-49.0	-48.5
189	.0	.0	16.0	-81.8	-87.5	-81.5	-81.8
193	.0	.0	14.0	-137.1	-136.5	-136.5	-137.1
197	.0	.0	12.0	-149.4	-149.6	-149.6	-149.4
201	.0	.0	10.0	-150.0	-150.0	-150.0	-150.0
205	.0	.0	8.0	-150.0	-150.0	-150.0	-150.0
209	.0	.0	6.0	-149.9	-149.9	-149.9	-149.9
213	.0	.0	4.0	-149.7	-149.7	-149.7	-149.7
217	.0	.0	2.0	-149.0	-149.0	-149.0	-149.0
221	.0	.0	.0	-147.4	-147.5	-147.5	-147.4

Table 9.9. Output data for example 1 (output file 'CUM_Q.OUT').

Example I · Colum Test

Program SWMS_3D
Date: 16. 8.   Time: 9:24: 9
Time independent boundary conditions
Units: L = cm , T = sec , M = ·
All cumulative fluxes (CumQ) are positive out of the region

Time [T]	CumQAP [V]	CumQRP [V]	CumQA [V]	CumQR [V]	CumQ3 [V]	CumQ1 [V]	CumQS [V]	CumQ5 [V]	CumQ6 [V]
60.0000	.000E+00	.000E+00	.000E+00	.000E+00	.000E+00	-.801E+00	.000E+00	.000E+00	.000E+00
900.0000	.000E+00	.000E+00	.000E+00	.000E+00	.000E+00	-.340E+01	.000E+00	.000E+00	.000E+00
1800.0000	.000E+00	.000E+00	.000E+00	.000E+00	.000E+00	-.506E+01	.000E+00	.000E+00	.000E+00
2700.0000	.000E+00	.000E+00	.000E+00	.000E+00	.000E+00	-.644E+01	.000E+00	.000E+00	.000E+00
3600.0000	.000E+00	.000E+00	.000E+00	.000E+00	.000E+00	-.768E+01	.000E+00	.000E+00	.000E+00
5400.0000	.000E+00	.000E+00	.000E+00	.000E+00	.000E+00	-.991E+01	.000E+0	.000E+00	.000E+00

Table 9.10.   Output data for example 2 (output file 'RUN_INF.OUT').

TLevel	Time	dt	Iter	ItCum
70	.120E+03	.500E+00	2	166
132	.151E+03	.500E+00	3	335
192	.181E+03	.500E+00	3	523
254	.212E+03	.500E+00	3	674
328	.243E+03	.500E+00	2	913
388	.273E+03	.500E+00	6	1068

Real time [sec]   64.000000000000000

Table 9.11. Output data for example 2 (part of output file 'A_LEVEL.OUT').

Example 2 - **Grass Field Problem (Hupselse Beek 1982)**

Program SUMS_30
Date: 16. 8.   Time: 9:33: 2
Time dependent boundary conditions
Units: L = cm   T = day   M= -
All cumulative fluxes (CunQ) are positive out of the region

Time	CunQAP	CunQRP	CumQA	CunQR	CunQ3	hAtm	hRoot	hKode3	A-level
[T]	[V]	[V]	[V]	[V]	[V]	[L]	[L]	[L]	
91.0000	.000E+00	.160E+00	.000E+00	.160E+00	.373E-01	-58.2	-37.1	171.9	1
92.0000	-.700E-01	.340E+00	-.700E-01	.340E+00	.722E-01	-59.5	-39.0	169.4	2
93.0000	-.900E-01	.470E+00	-.900E-01	.470E+00	.105E+00	-62.3	-40.9	167.4	3
94.0000	-.900E-01	.670E+00	-.900E-01	.670E+00	.136E+00	-66.3	-43.8	164.3	4
95.0000	-.900E-01	.950E+00	-.900E-01	.950E+00	.164E+00	-71.2	-47.9	160.3	5
96.0000	-.160E+00	.113E+01	-.160E+00	.113E+01	.190E+00	-71.2	-50.8	158.0	6
97.0000	-.450E+00	.121E+01	-.450E+00	.121E+01	.215E+00	-63.6	-49.7	159.0	7
98.0000	-.890E+00	.135E+01	-.890E+00	.135E+01	.240E+00	-57.8	-46.1	162.1	8
99.0000	-.109E+01	.146E+01	-.109E+01	.146E+01	.268E+00	-60.9	-44.1	164.0	9
100.0000	-.138E+01	.157E+01	-.138E+01	.157E+01	.298E+00	-57.8	-42.6	166.0	10
101.0000	-.170E+01	.168E+01	-.170E+01	.168E+01	.329E+00	-55.1	-40.2	168.6	11
102.0000	-.219E+01	.179E+01	-.219E+01	.179E+01	.362E+00	-48.7	-36.2	173.7	12
103.0000	-.220E+01	.195E+01	-.220E+01	.195E+01	.400E+00	-57.2	-35.3	172.4	13
104.0000	-.220E+01	.212E+01	-.220E+01	.212E+01	.435E+00	-60.8	-38.6	169.4	14
105.0000	-.220E+01	.234E+01	-.220E+01	.234E+01	.468E+00	-64.8	-42.1	165.8	15
106.0000	-.220E+01	.255E+01	-.220E+01	.255E+01	.497E+00	-68.4	-45.8	162.5	16
107.0000	-.220E+01	.278E+01	-.220E+01	.278E+01	.524E+00	-72.3	-49.4	159.1	17
108.0000	-.220E+01	.301E+01	-.220E+01	.301E+01	.549E+00	-76.0	-53.0	155.9	18
109.0000	-.220E+01	.325E+01	-.220E+01	.325E+01	.572E+00	-79.7	-56.5	152.7	19
110.0000	-.220E+01	.343E+01	-.220E+01	.343E+01	.593E+00	-82.1	-59.5	150.1	20
111.0000	-.220E+01	.358E+01	-.220E+01	.358E+01	.613E+00	-84.1	-61.7	148.0	21
112.0000	-.220E+01	.377E+01	-.220E+01	.377E+01	.631E+00	-87.0	-64.2	145.7	22
113.0000	-.221E+01	.392E+01	-.221E+01	.392E+01	.649E+00	-88.4	-66.3	143.7	23
114.0000	-.222E+01	.414E+01	-.222E+01	.414E+01	.665E+00	-91.7	-68.8	141.5	24
115.0000	-.222E+01	.437E+01	-.222E+01	.437E+01	.681E+00	-95.6	-71.8	139.0	25
116.0000	-.224E+01	.457E+01	-.224E+01	.457E+01	.695E+00	-97.0	-74.4	136.8	26
117.0000	-.224E+01	.474E+01	-.224E+01	.474E+01	.709E+00	-99.6	-76.4	134.9	27
118.0000	-.226E+01	.488E+01	-.226E+01	.488E+01	.722E+00	-99.7	-77.9	133.2	28
119.0000	-.252E+01	.501E+01	-.252E+01	.501E+01	.735E+00	-86.9	-76.1	132.6	29
120.0000	-.276E+01	.512E+01	-.276E+01	.512E+01	.747E+00	-84.2	-73.1	133.2	30
121.0000	-.337E+01	.520E+01	-.337E+01	.520E+01	.760E+00	-68.2	-67.1	136.0	31
122.0000	-.337E+01	.541E+01	-.337E+01	.541E+01	.774E+00	-89.2	-67.4	137.2	32
123.0000	-.356E+01	.555E+01	-.356E+01	.555E+01	.788E+00	-84.3	-70.1	137.4	33
124.0000	-.373E+01	.576E+01	-.373E+01	.576E+01	.802E+00	-85.9	-70.3	137.1	34
125.0000	-.451E+01	.583E+01	-.451E+01	.583E+01	.816E+00	-62.0	-63.5	140.5	35
126.0000	-.569E+01	.593E+01	-.569E+01	.593E+01	.833E+00	-48.2	-51.0	151.4	36
127.0000	-.637E+01	.603E+01	-.637E+01	.603E+01	.855E+00	-51.3	-43.6	162.7	37
128.0000	-.637E+01	.619E+01	-.637E+01	.619E+01	.884E+00	-65.3	-43.4	163.8	38
264.0000	-.238E+02	.429E+02	-.238E+02	.429E+02	.149E+01	-156.7	-246.6	15.3'	174
265.0000	-.238E+02	.431E+02	-.238E+02	.431E+02	.149E+01	-228.3	-229.7	14.6	175
266.0000	-.238E+02	.433E+02	-.238E+02	.433E+02	.149E+01	-257.4	-237.0	13.9	176
267.0000	-.238E+02	.435E+02	-.238E+02	.434E+02	.149E+01	-276.8	-245.2	13.2	177
268.0000	-.238E+02	.437E+02	-.238E+02	.436E+02	.149E+01	-293.1	-252.9	12.6	178
269.0000	-.243E+02	.438E+02	-.243E+02	.437E+02	.149E+01	-157.2	-236.4	12.0	179
270.0000	-.244E+02	.440E+02	-.244E+02	.439E+02	.149E+01	-206.6	-219.2	11.4	180
271.0000	-.244E+02	.442E+02	-.244E+02	.441E+02	.149E+01	-240.3	-225.3	10.8	181
272.0000	-.244E+02	.444E+02	-.244E+02	.443E+02	.149E+01	-264.1	-234.5	10.3	182
273.0000	-.254E+02	.444E+02	-.254E+02	.443E+02	.149E+01	-103.0	-203.9	9.8	183

Table 9.12. Output data for example 3b (part of output file 'SOLUTE.OUT').

```
All solute fluxes (SMean) and cumulative solute fluxes (ChemS) are positive out of the region

  Time     CumCh0       CumCh1       CumChR    ——————— --------- ChemS(i),i=1,NumKD——————————————————
  [T]       [M]          [M]          [M]                                    [M]

  1.00    .000E+00     .000E+00     .000E+00  -.750E+03    .000E+00    .000E+00    .000E+00    .000E+00    .00oE+0o
  2.29    .000E+00     .962E+0l     .000E+00  -.172E+04    .515E-36    .000E+00    .000E+00    .000E+00    .000E+00
  3.99    .000E+00     .386E+02     .000E+00  -.300E+04    .978E-33    .000E+00    .000E+00    .000E+00    .000E+00
  6.18    .000E+00     .103E+03     .000E+00  -.464E+04    .127E-29    .000E+00    .000E+00    .000E+00    .000E+00
  9.11    .000E+00     .234E+03     .000E+00  -.683E+04    .791E-27    .000E+00    .000E+00    .000E+00    .000E+00
 12.82    .000E+00     .477E+03     .000E+00  -.962E+04    .520E-24    .000E+00    .000E+00    .000E+00    .000E+00
 17.47    .000E+00     .897E+03     .000E+00  -.131E+05    .161E-21    .000E+00    .000E+00    .000E+00    .000E+00
 23.98    .000E+00     .168E+04     .000E+00  -.180E+05    .344E-19    .000E+00    .000E+00    .000E+00    .000E+00
 32.65    .000E+00     .307E+04     .000E+00  -.245E+05    .162E-16    .000E+00    .000E+00    .000E+00    .00oE+0o
 41.33    .000E+00     .488E+04     .00oE+0o  -.310E+05    .357E-14    .000E+00    .000E+00    .000E+00    .000E+0o
 50.00    .000E+00     .708E+04     .0ooE+0o  -.375E+05    .818E-1313  .000E+00    .000E+00    .000E+00    .000E+00
 62.50    .000E+00     .108E+05     .000E+00  -.469E+05    .148E-11    .000E+00    .000E+00    .000E+00    .000E+00
 75.00    .000E+00     .151E+05     .000E+00  -.563E+05    .620E-10    .000E+00    .000E+00    .000E+00    .000E+00
 87.50    .000E+00     .201E+05     .000E+00  -.656E+0S    .894E-09    .000E+0o    .000E+00    .000E+00    .000E+00
100.00    .000E+00     .256E+05     .000E+00  -.750E+05    .820E-08    .000E+00    .000E+00    .000E+00    .000E+00
114.72    .000E+00     .325E+05     .00oE+0o  -.861E+05    .651E-07    .0ooE+oo    .000E+00    .000E+00    .000E+00
129.44    .000E+00     .40lE+05     .000E+00  -.971E+05    .502E-06    .000E+0o    .000E+00    .000E+00    .000E+00
144.17    .000E+00     .481E+05     .000E+00  -.108E+06    .301E-05    .000E+0o    .000E+00    .000E+00    .000E+00
158.89    .000E+00     .565E+05     .000E+00  -.119E+06    .147E-04    .000E+00    .000E+00    .000E+00    .000E+00
173.61    .000E+00     .653E+05     .000E+00  -.130E+06    .609E-04    .000E+00    .000E+00    .o00E+o0    .000E+00
188.33    .000E+00     .744E+05     .000E+00  -.141E+06    .220E-03    .000E+00    .000E+00    .000E+00    .000E+00
203.06    .000E+00     .838E+05     .00oE+0o  -.152E+06    .709E-03    .000E+00    .000E+00    .000E+00    .00oE+0o
217.78    .000E+00     .934E+05     .000E+00  -.163E+06    .207E-02    .000E+00    .000E+00    .000E+00    .000E+00
232.50    .000E+00     .103E+06     .000E+00  -.174E+06    .550E-02    .00oE+0o    .000E+00    .000E+00    .000E+00
247.22    .000E+00     .113E+06     .000E+00  -.185E+06    .135E-01    .000E+0o    .000E+00    .000E+00    .000E+00
261.94    .000E+00    -123E+06     .00oE+0o  -.196E+06    .309E-01    .000E+00    .000E+00    .000E+00    .000E+00
276.67    .000E+00     .134E+06     .0o0E+00  -.208E+06    .662E-01    .000E+00    .000E+00    .000E+00    .000E+00
291.39    .000E+00     .144E+06     .000E+00  -.219E+06    .134E+00    .000E+00    .000E+00    .000E+00    .000E+o0
306.11    .000E+00     .154E+06     .00oE+0o  -.230E+06    .256E+00    .000E+00    .000E+00    .000E+00    .000E+00
320.83    .000E+00     .165E+06     .000E+0o  -.241E+06    .466E+00    .000E+00    .000E+00    .000E+00    .000E+00
335.56    .000E+00     .175E+06     .0ooE+00  -.252E+06    .812E+00    .000E+00    .000E+00    .000E+00    .000E+00
350.28    .000E+00     .186E+06     .0ooE+00  -.263E+06    .136E+0l    .0ooE+oo    .000E+00    .000E+00    .000E+00
365.00    .000E+00     .197E+06     .00oE+0o  -.274E+06    .218E+01    .000E+00    .000E+00    .000E+00    .000E+00
```

Table 9.13. Output data for example 3b (output file 'BALANCE.OUT').

```
Example 3b - Comparison with the 3-D analytical solution


Program SUMS_3D
Date:  1.  3.     Time:   16:10:17
Time independent boundary conditions
Units: L = m    , T = days , M ▫ -


Time [T]                 Total      Sub-region  number ...


        . 0000                          1
Volume  [L3]        . 288E+07    . 288E+07
Water    IL31       . 864E+06    . 864E+06
 Inflow [L3/T]      . 000E+00    . 000E+00
hMean    [L]        . 000E+00          . 0
ConcVol [M          . 000E+00    . 000E+00
cMean    [M/L3]     . 000E+00    . 000E+00


     50.0000                           I
Volume  CL31        . 288E+07    . 288E+07
Water    [L3]       . 864E+06    . 864E+06
 Inflow [L3/T]      . 000E+00    . 000E+00
hMean    [L]        . 000E+00          . 0
ConcVol [M          . 295E+05    . 295E+05
cMean    [M/L3]     . 114E-01    . 114E-01
CncBalT       [M] -'. 900E+03
CncBalR [%]            2. 018


    100.0000                           I
Volume   [L3]       . 288E+07    . 288E+07
ConcVol [M          . 474E+05    . 474E+05
cMean    [MI3]      . 183E-01    . 183E-01
CncBalT [M]        - . 202E+04
CncBalR [%]            2. 009


    365.0000                           I
Volume   [L3]       . 288E+07    . 288E+07
ConcVol [M          . 731E+05    . 731E+05
cMean    [MI3]      . 282E-01    . 282E-01
CncBalT [M]        -. 393E+04
CncBalR [%]            . 835
```

TABLE 9.14. Output data for example 3b (part of output file 'CONC.OUT').

```
Time • **   365.0000 • **

 n   x(n)   y(n)   z(n)  Conc(n)Conc(n+l)       . .

  1    .0     .0    .O  .970E+00 .971E+00  .970E+00  .971E+00  .969E+00  .965E+00  .880E+00  .128E+00 -.453E-02 -125E-03
 11  67.0     .0    .0 -.169E-03 .268E-04  .235E-04 -.275E-06  .273E-05  .971E+00  .970E+00  .971E+00  .970E+00  .971E+00
 21  45.0   10.0    .0  .974E+00 .843E+00  .899E-01  .589E-02  .106E-02 -.593E-04 -.309E-04 -.528E-05 -.754E-05  .109E-05
 31    .0   20.0    .0  .970E+00 .971E+00  .970E+00  .971E+00  .969E+00  .965E+00  .880E+00  .128E+00 -.454E-02 -.125E-03
 41  67.0   20.0    .O -.183E-03 .284E-04  .290E-04 -.671E-06  .939E-06  .971E+00  .970E+00  .971E+00  .970E+00  .971E+00
 51  45.0   30.0    .0  .975E+00 .843E+00  .901E-01  .589E-02  .114E-02 -.675E-04 -.582E-04 -.358E-05 -.519E-05  .970E-06
 61    .0   40.0    .O  .969E+00 .971E+00  .969E+00  .971E+00  .968E+00  .966E+00  .878E+00  .127E+00 -.539E-02 -.905E-04
 71  67.0   40.0    .0 -.474E-04 ,192E-04  .207E-04 ~564E-06  .500E-06  .965E+00  .974E+00  .965E+00  .975E+00  .966E+00
 81  45.0   45.0    .0  .983E+00 .843E+00  .994E-01  .480E-02  .108E-03 -.292E-04 -.251E-04 -.571E-06 -.236E-05  .353E-06
 91    .0   49.0    .0  .880E+00 .843E+00  .880E+00  .843E+00  .878E+00  .843E+00  .786E+00  .105E+00 -.529E-02 -.167E-03
101  67.0   49.0    .O  .106E-03 .243E-05  .150E-05 -.829E-07  .876E-06  .128E+00  .899E-01  .128E+00  .901E-01  .127E+00
111  45.0   51.0    .O  .994E-01 .105E+00  .286E-01  .2.50E-03 -.693E-03  .620E-05  .696E-05  .382E-06  .149E-06  .142E-06
121    .0   55.0    .O -.453E-02 .589E-02 -.454E-02  .589E-02 -.539E-02  .480E-02 -.529E-02  .250E-03 -.393E-03 -.442E-04
131  67.0   55.0    .0  .306E-05 .138E-05  .122E-05 -.378E-07 -.llOE-06 -.125E-03  .106E-02 -.125E-03  .114E-02 -.905E-04
141  45.0   60.0    .O  .108E-03 -.167E-03 -.693E-03 -.442E-04  .173E-04  .139E-05  .153E-05 -.189E-06 -.270E-06  .156E-07
151    .0   67.0    .O -.169E-03 -.593E-04 -.183E-03 -.675E-04 -.474E-04 -.292E-04  .106E-03  .620E-05  .306E-05  .139E-05
161  67.0   67.0    .0  .155E-05 -.489E-06 -.733E-06  .660E-07  .209E-06  .268E-04 -.309E-04  .284E-04 -.582E-04  .192E-04
171  45.0   75.0    .0 -.251E-04  243E-05  .696E-05  .138E-05  .153E-05 -.489E-06 -.108E-05  .151E-06  .207E-06 -.478E-07
181    .0   85.0    .O  .235E-04 -.528E-05  .290E-04 -.358E-05  .207E-04 -.571E-06  .150E-05  .382E-06  .122E-05 -.189E-06
191  67.0   85.0    .O -.733E-06  .151E-06  337E-06 -.338E-07 -.171E-06 -.275E-06 -.754E-05 -.671E-06 -.519E-05 -.564E-06
201  45.0  100.0    .O -.236E-05 -.829E-07  .149E-06 -.378E-07 -.270E-06  .660E-07  .207E-06 -.338E-07 -.457E-07  .158E-07
211    .o  120.0    .O  .273E-05  .109E-05  .939E-06  .970E-06  .500E-06  .353E-06  .876E-06  .142E-06 -.llOE-06  .156E-07
221  67.0  120.0    .O  .209E-06 -.478E-07 -.171E-06  .158E-07  .117E-06
226    .0     .0   -5.0  .842E+00 .838E+00  .842E+00  .836E+00  .841E+00  .849E+00  .602E+00  .279E+00  .437E-01 -.475E-03
236  67.0     .0   -5.0 -.298E-03 -.521E-03  .257E-04  .328E-05  .382E-05  .838E+00  .842E+00  .838E+00  .842E+00  .838E+00
246  45.0   10.0   -5.0  .797E+00 .559E+00  .238E+00 -.113E-01  .352E-03  .138E-02  .146E-04  .960E-04 -.lllE-04 -.183E-04
256    .0   20.0   -5.0  .842E+00 .838E+00  .842E+00  .837E+00  .841E+00  .850E+00  .602E+00  .279E+00  .437E-01 -.491E-03
266  67.0   20.0   -5.0 -.307E-03 ~557E-03  .304E-04  .107E-04  .169E-05  .836E+00  .842E+00  .837E+00  .842E+00  .837E+00
276  45.0   30.0   -5.0  .797E+00 .559E+00  238E+00 -.lllE-Ol  .412E-03  .157E-02 -.527E-05  .626E-04 -.807E-05 -.166E-04
286    .0   40.0   -5.0  .841E+00 .838E+00  .841E+00  .837E+00  .841E+00  .848E+00  .599E+00  .276E+00  .401E-01 -.163E-02
296  67.0   40.0   -5.0 ~155E-03 -.383E-03  225E-04  .838E-05  .500E-06  .849E+00  .797E+00  .850E+00  .797E+00  .848E+00
306  45.0   45.0   -5.0  .777E+00 .570E+00  243E+00  .2llE-02  .153E-03  .686E-03 -.492E-04  .280E-04 -.195E-05 -.530E-05
316    .0   49.0   -5.0  .602E+00 .559E+00  .602E+00  .559E+00  .599E+00  .570E+00  .423E+00  .186E+00  .182E-01 -.187E-02
326  67.0   49.0   -5.0  .780E-04 -.477E-04  .523E-05 -.164E-05 -.365E-Q6  .279E+00  .238E+00  .279E+00  .238E+00  .276E+00
336  45.0   51.0   -5.0  .243E+00 .186E+00  .967E-01  .656E-02 -.451E-03  .572E-06 -.186E-04 -.292E-06 -.516E-06 -.254E-06
346    .0   55.0   -5.0  .437E-01 -.113E-01  .4378-01 -.lllE-Ol ,401E-Ol  .2llE-02  .182E-01  .656E-02  .161E-02 -.151E-03
356  67.0   55.0   -5.0 -.188E-04 ~166E-04  .144E-05  .690E-06 -.116E-06 -.475E-03  .352E-03 -.491E-03  .412E-03 -.163E-02
366  45.0   60.0   -5.0  .153E-03 ~187E-02 -.451E-03 -.151E-03 -.331E-04 -.168E-04  .173E-05  .412E-05 -.309E-06 -.262E-06
376    .0   67.0   -5.0 -.298E-03  .138E-02 -.307E-03  .157E-02 -.155E-03  .686E-03  .780E-04  .572E-06 -.188E-04 ~168E-o04
386  67.0   67.0   -5.0  .397E-05 .933E-05 -.971E-06 -.123E-05  .289E-06 -.521E-03  .146E-04 -.557E-03 -.527E-05 -.383E-03
396  45.0   75.0   -5.0 -.492E-04 -.477E-04 -.186E-04 -.166E-04  .173E-05  .933E-05 -.141E-05 -.289E-05  .310E-06  .851E-06
406    .0   85.0   -5.0  .257E-04 .960E-04  .304E-04  .626E-04  .225E-04  .280E-04  .523E-05 -.292E-06  .144E-05  .412E-05
416  67.0   85.0   -5.0 -.971E-06 -.289E-05  .473E-06  .611E-06 -.266E-06  .328E-05 -.lllE-04  .107E-04 -.807E-05  .838E-05
426  45.0  100.0   -5.0 -.195E-05 -.164E-05 -.516E-06  .690E-06 -.309E-06 -.123E-05  .310E-06  .611E-06 -.828E-07 -.271E-06
436    .o  120.0   -5.0  .382E-05 -.183E-04  .169E-05 -.166E-04  .500E-06 -.530E-05 -.365E-06 -.254E-06 -.116E-06 -.262E-06
446  67.0  120.0   -5.0  .289E-06 .851E-06 -.266E-06 -.271E-06  .205E-06
451    .o    .O   -10.0  .724E+00 .727E+00  .724E+00  .726E+00  .733E+00  .690E+00  .470E+00  .290E+00  .453E-01  .487E-02
461 67.0    .O   -10.0  .185E-02 -.380E-03 -.117E-03  .51OE-05 -.234E-04  .727E+00  .725E+00  .727E+00  .723E+00  .723E+00
```

130

Table 9.15. Output data for example 4 (output file 'CUM_Q.OUT').

```
Example 4 · Contaminant Transport from a Waste Disposal Site in a Pumped Aquifer

Program SUMS-30
Date:  6.  3.     Time:   15:50:52
Time independent boundary conditions
Units: L = cm   , T  =  day  , M = ·
All cumulative fluxes (CumQ) are positive out of the region
```

Time	CumQAP	CumQRP	CumQA	CumQR	CumQ3	CumQ1	CumQS	CumQ5	CumQ6
[T]	[L3]	[L3]	[L3]	[L3]	[L3]	[L3]	[L3]	[L3]	[L3]
.2500	.000E+00	.000E+00	.000E+00	.000E+00	.000E+00	-.671E+02	.297E+02	.000E+00	.000E+00
1.5000	.000E+00	.000E+00	.000E+00	.000E+00	.000E+00	-.730E+03	.123E+03	.000E+00	.000E+00
5.0000	.000E+00	.000E+00	.000E+00	.000E+00	.000E+00	-.129E+04	.257E+03	.000E+00	.000E+00
10.0000	.000E+00	.000E+00	.000E+00	.000E+00	.000E+00	-.135E+04	.372E+03	.000E+00	.000E+00
20.0000	.000E+00	.000E+00	.000E+00	.000E+00	.000E+00	-.166E+04	.532E+03	.000E+00	.000E+00
30.0000	.000E+00	.000E+00	.000E+00	.000E+00	.000E+00	-.198E+04	.680E+03	.000E+00	.000E+00
50.0000	.000E+00	.000E+00	.000E+00	.000E+00	.000E+00	-.240E+04	.984E+03	.000E+00	.000E+00
100.0000	.000E+00	.000E+00	.000E+00	.000E+00	.000E+00	-.322E+04	.175E+04	.000E+00	.000E+00
200.0000	.000E+00	.000E+00	.000E+00	.000E+00	.000E+00	-.475E+04	.330E+04	.000E+00	.000E+00

Table 9.16. Output data for example 4 (part of output file 'BOUNDARY.OUT').

Example 4 · Contaminant Transport from a Waste Disposal Site in a Pumped Aquifer

Program SWMS_3D
Date: 6. 3.   Time: 15:50:52
time independent boundary conditions
Units: L=cm , T=day , M=-

Time: 200.0000

i	n	x	Y	z	Code	Q [L3/T]	v [L/T]	h [L]	th t-1	Qc [M/T]	vc [M/L2/T]	Conc [M13]
1	3	20.0	.0	38.0	1	.184E+02	-.368E+0l	.0	.450	.000E+00	..000E+00	.255E-07
2	4	25.0	.0	38.0	1	.573E+0l	-.344E+0l	.0	.450	.000E+00	.000E+00	-.311E-07
3	5	30.0	.0	38.0	1	.105E+02	-.316E+0l	.0	.450	.000E+00	.000E+00	.301E-07
4	6	35.0	.0	38.0	1	.500E+0l	-.600E+0l	.0	.450	.000E+00	.000E+00	-.135E-07
5	7	40.0	.0	38.0	1	.983E+0l	-.295E+0l	.0	.450	.000E+00	.000E+00	.428E-07
6	8	45.0	.0	38.0	1	.491E+0l	-.294E+0l	.0	.450	.000E+00	.000E+00	-.10lE-06
7	9	50.0	.0	38.0	1	.102E+02	-.305E+0l	.0	.450	.000E+00	.000E+00	.517E-06
8	10	55.0	.0	38.0	1	.548E+0l	-.329E+0l	.0	.450	.000E+00	.000E+00	-.116E-05
9	11	60.0	.0	38.0	1	.174E+02	-.348E+0l	.0	.450	.000E+00	.000E+00	.318E-05
10	36	20.0	1.0	38.0	1	.176E+02	-.352E+0l	.0	-450	.000E+00	.000E+00	-.200E-07
11	37	25.0	1.0	38.0	1	.229E+02	-.344E+0l	.0	.450	.000E+00	.000E+00	-.291E-07
12	38	30.0	1.0	38.0	1	.106E+02	-.319E+0l	.0	.450	.000E+00	.000E+00	.270E-07
13	39	35.0	1.0	38.0	1	.203E+02	-.608E+0l	.0	.450	.000E+00	.000E+00	-.181E-07
14	40	40.0	1.0	38.0	1	.989E+0l	-.297E+0l	.0	.450	.000E+00	.000E+00	.24lE-07
15	41	45.0	1.0	38.0	1	.199E+02	-.298E+0l	.0	.450	.000E+00	.000E+00	-.142E-06
16	42	50.0	1.0	38.0	1	.103E+02	-.309E+0l	.0	.450	.000E+00	.000E+00	.370E-06
17	43	55.0	1.0	38.0	1	.220E+02	-.330E+0l	.0	.450	.000E+00	.000E+00	-.173E-05
18	44	60.0	1.D	38.0	1	.167E+02	-.333E+0l	.D	.450	.000E+00	.000E+00	.276E-05
19	69	20.0	2.0	38.0	1	.38lE+02	-.38lE+0l	.0	.450	.000E+00	.000E+00	-.163E-06
20	70	25.0	2.0	38.0	1	.119E+02	-.358E+0l	.0	.450	.000E+00	.000E+00	-.312E-07
21	71	30.0	2.0	38.0	1	.221E+02	-.332E+0f	.0	.450	.000E+00	.000E+00	.393E-07
22	72	35.0	2.0	38.0	1	.104E+02	-.626E+0l	.0	.450	.000E+00	.000E+00	.223E-08
23	73	40.0	2.0	38.0	1	.207E+02	-.311E+0l	.0	.450	.000E+00	.000E+00	.199E-07
24	74	45.0	2.0	38.0	1	.103E+02	-.308E+0l	.D	.450	.000E+00	.000E+00	-.562E-07
25	75	50.0	2.0	38.0	1	.214E+02	-.321E+0l	.0	.450	.000E+00	.000E+00	.593E-06
26	76	55.0	2.0	38.0	1	.114E+02	-.343E+0l	.0	.450	.000E+00	.000E+00	-.130E-05
27	77	60.0	2.0	38.0	1	.364E+02	-.364E+0l	.0	.450	.000E+00	.000E+00	.324E-05
28	102	20.0	3.0	38.0	1	.189E+02	-.378E+0l	.0	.450	.000E+00	.000E+00	-.112E-05
29	103	25.0	3.0	38.0	1	.25lE+02	-.377E+0l	.O	.450	.000E+00	.000E+00	-.349E-07
30	104	30.0	3.0	38.0	1	.117E+02	-.350E+0l	.0	.450	.000E+00	.000E+00	.665E-07
618	11914	.0	20.0	.0	1	-.127E+0l	.381E+00	28.0	.450	-.166E-01	.499E-02	.131E-01
619	11946	260.0	20.0	.o	1	.436E+00	-.131E+00	26.0	.450	.000E+00	.000E+00	.196E-05
620	11947	.O	25.0	.0	1	-.237E-0l	.356E+00	28.0	-450	-.557E-01	.835E-02	.234E-01
621	11979	260.0	25.0	.0	1	.86lE+00	-.129E+00	26.0	.450	.000E+00	.000E+00	.16lE-05
622	11980	.0	30.0	.o	1	-.111E+0l	.334E+00	28.0	.450	-.585E-01	.176E-01	.524E-01
623	12012	260.0	30.0	.o	1	.426E+00	-.128E+00	26.0	.450	.000E+00	.000E+00	.389E-06
624	12013	.0	35.0	.o	1	-.203E+0l	.305E+00	28.0	.450	-.346E+00	.519E-01	.170E+00
625	12045	260.0	35.0	.o	1	.839E+00	-.126E+00	26.0	.450	.000E+00	.000E+00	.239E-06
626	12046	.0	40.0	.o	1	-.100E+0l	.301E+00	28.0	.450	-.317E+oo	.951E-01	.316E+00
627	12078	260.0	40.0	.D	1	.419E+00	-.126E+00	26.0	.450	.000E+00	.000E+00	.349E-07
628	12079	.0	45.0	.o	1	-.186E+0l	.279E+00	28.0	.450	-.602E+00	.903E-01	.324E+00
629	12111	260.0	45.0	.D	1	.826E+00	-.124E+00	26.0	.450	.000E+00	.000E+00	.146E-07
630	12112	.0	50.0	.0	1	-.482E+00	.289E+00	28.0	.450	-.128E+00	.766E-01	.265E+00
631	12144	260.0	50.0	.o	1	.208E+00	-.125E+00	26.0	.450	.000E+00	.000E+00	.239E-08

10. PROGRAM ORGANIZATION AND LISTING

10.1. Description of Program Units

The program consists of a main program and 61 subprograms. The subprograms are organized by means of 8 source files which are stored and compiled separately and then linked together with the main program to form an executable program. Below are a list and brief descriptions of the source files and the associated subprograms.

SWMS_3D.FOR	(Main program unit)
INPUT3 .FOR	BasInf, MatIn, GenMat, TmIn, SeepIn, NodInf, EIemIn, GeomIn, AtmIn, SinkIn, ChemIn, DrainIn, Elem
WATFLOW3.FOR	WatFIow, Reset, Dirich, Solve, Shift, SetMat, Veloc
TIME3 .FOR	TmCont, SetAtm, Fgh
MATERIA3 .FOR	FK, FC, FQ, FH
SINK3.FOR	SetSnk, FAlfa
OUTPUT3.FOR	TLInf, ALInf, hOut, thOut, QOut, FIxOut, SubReg, BouOut, cOut, SolInf, ObsNod
SOLUTE3.FOR	Solute, cBound, ChInit, Disper, SolveT, WeFact, PeCour
ORTHOFEM.FOR	IADMake, Insert, Find, ILU, DU, ORTHOMIN, LUSolv, MatM2, SDot, SDotK, SNRM, SAXPYK, SCopy, SCopyK

Main program unit SWMS_3D. FOR

This is the main program unit of SWMS_3D   This unit controls execution of the program and determines which optional subroutines are necessary for a particular application.

Source file INPUT3. FOR

Subroutines included in this source file are designed to read data from different input blocks. The following table summarizes from which input file and input block (described in Section 8) a particular subroutine reads.

Table 10.1. Input subroutines/files.

Subroutine	Input Block	Input File
BasInf	A. Basic Information	
MatIn	B. Material Information	
TmIn	C. Time Information	
SinkIn	D. Sink Information	SELECTOR.IN
SeepIn	E. Seepage Information	
DrainIn	F. Drain Information	
ChemIn	G. Solute Transport Information	
NodInf	H. Nodal Information	
ElemIn	I. Element Information	GRID.IN
GeomIn	J. Boundary Geometry Information	
AtmIn	K. Atmospheric Information	ATMOSPH.IN

Subroutine **GenMat** generates for each soil type in the flow domain a table of water contents, hydraulic conductivities, and specific water capacities from the set of hydraulic parameters.

Subroutine **Elem** subdivides the input hexahedral and triangular prismatic elements into tetrahedrals which are subsequently treated as subelements.

Source file WATFLOW3. FOR

Subroutine **WatFlow** is the main subroutine for simulating water flow; this subroutine controls the entire iterative procedure of solving the Richards equation.

Subroutine **Reset** constructs the global matrix equation for water flow, including the right-hand side vector.

Subroutine **Dirich** modifies the global matrix equation by incorporating prescribed pressure head nodes.

Subroutine Solve solves the banded symmetric matrix equation for water flow by Gaussian elimination.

Subroutine **Shift** changes atmospheric or seepage face boundary conditions from Dirichlet type to Neumann type conditions, or vice versa, as needed. Also updates boundary conditions for the variable boundary fluxes (free and deep drainage).

Subroutine **SetMat** determines the nodal values of the hydraulic properties K(h), C(h) and $\theta(h)$ by interpolation between intermediate values in the hydraulic property tables.

Subroutine **Veloc** calculates nodal water fluxes.

Source file TIME3. FOR

Subroutine **TmCont** adjusts the current value of the time increment At.

Subroutine **SetAtm** updates time-dependent boundary conditions.

Function **Fqh** describes the groundwater level - discharge relationship, q(h), defined by equation (6.1). This function is called only from subroutine SetAtm.

Source file MA TERIA3. FOR

This file includes the functions **FK, FC, FQ** and **FH** which define the unsaturated hydraulic properties K(h), C(h), $\theta(h)$, and $h(\theta)$, for each soil material.

Source file SINK3. FOR

This file includes subroutine **SetSnk** and function **FAlfa.** These subroutines calculate the

135

actual root water extraction rate as a function of water stress in the soil root zone.

Source file OUTP UT3. FOR

The subroutines included in this file are designed to print data to different output files. Table 10.2 summarizes which output files are generated by a particular subroutine.

Table 10.2. Output subroutines/files.

Subroutine	Output File
TLInf	H_MEAN.OUT
	V_MEAN.OUT
	CUM_Q.OUT
	RUN_INF.OUT
SolInf	SOLUTE.OUT
hOut	H.OUT
thout	TH.OUT
cOut	CONC.OUT
QOut	Q.OUT
FlxOut	VX.OUT
	VY.OUT
	VZ.OUT
BouOut	BOUNDARY.OUT
SubReg	BALANCE.OUT
ALInf	A_LEVEL.OUT
ObsNod	OBSNOD.OUT

Source file SOL UTE3. FOR

Subroutine **Solute** is the main subroutine for simulating solute transport; it constructs the global matrix equation for transport, including the right-hand side vector.

Subroutine **c-Bound** determines the values of the solute transport boundary codes, cKod(n), and

136

incorporates prescribed boundary conditions in the global matrix equation for solute transport.

Subroutine **ChInit** initializes selected transport parameters at the beginning of the simulation.

Subroutine **Disper** calculates nodal values of the dispersion coefficients.

Subroutine **SolveT** solves the final asymmetric banded matrix equation for solute transport using Gaussian elimination.

Subroutine **WeFact** computes the optimum weighing factors for all sides of all elements.

Subroutine **PeCour** computes the maximum local Peclet and Courant numbers and the maximum permissible time step.

Source file *ORTHOFEM. FOR*

The subroutines included in this file solve large sparse systems of linear algebraic equations using the preconditioned conjugate gradient method for symmetric matrices, and the ORTHOMTN method for asymmetric matrices. The subroutines were adopted from *Mendoza et al. [* 1991] (see *Mendoza et al. [* 1991] for a detailed description of both methods).

Subroutine **IADMake** generates the adjacency matrix which determines nodal connections from the finite element incidence matrix.

Subroutine **Insert** adds node **j** to the adjacency list for node *i*.

Subroutine **Find** retrieves from the adjacency matrix the appropriate position of two global points in the coefficient matrix.

Subroutine **ILU** performs incomplete lower-upper decomposition of matrix [A].

Function **DU** searches the *ith* row of the upper diagonal matrix for an adjacency of node j.

Subroutine **ORTHOMIN governs the** ORTHOMIN (conjugate gradient) acceleration.

Subroutine **LUSolv** performs lower diagonal matrix inversion by forward substitution, and upper diagonal matrix inversion by backward substitution.

Subroutine MatM2 multiplies a matrix by a vector.

Function SDot calculates the dot product of two vectors.

Function SDotK calculates the dot product of a column in matrix by a vector.

Function SNRM computes the maximum norm of a vector.

Subroutine SAXPYK multiplies a column in a matrix by a scalar, and adds the resulting value to another vector.

Subroutine SCopy copies a vector into another vector.

Subroutine SCopyK copies a column in a matrix into a vector.

Source file GENER3. FOR

In addition to the main code SWMS_3D, we also provide a simple mesh generator, GENER3, which may be used to generate the input file GRID.IN for simple hexahedral flow regions. Generator assumes that the local anisotropy is the same throughout the flow region and that the initial pressure head and concentration, as well as the scaling factors, root distribution, material numbers, recharge/discharge and boundary codes are all the same within a particular horizontal layer. If this is not the case, then the user must modify the resulting output file GRID.IN manually or with available word- or data-processing software. The source code is stored in the source file GENER3.FOR. The GENER3 code reads input file GENER3.IN, which must be included, as well as other input files for SWMS_3D, in subdirectory SWMS_3D.lN.

10.2. *List of Significant SWMS_3D Program Variables.*

Variables which appear in subroutines of the ORTHOFEM package are not given in following tables. Consult the user's guide of ORTHOFEM *[Mendoza et al.,* 1991] for their definition.

Table 10.3. List of significant integer variables.

ALevel	Time level at which a time-dependent boundary condition is specified.
cKod	Code which specifies the type of boundary condition used for solute transport.
IJ	Maximum number of nodes on any transverse line (Table 8.8).
ItCum	Cumulative number of iterations (Table 9.4).
Iter	Number of iterations (Table 9.4).
MaxAl	Number of atmospheric data records (Table 8.11).
MaxIt	Maximum number of iterations allowed during any time step for the solution of water flow equation (Table 8.1).
MBand	Bandwidth (or half-bandwidth) of the symmetric (or asymmetric) matrix *A* when Gaussian elimination is used. Maximum number of nodes adjacent to another node when iterative solvers are used.
MBandD	Maximum permitted bandwidth of matrix *A* when Gaussian elimination is used. Maximum permitted number of nodes adjacent to another node when iterative solvers are used (Table 6.7).
MPL	Number of specified print-times at which detailed information about the pressure head, the water content, flux, concentration, and the soil water and solute balances is printed (Table 8.3).
NDr	Number of drains.
NDrD	Maximum permitted number of drains.
NLay	Number of subregions for which separate water balances are being computed (Table 8.2).
NLevel	Number of time levels at which matrix *A* and vector *B are* assembled for solute transport.
NMat	Number of soil materials (Table 8.2).
NMatD	Maximum permitted number of soil materials (Table 6.7).
NObs	Number of observation nodes for which values of the pressure head, water content, and concentration are printed at each time level.
NObsD	Maximum number of observation nodes for which values of pressure head, water content, and concentration are printed at each time level.
NPar	Number of unsaturated soil hydraulic parameters specified for each material (Table 8.2).
NSeep	Number of seepage faces expected to develop (Table 8.5).

Table 10.3. (continued)

NSeepD	Maximum permitted number of seepage faces (Table 6.7).
NTab	Number of entries in the internally generated tables of the hydraulic properties (see Section 4.3.11).
NTabD	Maximum permitted number of entries in the internally generated tables of the hydraulic properties (Table 6.7).
NumBP	Number of boundary nodes for which $Kode(N) \neq 0$ (Table 8.8).
NumBPD	Maximum permitted number of boundary nodes for which $Kode(n) \neq 0$ (Table 6.7).
NumEl	Number of elements (tetrahedrals, hexahedrals, and/or triangular prisms) (Table 8.8).
NumElD	Maximum permitted number of elements in finite element mesh (Table 6.7).
NumKD	Maximum permitted number of available code number values (Table 6.7).
NumNP	Number of nodal points (Table 8.8).
NumNPD	Maximum permitted number of nodes in finite element mesh (Table 6.7).
NumSEl	Number of subelements (tetrahedrals).
NumSPD	Maximum number of nodes along a seepage face (Table 6.7).
NUS	Number of comer nodes of a particular element.
PLevel	Print time-level (current print-time number).
TLevel	Time-level (current time-step number) (Table 9.4).

Table 10.4. List of significant real variables.

Alf	*1-Epsi,* where *Epsi* is a temporal weighing coefficient [-].
Alfa	Parameter in the soil water retention function $[\text{L}^{-1}]$ (see Section 2.3).
Aqh	Parameter *A, in* equation (6.1) $[\text{LT}^{-1}]$ (Table 8.11).
Bqh	Parameter B_{qh} *in* equation (6.1) $[\text{L}^{-1}]$ (Table 8.11).
cBalR	Relative error in the solute mass balance of the entire flow domain [%] (see equation (5.31)) *(CncBalR* in Table 9.6).
cBalT	Absolute error in the solute mass balance of the entire flow domain [M] (see equation (5.30)) *(CncBalT in* Table 9.6).
cBnd	Value of the boundary condition for solute transport [ML^-3].
cCumA	Sum of the absolute values of all cumulative solute fluxes across the flow boundaries, including those resulting from sources and sinks in the flow domain [M] (see equation (5.3 1)).
cCumT	Sum of all cumulative solute fluxes across the boundaries, including those resulting from sources and sinks in the flow domain [M] (see right hand side of equation (5.30)).
cE	Average concentration of an element [ML^-3].
Change	Inflow/Outflow to/from the flow domain $[\text{L}^{3}\text{T}^{-1}]$ *(InFlow in* Table 9.6).
cht	Time-dependent concentration for the first-type boundary condition assigned to nodes for which *Kode(n)=+3* $[\text{ML}^{-3}]$ (Table 8.11).
cNewE	Amount of solute in a particular element at the new time-level [M].
ConA 1	First principal component, K_1^A, of the dimensionless anisotropy tensor $\boldsymbol{K}^A$ [-] assigned to each element (Table 8.9).
conA2	Second principal component, K_2^A of $\boldsymbol{K}^A$ [-] (Table 8.9).
ConA3	Third principal component, K_3^A of $\boldsymbol{K}^A$ [-] (Table 8.9).
con Vol	Amount of solute in the entire flow domain [M] *(ConVol in* Table 9.6).
Cos11	Cosine of an angle between the principal direction of K_1^A and the x-axis of the global coordinate system assigned to each element (Table 8.9).
cos22	Cosine of an angle between the principal direction of K_2^A and the y-axis of the global coordinate system assigned to each element (Table 8.9).
cos33	Cosine of an angle between the principal direction of K_3^A and the z-axis of the global coordinate system assigned to each element (Table 8.9).
cos12	Cosine of an angle between the principal direction of K_1^A and the y-axis of the global coordinate system assigned to each element (Table 8.9).
Cosl3	Cosine of an angle between the principal direction of K_1^A and the z-axis of the global coordinate system assigned to each element (Table 8.9).
cos23	Cosine of an angle between the principal direction of K_2^A and the z-axis of the global coordinate system assigned to each element (Table 8.9).
Courant	Maximum local Courant number [-] (Table 9.4).

Table 10.4. (continued)

cPrec	Solute concentration of rainfall water [ML^-3] (Table 8.11).
crt	Time-dependent concentration of the drainage flux, or some other time-dependent prescribed flux for nodes were *Kode(n)= -3* $[ML^{-3}]$ (Table 8.11).
cSink	Concentration of the sink term [ML^-1].
cTot	Mean concentration in the flow domain [ML^-3] *(cMean* in Table 9.6).
CumCh0	Cumulative amount of solute removed from the entire flow domain by zero-order reactions [M] (Table 9.5).
CumCh 1	Cumulative amount of solute removed from the entire flow domain by first-order reactions [M] (Table 9.5).
CumChR	Cumulative amount of solute removed from the entire flow domain by root water uptake [M] (Table 9.5).
CumQrR	Cumulative total potential transpiration from the entire flow domain $[L^3]$ *(CumQRP in* Tables 9.3 and 9.7).
CumQrT	Cumulative total potential flux across the atmospheric boundary $[L^3]$ *(CumQAP* in Tables 9.3 and 9.7).
CumQvR	Cumulative total actual transpiration from the entire flow domain $[L^3]$ *(CumQR in* Tables 9.3 and 9.7).
c VolI	Initial amount of solute in the entire flow domain [M].
DeltC	Sum of the absolute changes in concentrations as summed over all elements [M] (see equation (5.3 1)).
DeltW	Sum of the absolute changes in water content as summed over all elements $[L^3]$ (see equation (4.24)).
dlh	Spacing (logarithmic scale) between consecutive pressure heads in the internally generated tables of the hydraulic properties [-] (see equation (4.27)).
dMul	Dimensionless number by which At is multiplied if the number of iterations is less than or equal to 3 [-] (Table 8.3).
dMul2	Dimensionless number by which At is multiplied if the number of iterations is greater than or equal to 7 [-] (Table 8.3).
dt	Time increment At [T] (Table 8.3).
dtMax	Maximum permitted time increment change in t$_{max}$ [T] (Table 8.3).
dtMaxC	Maximum permitted time increment change in t$_{max}$ for solute transport [T] (see equation (5.32)).
dtMin	Minimum permitted time increment Δt_{min} [T] (Table 8.3).
dtOld	Old time increment [T].
dtOpt	Optimal time increment [T].
EI	Potential surface flux per unit atmospheric boundary [LT'] *(=rTop).*
Epsi	Temporal weighing coefficient [-] (Table 8.7).

Table 10.4. (continued)

EpsH	Absolute change in the nodal pressure head between two successive iterations [L].
EpsTh	Absolute change in the nodal water content between two successive iterations [L].
GWL	Time-dependent prescribed head boundary condition [L] for nodes indicated by *Kode(n)=+3* (Table 8.11).
G WLOL	Parameter in equation (6.1) [L] (Table 8.11).
hCritA	Minimum allowed pressure head at the soil surface [L] (Table 8.11).
hCritS	Maximum allowed pressure head at the soil surface [L] (Table 8.11).
hE	Mean element value of the pressure head [L].
hMeanG	Mean value of the pressure head calculated over a set of nodes for which $Kode(n)=\pm3$ [L] *(hKode3 in Tables 9.1 and 9.7).*
hMeanR	Mean value of the pressure head within the root zone [L] *(hRoot in Table 9.1 and 9.7).*
hMean T	Mean value of the pressure head calculated over a set of nodes for which $Kode(n)=\pm4$ [L] *(hAtm in Tables 9.1 and 9.7).*
hTab 1	Lower limit [L] of the pressure head interval for which tables of hydraulic properties is generated internally for each material (ha in Table 8.2).
hTabN	Upper limit [L] of the pressure head interval for which tables of hydraulic properties is generated internally for each material *(hb in* Table 8.2).
hTot	Mean pressure head in the entire flow domain [L] *(hMean in* Table 9.6).
Kk	Unsaturated hydraulic conductivity corresponding to θ_k [LT⁻¹] (see Section 2.3) (Table 8.2).
Ks	Saturated hydraulic conductivity [LT⁻¹] (Table 8.2).
m	Parameter in the soil water retention function [-] (see Section 2.3) (Table 8.2).
n	Parameter in the soil water retention function [-] (see Section 2.3) (Table 8.2).
Peclet	Maximum local Peclet number [-] (Table 9.4).
PeCr	Stability criterion [-] (Table 9.4).
PeCrMax	Maximum local product of Peclet and Courant numbers [-] (Table 9.4).
Prec	Precipitation [LT⁻¹] (Table 8.11).
PO	Value of the pressure head [L], $h_,$, below which roots start to extract water from the soil (Table *8.4).*
P2H	Value of the limiting pressure head [L], $h_,$, below which the roots cannot extract water at the maximum rate (assuming a potential transpiration rate of *r2P)* (Table 8.4).
P2L	As above, but for a potential transpiration rate of *r2L* (Table 8.4).
P3	Value of the pressure head [L], $h_,$, below which root water uptake ceases (usually equal to the wilting point) (Table 8.4).
Qa	Parameter in the soil water retention function [-] (see Section 2.3) (Table 8.2).

Table 10.4. (continued)

θk	Volumetric water content corresponding to K_k [-] (see Section 2.3) (Table 8.2).
θm	Parameter in the soil water retention function [-] (see Section 2.3) (Table 8.2).
θr	Residual soil water content [-].
θs	Saturated soil water content [-].
rQWL	Time-dependent prescribed flux boundary condition [LT^-1] for nodes *wereKode(n)=-3* (Table 8.11).
rLen	Surface area of soil surface associated with transpiration [L^2] (Table 8.10).
RootCh	Amount of solute removed from a particular subelement during one time step by root water uptake [M].
rRoot	Potential transpiration rate [LT^{-1}] (Table 8.11).
rSoil	Potential evaporation rate [LT^{-1}] (Table 8. 11).
rTop	Potential surface flux per unit atmospheric boundary [LT^{-1}] *(rAtm in Table 9.2)*.
r2H	Potential transpiration rate [LT^{-1}] (see Table 8.4).
r2L	Potential transpiration rate [LT^{-1}] (see Table 8.4).
t	Time, t, at current time-level [T].
tAtm	Time for which the *i-th* data record is provided [T] (Table 8.11).
Tau	Tortuosity factor [-].
tFix	Next time resulting from time discretizations 2 and 3 [T] (see Section 4.3.3).
tInit	Starting time of the simulation [T] (Table 8.11).
tMax	Maximum duration of the simulation [T].
tOld	Previous time-level [T].
TolH	Maximum desired absolute change in the value of the pressure head, *h* [L], between two successive iterations during a particular tune step (Table 8.1).
TolTh	Maximum desired absolute change in the value of the water content, θ [-], between two successive iterations during a particular time step (Table 8.1).
tPulse	Time duration of the concentration pulse [T] (Table 8.7).
Vabs	Absolute value of the nodal Darcy fluid flux density [LT^{-1}].
VE	Volume of a tetrahedral element [L^3].
vMeanR	Actual transpiration rate [LT^{-1}] *(vRoot in Table 9.2)*.
vNewE	Volume of water in a particular element at the new time-level [L^3].
vOldE	Volume of water in a particular *element* at the old time-level [L^3].
VolR	Volume of the domain occupied by the root zone [L^3].
Volume	Volume of water in the entire flow domain [L^3] (Table 9.6).
VTot	Volume of the entire flow domain [L^3] *(Area in Table 9.6)*.

Table 10.4. (continued)

wBalR	Relative error in the water mass balance in the entire flow domain [%] (see equation (4.24)).
wBaiT	Absolute error in the water mass balance in the entire flow domain $[L^3]$ (see equation (4.23)).
wCumA	*Sum* of the absolute values of all fluxes across the flow boundaries, including those resulting from sources and sinks in the region $[L^3]$ (see equation (4.24)).
wCumT	*Sum* of all cumulative fluxes across the flow boundaries, including those resulting from sources and sinks in the region $[L^3]$ (see equation (4.23)).
w *VolI*	Initial volume of water in the flow domain $[L^3]$.

Table 10.5. List of significant logical variables.

AtmInf	Logical variable indicating whether or not the input file ATMOSPH.IN is provided (Table 8.1).
CheckF	Logical variable indicating whether or not the grid input data are to be printed for checking (Table 8.1).
DrainF	Logical variable indicating whether drains are, or are not, present in the transport domain (Table 8.1); if drams are present, they are represented by an electrical resistance network analog.
Explic	Logical variable indicating whether an explicit or implicit scheme was used for solving the water flow equation.
FluxF	Logical variable indicating whether or not detailed flux information is to be printed (Table 8.1).
FreeD	Logical variable indicating whether a unit hydraulic gradient (free drainage) is, or is not, invoked at the bottom of the *transport* domain (Table 8.1).
ItCrit	Logical variable indicating whether or not convergence was achieved.
lArtD	Logical variable indicating whether an artificial dispersion is, or is not, to be added in order to satisfy the stability criterion *PeCr* (Table 8.7).
lChem	Logical variable indicating whether or not the solute transport equation is to be solved (Table 8.1).
tConst	Logical variable indicating whether or not there is a constant number of nodes at any transverse line.
lUpw	Logical variable indicating if upstream weighing or the standard Galerkin formulation is to be used (Table 8.7).
IWat	Logical variable indicating if steady-state or transient water flow is to be considered (Table 8.1).
qG WLF	Logical variable indicating whether or not the discharge-groundwater level relationship is used as bottom boundary condition (Table 8.11).
SeepF	Logical variable indicating whether or not a seepage face is to be expected (Table 8.1).
ShortF	Logical variable indicating whether or not the printing of time-level information is to be suppressed on each time level (Table 8.1).
SinkF	Logical variable indicating whether or not plant water uptake will take place (Table 8.11).

146

Table 10.6. List of significant arrays.

A(MBandD,NumNPD)	Coefficient matrix.
Ac(NumNPD)	Nodal values of the product θR [-].
Axz(NumNPD)	Nodal values of the dimensionless scaling factor α_h associated with the pressure head [-] (Table 8.8).
B(NumNPD)	Coefficient vector.
Beta(NumNPD)	Nodal values of the normalized rootwater uptake distribution [L^{-3}] (Table 8.8).
Bi(4)	Geometric shape factors [L^2].
Bxz(NumNPD)	Nodal value of the scaling factor α_K associated with the saturated hydraulic conductivity [-] (Table 8.8).
Cap(NumNPD)	Nodal values of the soil water hydraulic capacity [L^{-1}].
CapTab(NTabD,NMatD)	Internal table of the soil water hydraulic capacity [L^{-1}].
cBound(12)	Values of the time independent concentration boundary condition [ML"] (Table 8.7).
ChemS(NumKD)	Cumulative boundary solute fluxes [M] (Table 9.5).
ChPar(10,NMatD)	Parameters which describe the transport properties of the porous media (Table 8.7).
Ci(4)	Geometric shape factors [L^2].
cMean(10)	Mean concentrations of specified subregions [ML^-3] (Table 9.6).
Con(NumNPD)	Nodal values of the hydraulic conductivity at the new time level [LT^{-1}].
ConAxx(NumElD)	Nodal values of the component K_{xx}^A of the anisotropy tensor $\boldsymbol{K}^A$ [-].
ConAxy(NumElD)	Nodal values of the component K_{xy}^A of the anisotropy tensor $\boldsymbol{K}^A$ [-].
ConAxz(NumElD)	Nodal values of the component K_{xz}^A of the anisotropy tensor $\boldsymbol{K}^A$ [-].
ConAyy(NumElD)	Nodal values of the component K_{yy}^A of the anisotropy tensor $\boldsymbol{K}^A$ [-].
ConAyz(NumElD)	Nodal values of the component K_{yz}^A of the anisotropy tensor $\boldsymbol{K}^A$ [-].
ConAzz(NumElD)	Nodal values of the component K_{zz}^A of the anisotropy tensor $\boldsymbol{K}^A$ [-].
Conc(NumNPD)	Nodal values of the concentration [ML"] (Table 8.8).
ConO(NumNPD)	Nodal values of the hydraulic conductivity at the old time level [LT^{-1}].
ConSat(NMatD)	Saturated hydraulic conductivities of the material [LT^{-1}].
ConSub(10)	Amounts of solute in the specified subregions [M] (Table 9.6).
ConTab(NTabD,NMatD)	Internal table of the hydraulic conductivity [LT^-1].
CumQ(NumKD)	Cumulative boundary fluxes [L^3] (Table 9.3).
Di(4)	Geometric shape factors [L^2].
Dispxx(NumNPD)	Nodal values of the component D_{xx} of the dispersion tensor [L^2T^{-1}].
Dispxy(NumNPD)	Nodal values of the component D_{xy} of the dispersion tensor [L^2T^{-1}].

Table 10.6. (continued)

Dispxz(NumNPD)	Nodal values of the component D_{xz} of the dispersion tensor $[L^2T^{-1}]$.
Dispyy(NumNPD)	Nodal values of the component D_{yy} of the dispersion tensor $[L^2T^{-1}]$.
Dispyz(NumNPD)	Nodal values of the component D_{yz} of the dispersion tensor $[L^2T^{-1}]$.
Dispzz(NumNPD)	Nodal values of the component D_{zz} of the dispersion tensor $[L^2T^{-1}]$.
DS(NumNPD)	Vector *{D}* in the global matrix equation for water flow $[L^3T^{-1}]$ (see equation (4.9)); also used for the diagonal of the coefficient matrix [Q] in the global matrix equation for solute transport [L^3] (see equation (5.5)).
Dxz(NumNPD)	Nodal values of the scaling factor α_θ associated with the water content (Table 8.8).
E(4,4)	Element contributions to the global matrix A for water flow $[L^4]$ (see equation (4.5)).
EfDim(2,NDr)	Effective diameter of drains and side lengths of the finite element mesh representing the dram (Table 8.6).
F(NumNPD)	Diagonal of the coefficient matrix [F] in the global matrix equation for water flow, $[L^3]$ (see equation (4.7)).
Fc(NumNPD)	Nodal values of the parameter *F* $[T^{-1}]$ *(see* equation (3.5)).
Gc(NumNPD)	Nodal values of the parameter G $[ML^{-3}T^{-1}]$ (see equation (3.5)).
hMean(10)	Mean values of the pressure head in specified subregions [L] (Table 9.6).
hMean(NumKD)	Mean values of the pressure head along a certain type of boundary [L] (Table 9.6).
hNew(NumNPD)	Nodal vaiues of the pressure head [L] at the new time-level (Table 8.8).
hOld(NumNPD)	Nodal values of the pressure head [L] at the old time-level.
hSat(NMatD)	Air-entry values for each material [L].
hTab(NTabD)	Internal table of the pressure head [L].
hTemp(NumNPD)	Nodal values of the pressure head [L] at the previous iteration.
iLock(4)	Global nodal numbers of element comer nodes.
IU(11)	Vector which contains identification numbers of output files.
KNoDr(NDr, ND)	Global numbers of nodes representing a particular drain (Table 8.6).
KElDr(NDr, NEID)	Global numbers of elements surrounding a particular drain (Table 8.6).
KodCB(NumBPD)	Codes which identify type of boundary condition and refer to the vector *cBound* for time-independent solute transport boundary conditions (Table 8.7).
Kode(NumNPD)	Codes which specify the type of boundary condition (Table 8.8).
KX(NumElD,9)	Global nodal numbers of element comer nodes (Table 8.8). *Kx(i,9)* represents the code specifying the subdivision of the element into subelements.
KXB(NumBPD)	Global nodal numbers of sequentially numbered boundary nodes for which $Kode(n) \neq 0$ (Table 8.8).
LayNum(NumElD)	Subregion numbers assigned to each element (Table 8.9).

Table 10.6. (continued)

List(4)	Global nodal numbers of element comer nodes.
ListNE(NumNPD)	Number of subelements adjacent to a particular node.
MatNum(NumNPD)	Indices for material whose hydraulic and transpon properties are assigned to a particular node (Table 8.8).
ND(NDr)	Number of nodes representing a drain (Table 8.6).
NElD(NDr)	Number of elements surrounding a drain (Table 8.6).
Node(NObsD)	Observation nodes for which values of the pressure head, water content, and concentration are printed at each time level (Table 8.10).
NP(NSeepD,NumSPD)	Sequential global numbers of nodes on the seepage face (Table 8.5).
NSP(NSeepD)	Numbers of nodes on seepage face (Table 8.5).
Par(10,NMatD)	Parameters which describe the hydraulic properties of the porous medium (Table 8.2).
POptm(NMatD)	Values of the pressure head [L], h_2, below which roots start to extract water at the maximum possible rate (Table 8.4).
Q(NumNPD)	Nodal values of the recharge/discharge rate $[L^3T^{-1}]$ (Table 8.8).
Qc(NumNPD)	Nodal values of solute fluxes [MT'].
S(4,4)	Element contributions to the global matrix S for solute transport $[L^3T^{-1}]$ (see equation (5.6)).
Sink(NumNPD)	Nodal values of the sink term $[T^{-1}]$ (see equation (2.3)).
SMean(NumKD)	Total solute fluxes [MT^-1] (Table 9.5).
SolIn(NumElD)	Element values of the initial amount of solute [M] (Table 9.6).
SubCha(10)	Inflow/Outflow to/from specified subregions $[L^3T^{-1}]$ (Table 9.6).
Sub Vol(10)	Volumes of water in specified subregions [L^3] (Table 9.6).
S *Width(NumKD)*	Surface area of a boundary associated with a certain type of boundary condition $[L^2]$.
TheTab(NTabD,NMatD)	Internal table of the soil water content [-].
ThNew(NumNPD)	Nodal values of the water content at the new time level [-].
ThOld(NumNPD)	Nodal values of the water content at the old time level [-].
thr(NMatD)	Residual water contents for specified materials [-].
thSat(NMatD)	Saturated water contents for specified materials [-].
TPrint(MPL)	Specified print-times [T] (Table 8.3).
vMean(NumKD)	Values of boundary fluxes across a certain type of boundary $[L^3T^{-1}]$.
Vol(10)	Volume of the specified subregions $[L^3]$ (Table 9.6).
Vx(NumNPD)	Nodal values of the x-component of the Darcian velocity vector $[LT^{-1}]$.

Table 10.6. (continued)

VxE(4)	Nodal values of the x-component of the Darcian velocity vector for a particular element $[LT^{-1}]$.
Vy(NumNPD)	Nodal values of the y-component of the Darcian velocity vector $[LT^{-1}]$.
VyE(4)	Nodal values of the y-component of the Darcian velocity vector for a particular element $[LT^{-1}]$.
Vz(NumNPD)	Nodal values of the z-component of the Darcian velocity vector $[LT^{-1}]$.
VzE(4)	Nodal values of the z-component of the Darcian velocity vector for a particular element $[LT^{-1}]$.
WatIn(NumElD)	Element values of the initial volume of water $[L^3]$.
*WeTab(6,5*NumElD)*	Weighing factors associated with the sides of subelements [-].
Width(NumBPD)	Surface area of the boundary $[L^2]$ associated with boundary nodes (Table 8.10).
Wx(4)	Additional upstream weighting contributions to the global matrix S from the x-direction from a particular element $[LT^{-1}]$.
WY(4)	Additional upstream weighting contributions to the global matrix S from the y-direction from a particular element $[LT^{-1}]$.
Wz(4)	Additional upstream weighting contributions to the global matrix S from the z-direction from a particular element $[LT^{-1}]$.
x(NumNPD)	x-coordinates [L] of the nodal points (Table 8.8).
y(NumNPD)	y-coordinates [L] of the nodal points (Table 8.8).
z(NumNPD)	z-coordinates [L] of the nodal points (Table 8.8).

11. REFERENCES

Bear, J. 1972. *Dynamics of Fluid in Porous Media.* Elsevier, New York.

Behie, A., and P. K. W. Vinsome. 1982. Block iterative methods for fully implicit reservoir simulation, Soc. *Pet. Eng. J., 22, 658-668.*

Belmans, C., J. *G.* Wesseling, and R. A. Feddes. 1983. Simulation model of the water balance of a cropped soil: SWATRE, J. *Hydrol., 63, 271- 286.*

Celia, M. A., E. T. Bouloutas, and R. L. Zarba. 1990. A general mass-conservative numerical solution for the unsaturated flow equation, *Water Resour. Rex, 26,* 1483-1496.

Christie, L. D., D. F. Griffiths, A. R. Mitchell, and 0. C. Zienkiewicz. 1976. Finite element methods for second order differential equations with significant first derivatives, *Int. J Num. Methods in Engineering, 10,* 13 89- 13 96.

Cislerova, M. 1987. Comparison of simulated water balance for ordinary and scaled soil hydraulic characteristics, *Publ. No. 82,* Dept. of Hydraulics and Catchment hydrology, Agricultural Univ., Wageningen, The Netherlands.

Cleary, R. W., and M. J. Ungs. 1978. Groundwater pollution and hydrology, Mathematical models and computer programs, *Research Report No. 78- WR-15,* Water Resour. Program, Princeton Univ. Princeton, New Jersey.

Davis, L. A., and S. P. Neurnan. 1983. Documentation and user's guide: UNSAT2 - Variably saturated flow model, *Final Report, WWL/TM-1 791-1,* Water, Waste & Land, Inc., Ft. Collins, Colorado.

Feddes, R. A., E. Bresler, and S. P. Neuman. 1974. Field test of a modified numerical model for water uptake by root systems, *Water Resow. Res., 10(6),* 1199- 1206.

Feddes, R. A., P. J. Kowalik, and H. Zaradny. 1978. *Simulation of Field Water Use and Crop Yield,* Simulation Monographs, 188 p., Pudoc, Wageningen, The Netherlands.

Fipps, G., R. W. Skaggs, and J. L. Nieber. 1986. Drain as a boundary condition in finite element, *Water Resour. Res., 22(1* l), 1613-1621.

Hopmans, J. W., and J. N. M. Stricker. 1989. Stochastic analysis of soil water regime in a watershed, J. *Hydrol., 105, 57-84.*

Huyakom, P. S., and G. F. Pinder. 1983. *Computational Methods in Subsurface Flow,* Academic press, London, United Kingdom.

Javandel, I., Ch. Doughty, and Chin-Fu Tsang. 1984. *Groundwater Transport: Handbook of Mathematical Models,* Water Resour. Monograph No. 10, 228 p., Am. Geophys. Union, Washington, D.C.

Leij, F. J., T. H. Skaggs, and M. Th. van Genuchten. 1991. Analytical solutions for solute transport in three-dimensional semi-infinite porous media, *Water Resour. Res., 27(l0), 27 19-2733.*

Leij, F. J., and S. A. Bradford. 1994. 3DADE: A computer program for evaluating three-dimensional equilibrium solute transport in porous media. *Research Report No. 134, 82* p., U.S. Salinity Laboratory, USDA, ARS, Riverside, California.

Letniowski, F. W. 1989. An overview of preconditioned iterative methods for sparse matrix equations. *Research Report U-89-26,* Faculty of Mathematics, Univ. of Waterloo, Waterloo, Ontario, Canada.

Luckner, L., M. Th. van Genuchten, and D. R. Nielsen. 1989. A consistent set of parametric models for the two-phase flow of immiscible fluids in the subsurface. *Water Resour. Res., 25(10), 2187-2193.*

Lynch, D. 1984. Mass conservation in finite element groundwater models. *Adv. Water Resour., 7, 67-75.*

McCord, J. T. 1991. Application of second-type boundaries in unsaturated flow modeling. *Water Resour. Res., 27(12), 3257-3260.*

Meijerink, J. A. , and H. A. van der Vorst. 1977. An iterative solution method for linear systems of which the coefficient matrix is a symmetric M-matrix. *Mathematics of Computation, 31(137), 148-162.*

Mendoza, C. A., R. Therrien, and E. A. Sudicky. 1991. *ORTHOFEM User's Guide, Version 1.02.* Waterloo Centre for Groundwater Research, Univ. of Waterloo, Waterloo, Ontario, Canada.

Miller, E. E., and R. D. Miller. 1956. Physical theory for capillary flow phenomena, J. *Appl. Phys., 27, 324-332.*

Millington, R. J., and J. M. Quirk. 196 1. Permeability of porous solids, *Trans. Faraday Soc., 57, 1200-1207.*

Mls, J. 1982. Formulation and solution of fundamental problems of vertical infiltration, *Vodohosp. Cas., 30, 304-313* (in Czech).

Mohammad, F. S., and R. W. Skaggs. 1983. Drain tube opening effects on drain inflow, J. *Irrig. Drain. Div. Am. Soc. Civ. Eng., 109(4), 393-404.*

Mualem, Y. 1976. A new model for predicting the hydraulic conductivity of unsaturated porous media, *Water Resow. Res., 12(3), 5 13-522.*

Neuman, S. P. 1972. Finite element computer programs for flow in saturated-unsaturated porous media, *Second Annual Report, Part 3, Project No. AIO-SWC-77, 87* p. Hydraulic Engineering Lab., Technion, Haifa, Israel.

Neuman, S. P. 1973. Saturated-unsaturated seepage by finite elements, J. *Hydraul. Div.,* ASCE, 99 (HY 12), 2233-2250.

Neuman, S. P. 1975. Galerkin approach to saturated-unsaturated flow in porous media, Chapter 10 in *Finite Elements in Fluids, Vol. I, Viscous Flow and Hydrodynamics,* edited by R. H. Gallagher, J. T. Oden, C. Taylor, and O.C. Zienkiewicz., pp. 201-217, John Wiley and Sons, London.

Neuman, S. P., R. A. Feddes, and E. Bresier. 1974. Finite element simulation of flow in saturated-unsaturated soils considering water uptake by plants, *Third Annual Report, Project No. A IO-SWC- 77,* Hydraulic Engineering Lab., Technion, Haifa, Israel.

Perrochet, P., and D. Berod. 1993. Stability of the standard Crank-Nicholson-Galerkin scheme applied to the diffusion-convection equation: some new insights, *Water Resour. Res., 29(9), 329 1-3297.*

Pinder, G. F., and W. G. Gray. 1977, *Finite Element Simulation in Surface and Subsurface Hydrology,* Academic Press, New York, N.Y.

Simmons, C. S., D. R. Nielsen, and J. W. Biggar. 1980. Scaling of field-measured soil water properties, *Hilgardia, 4 7, 10* 1 - *122.*

Šimůnek, J., T. Vogel, and M. Th. van Genuchten. 1992. The SWMS_2D code for simulating water flow and solute transport in two-dimensional variably saturated media, Version 1.1. *Research Report No. 126, 169* p., U.S. Salinity Laboratory, USDA, ARS, Riverside, California.

Šimůnek, J., and D. L. Suarez. 1993. UNSATCHEM-2D code for simulating two-dimensional variably saturated water flow, heat transport, carbon dioxide production and transport, and multicomponent solute transport with major ion equilibrium and kinetic chemistry, Version 1.1. *Research Report No. 128, 218* p., U.S. Salinity Laboratory, USDA, ARS, Riverside, California.

Šimůnek, J., T. Vogel, and M. Th. van Genuchten. 1994. The SWMS_2D code for simulating water flow and solute transport in two-dimensional variably saturated media, Version 1.2 1. *Research Report No. 132,* 197 p., U.S. Salinity Laboratory, USDA, ARS, Riverside, California.

Sir, M., T. Vogel, and M. Císlerová. 1985. Analytical expression of the retention curve and hydraulic conductivity for porous material, *Vodohosp. Čas.,* 33(l), 74-85 (in Czech).

Sisson, J. B. 1987. Drainage from layered field soils: Fixed gradient models, *Water Resour. Res.,* 23(11), 2071-2075.

Skaggs, R. W., E. J. Monke, and L. F. Huggins. 1970. An approximate method for determining the hydraulic conductivity function of an unsaturated soil, *Techn. Report No. II,* Water Resour. Res. Center, Purdue University, Lafayette, Indiana.

Sudicky, E. A., and P. S. Huyakom. 199 1. Contaminant migration in imperfectly known heterogeneous groundwater systems, *Reviews of Geophysics,* Supplement, U.S. National Report. to Int. Union of Geodesy and Geophysics 1987-1990, pp. 240-253, Am. Geophys. Union, Washington, DC.

van Genuchten, M. Th. 1976. On the accuracy and efficiency of several numerical schemes for solving the convective-dispersive equation, in *Finite elements in Water Resources,* edited by W. G. Gray et al., pp. 1.71- 1.90, Pentech Press, London.

van Genuchten, M. Th. 1978. Mass transport in saturated-unsaturated media: one-dimensional solutions, *Research Report No. 78- WR-I I,* 118 p., Water Resources Program, Princeton Univ., Princeton, New Jersey.

van Genuchten, M. Th. 1980. A closed-form equation for predicting the hydraulic conductivity of unsaturated soils, Soil Sci. Soc. *Am. J., 44, 892-898.*

van Genuchten, M. Th., and J. Parker. 1984. Boundary conditions for displacement experiment through short laboratory soil columns, Soil Sci. Soc. *Am. J., 48, 703-708.*

Vimoke, B. S., and G. S. Taylor. 1962. Simulating water flow in soil with an electric resistance network, *Report No. 41-65, 5* 1 p., Soil and Water Conserv. Res. Div., U. S. Agric. Res. Serv., Columbus, Ohio.

Vimoke, B. S., T. D. Yura, T. J. Thiel, and G. S. Taylor. 1963. Improvements in construction and use of resistance networks for studying drainage problems, *Soil Sci. Soc. Am. J., 26(2), 203-207.*

Vogel, T. 1987. SWMII - Numerical model of two-dimensional flow in a variably saturated porous medium, *Research Report No. 87,* Dept. of Hydraulics and Catchment Hydrology, Agricultural Univ., Wageningen, The Netherlands.

Vogel, T., and M. Císlerová. 1988. On the reliability of unsaturated hydraulic conductivity calculated from the moisture retention curve, *Transport in Porous Media, 3,* l-l 5.

Vogel, T., M. Císlerová, and J. W. Hopmans. 1991. Porous media with linearly variable hydraulic properties, *Water Resow, Res., 27(l0), 2735-2741.*

Wesseling, J. G., and T. Brandyk. 1985. Introduction of the occurrence of high groundwater levels and surface water storage in computer program SWATRE, Nota 1636, Institute for Land and Water Management Research (ICW), Wageningen, The Netherlands.

Zienkiewicz, 0. C. 1977. The *Finite Element Method,* 3rd ed., McGraw-Hill, London, United Kingdom.